Institut für Medizinische Mikrobiologie, Immunologie und Hygiene
der Technischen Universität München

Direct *ex vivo* identification of individual antigen-specific T cells with optimal avidity for protection

Robert A. Knall

Vollständiger Abdruck der von der Fakultät Wissenschaftszentrum Weihenstephan für Ernährung, Landnutzung und Umwelt der Technischen Universität München zur Erlangung des akademischen Grades eines

Doktors der Naturwissenschaften

genehmigten Dissertation.

Vorsitzender:	Univ.-Prof. Dr. S. Scherer
Prüfer der Dissertation:	1. Univ.-Prof. Dr. D. Busch
	2. Univ.-Prof. Dr. D. Haller

Die Dissertation wurde am 07.08.2007 bei der Technischen Universität München eingereicht und durch die Fakultät Wissenschaftszentrum Weihenstephan für Ernährung, Landnutzung und Umwelt am 23.10.2007 angenommen.

I TABLE OF CONTENTS

II INDEX OF FIGURES

II INDEX OF FIGURES

III ABBREVIATIONS

ACT	Ammoniumchloride/Tris
Ag	Antigen
α-MM	α-Methylmannopyranoside
APC	Allophycocyanin
APC	antigen presenting cell
APL	altered peptide ligand
APS	Ammoniumpersulfate
ATCC	American type culture collection
β_2m	beta-2-microglobuline
BHI	brain-heart infusion medium
BSA	bovine serum albumin
CCR	receptor for CC-type chemokines
CD	cluster of differentiation
CDR	complementarity determining region
CFU	colony forming unit
CMV	Cytomegalovirus
ConA	Concanavalin A
^{51}Cr	Chromium-51
CTL	cytotoxic T lymphocyte
d	day
DC	dendritic cell
dH_2O	distilled, deionized water
DNA	Deoxyribonucleic acid
DTT	Dithiothreitol
EBV	Epstein-Barr virus
EDTA	Ethylendiaminetetraacetate
ELISPOT	enzyme linked immunospot technique
EMA	Ethidiummonazidebromide
Fab	antigen-binding fragment
FACS	fluorescence activated cell sorting
FCS	fetal calf serum

FITC	Fluoresceinisothiocyanate
FPLC	fast protein liquid chromatography
Gy	Gray
h	hour
h	human
HIV	human immunodeficiency virus
HLA	human leukocyte antigen
HSCT	hematopoetic stem cell transplant
HSV	Herpes simplex virus
IC_{50}	peptide concentration mediating 50% IFN-γ production in ICCS
ICCS	intracellular cytokine staining
IFN	Interferon
Ig	Immunoglobulin
IL	Interleukin
IPTG	Isopropyl-β-D-thiogalactopyranoside
i.v.	intravenously
kDa	kilodalton
LB	Luria Bertoni medium
Lck	leukocyte-specific protein tyrosine kinase
LFA	leukocyte function-associated antigen
LLO	Listeriolysin O
L.m.	*Listeria monocytogenes*
LSM	laser scanning microscope
m	murine
M	molar
MHC	major histocompatibility complex
min	minutes
mRNA	messenger RNA
NK cell	natural killer cell
OD	optical density
PAGE	polyacrylamide gel electrophoresis
PBMC	peripheral blood mononuclear cell
PCR	polymerase chain reaction
PBS	phosphate-buffered saline

PE	Phycoerythrin
PFA	Paraformaldehyde
PFU	plaque forming units
pMHC	peptide loaded MHC molecule
PTLD	post-transplant lymphoproliferative disease
RAG	recombination activating gene
RNA	Ribonucleic acid
rpm	rounds per minute
RT	room temperature
RU	response unit
SA	Streptavidin
SDS	Sodiumdodecylsulfate
SPF	specific pathogen free
SPR	surface plasmon resonance
ST	Streptactin
TAA	tumor-associated antigen
TBE	Tris/Borate/EDTA buffer
T_{CM}	central memory T cell
TCR	T cell receptor
TdT	terminal deoxynucleotide transferase
T_E	effector T cell
T_{EM}	effector memory T cell
TEMED	N,N,N´,N´-Tetramethylethylendiamine
T_H	T helper cell
TL	thymic leukemia; MHC class Ib molecule
TNF	tumor necrosis factor
Tris	Tris-(hydroxylmethyl)-aminomethane
Vα/Vβ	V alpha/V beta region of the TCR
VSV	vesicular stomatitis virus
wt	wildtype
ZAP-70	ζ-associated protein of 70 kDa

1 INTRODUCTION

1.1 THE IMMUNE SYSTEM

The immune system is the organisms defense system against pathogens like bacteria, viruses and parasites, as well as against certain tumors. It is formed by a highly complex interplay of different cell types and molecules that as a whole enable the body to fight these threats. In general, the immune system can be divided into the innate and the adaptive compartment (Abbas, 2003).

The innate immune system represents the first line of defense against pathogens. It includes epithelial barriers, the complement system, anti-microbial molecules (defensins) and enzymes, as well as mediators of inflammation like interferons and interleukins. On a cellular level, granulocytes, monocytes, macrophages, dendritic cells, neutrophils, mast cells and natural killer (NK) cells are part of the innate immune system, all of which can attack and eliminate pathogens. Some innate cells, like NK cells are involved in self/non-self discrimination, others are crucial for the presentation of foreign antigen to cells of the adaptive immune system (Janeway and Medzhitov, 2002). Once cells of the innate immune system detect a pathogen, they can secrete cytokines that deliver specific signals to immune cells in an auto- or paracrine fashion. Other cells secrete mediators of inflammation that can recruit effector cells both of the innate and adaptive immune system to the site of infection (Abbas, 2003). Especially when certain pathogens overcome these first and early defense mechanisms, the adaptive immune system has to come into play.

1.2 ADAPTIVE IMMUNITY

Due to their highly diversified receptors, cells of the adaptive or acquired immune system can generate immune reactions that are directed against defined molecules of the pathogen (so called antigens) in a highly specific manner. Since the antigen has to be processed and presented by phagocytic antigen presenting cells (APC) of the innate immune system, the initiation and maintenance of an adaptive immune response requires tight and complex interactions between innate and adaptive immunity. Both arms of the immune system

contribute essential factors important for antigen-processing, -presentation, -recognition, T and B cell activation, differentiation and memory development.

After antigen recognition, B cells, which comprise the humoral part of adaptive immunity, differentiate and proliferate in the B cell regions of secondary lymphatic organs. They develop into antibody producing plasma cells. These antibodies can reach toxins and pathogens in the blood and in extracellular compartments, bind to specific molecular structures, and by this neutralize the toxin or pathogen and mark it for elimination by the complement system or by cells of the innate immune system like NK cells or phagocytes (Abbas, 2003).

Certain pathogens have developed strategies to escape from the immune system by hiding in the inside of cells. This is true for all viruses, which have to make use of their hosts´ protein production machinery for replication, but also for some bacteria and parasites. These pathogens cannot be reached by antibodies. However, defined parts of the pathogens proteins are presented on the surface of the infected cell by MHC (major histocompatibility complex) molecules in the form of short peptide sequences. These peptide loaded MHC molecules (pMHC) can be recognized by T cells, which form the cellular compartment of adaptive immunity (Abbas, 2003).

1.3 T CELLS

T cells recognize antigenic peptides in the context of MHC molecules with their T cell receptor (TCR) (Cresswell, 1994; Pamer and Cresswell, 1998). This way they can react to cells that have taken up or are infected by a certain pathogen in a highly specific manner.

T cells are classified into two major compartments, cytotoxic T cells (CTL) and T helper cells (T_H cells). T_H cells use CD4 as coreceptor for the TCR and are, therefore, also called $CD4^+$ T cells. They recognize antigen in the context of MHC class II molecules (MHC II). CTL use CD8 as coreceptor and are also called $CD8^+$ T cells. They recognize antigen in the context of MHC class I molecules (MHC I). Both coreceptors cooperate structurally with the TCR by binding to constant regions of the MHC molecule and functionally by enhancing TCR signaling (Rudolph et al., 2006).

The main function of $CD4^+$ T cells after activation through contact with antigen in the context of MHC II is to control antibody production by B cells or the effector functions of $CD8^+$ T cells (Kalams and Walker, 1998). T_H cells can be classified into different subtypes

depending on their cytokine secretion profiles. These subtypes are T_H0, T_H1 and T_H2 cells (Mosmann and Sad, 1996). T_H0 are naïve or weakly activated $CD4^+$ T cells that cannot yet be divided into the other subsets. For the differentiation into T_H1 or T_H2, the nature and the amount of antigen, as well as the cytokines that are produced by the antigen presenting cell (APC) are crucial (Morel and Oriss, 1998; Rogers et al., 1998; Romagnani, 1992). Presence of IL-12 and/or IL-18 during presentation leads to differentiation into T_H1 cells. These cells mainly produce IL-2, IFN-γ and TNF-α, which among other functions can activate macrophages and thus facilitate the killing of intracellular pathogens (O'Garra, 1998). Presence of IL-4 during antigen presentation leads primarily to differentiation into T_H2 cells, which mainly produce IL-4, IL-5, IL-10 and IL-13, which can activate B cells to produce antibodies (Medzhitov and Janeway, 1998; Morel and Oriss, 1998). Once this initial polarization of the response to a T_H1 or T_H2 response is established, it is self perpetuating since T_H1 cytokines further enhance the T_H1 response and down-regulate T_H2 differentiation and vice versa (Morel and Oriss, 1998).

After activation through contact with antigen in the context of MHC I and co-stimulatory molecules, $CD8^+$ T cells differentiate into CTLs. These cells can lyse infected cells or tumor cells that present antigen on their surface, secrete cytokines like IFN-γ and TNF-α that directly attack the pathogen, or stimulate other immune cells. The killing of cells is mediated by Fas – Fas-ligand interactions and cytotoxic effector molecules like granzymes and perforin (Griffiths, 1995). Other effector functions, like the negative regulation of viral reproduction by T cell effector mechanisms have also been described (Nakamoto et al., 1997).

The initiation of target cell lysis has been named “lethal hit” (Berke, 1995). Within minutes of the first contact of a CTL with a target cell, the Golgi apparatus and lytic granula migrate to the contact zone. The granula fuse with the surface membrane, and perforins and granzymes are released. Perforins polymerize and form a pore in the target cell membrane, leading to water influx and osmotic lysis. Apoptosis inducing proteins like granzymes also enter the target cell via this pore. Besides these mechanisms, apoptosis can also be induced by signaling of Fas (CD95) on the target cell upon ligation of Fas-Ligand (CD95L) from the CTL. Activated $CD8^+$ T cells express large amounts of CD95L and can kill Fas-expressing target cells via this route. Under certain conditions, IFN-γ and TNF-α can also lead to apoptosis in target cells (Abbas, 2003).

In recent years, another T cell population has been described, so called γ/δ-T cells. This population makes up about 5% of overall T cells. They have been described to be involved in both innate and adaptive immunity. Naïve γ/δ-T cells can respond very rapidly to their

specific ligand, a characteristic normally typical for cells of the innate immune system. However, since they express rearranged surface receptors and are able to develop into memory cells, they also bear specific characteristics of cells of the adaptive immune system. Interestingly, in humans γ/δ-T cells have been implicated also to function as APC, being able to present ligands to other γ/δ-T cells (Modlin and Sieling, 2005).

A special feature of the adaptive immune system is the ability to generate cells that persist after the first period of contact with an antigen. These so called "memory cells" are long living and can react faster and more efficient to repeated antigen contact than naïve T cells (Kalia et al., 2006). The clonal expansion phase of an adaptive T cell response is followed by a contraction phase, where more than 90% of the antigen-specific cells die by apoptosis, leaving only a small pool of memory T cells. The programming of naïve T cells to become memory cells takes place very early during the primary response. Already 24 hours of antigenic stimulation are sufficient to induce a program of clonal expansion, expression of effector functions and differentiation into memory cells (Bevan and Fink, 2001; Masopust et al., 2004; Wong et al., 2004). Memory T cells can be immediately activated through re-encounter with antigen, resulting in rapid proliferation of antigen-specific T cells, this way providing protection against re-encounter of a pathogen. Many studies have been performed to distinguish long living memory T cells from the pool of short living effector T cells via distinct markers. In humans this distinction was made using the markers CD45RA and CD45R0, which are predominantly expressed on naïve or memory T cells, respectively. Further distinctions can be made via the markers CD62L, CD27 and CCR7. CCR7 is a homing receptor and can be used in combination with CD45RA to distinguish so called central memory cells (T_{CM} – $CCR7^{high}/CD45RA^{low}$) and effector memory cells (T_{EM} – $CCR7^{low}/CD45RA^{low}$). T_{CM} are believed to be the main source for long-term maintenance of antigen-specific immune responses, whereas T_{EM} are crucial for providing immediate protective capacity (Sallusto et al., 1999). With the recent identification of the marker CD127 (the IL-7 receptor α-chain) in combination with CD62L, the discrimination between effector and memory T cell subsets could also be made in the murine system. T_{CM} ($CD127^{high}/CD62L^{high}$) can now be distinguished from T_{EM} ($CD127^{high}/CD62L^{low}$) and effector T cells (T_E – $CD127^{low}/CD62L^{low}$) (Huster et al., 2004). The different memory T cell subsets differ in their cytokine expression profiles and their proliferative capacities. T_{EM}, like T_E, show immediate effector function characterized by the production of IFN-γ and TNF-α, which are not typically produced by T_{CM}. Regarding their proliferative capacity, T_{EM} show poor proliferative capacity upon antigenic stimulation and show poor IL-2 production. In

contrast, like it has been described in the human system, T_{CM} can vigorously proliferate after re-stimulation with antigen (Huster et al., 2004).

1.4 MOLECULAR STRUCTURE OF THE T CELL RECEPTOR

T cells recognize antigen in the context of MHC molecules presented by professional APCs. Antigen specificity is defined by the T cell receptor (TCR) (Davis and Bjorkman, 1988). Each T cell carries about 100000 copies of the same TCR on its surface. Technological advances like the development of monoclonal T cell populations and the cloning of T cell-specific genes led to the identification of the TCR. This process culminated in the x-ray crystallographic analysis of TCRs, and even of trimolecular complexes of MHC molecules, bound peptides and specific TCRs, generating very exact data about the molecular structure of the TCR, and of TCR – MHC interactions (Garboczi et al., 1996; Garcia et al., 1996).

The T cell receptor is composed of two different transmembrane polypeptide chains, the TCR α- and β-chain, which are covalently linked by a disulfide bridge to a heterodimeric structure (Fig. 1). The α-chain has a molecular weight of 40-60 kDa for humans, and 44-55 kDa in the mouse, the β-chain of 40-50 kDa in humans and 40-55 kDa in the mouse. Each α- and β-chain consists of one Ig-like N-terminal variable (V) domain, one Ig-like constant (C)

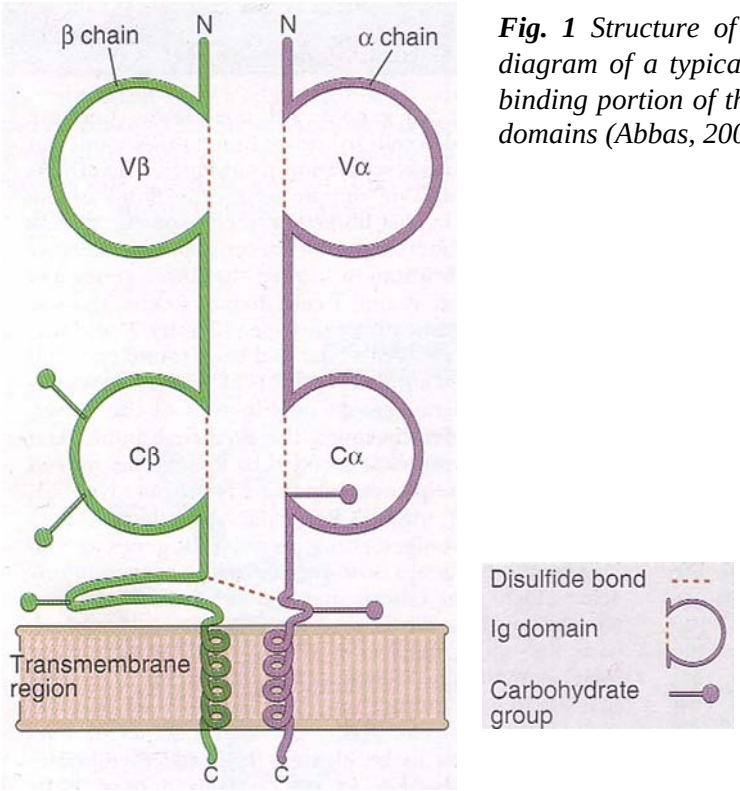

Fig. 1 *Structure of the T cell receptor. A schematic diagram of a typical α/β-TCR is shown. The antigen-binding portion of the TCR is formed by the V_α and V_β domains (Abbas, 2003).*

domain, a hydrophobic transmembrane region, and a short cytoplasmic tail (Abbas, 2003). The V regions of the TCR α- and β-chains contain short stretches of amino acids, where the variability between different TCRs is at a maximum. These form the hypervariable or complementarity-determining regions (CDRs). Three CDRs in the α-chain are opposed to three similar regions in the β-chain to form the part of the TCR that specifically recognizes pMHC complexes (Bjorkman, 1997; Garcia et al., 1996).

Each TCR chain is encoded by multiple gene segments that undergo somatic rearrangements during the maturation of a T cell (see 1.5). In the α- and β-chains, the third hypervariable regions (which form CDR3) are composed of sequences encoded by V and J (joining) gene segments (in the α-chain) or by V, D (diversity) and J segments (in the β-chain). The CDR3 regions also contain sequences that are not derived from the genome, but are encoded by different types of nucleotide additions. Therefore, most of the sequence variability in TCRs is concentrated in CDR3.

The C regions of both the α- and β-chain continue into short hinge regions, which contain cysteine residues that contribute to a disulfide-bridge linking the two chains. The hinge is followed by the hydrophobic transmembrane regions. Atypical for transmembrane regions, these contain positively charged amino acid residues, which interact with negatively charged amino acids of the transmembrane regions of other polypeptides (CD3 and ζ) that form the TCR complex (Campbell et al., 1994). Both α- and β-chains have C-terminal cytoplasmic tails that are 5 to 12 amino acids long, but do not contribute to TCR signal-transduction.

A small population of T cells, so called γ/δ-T cells, carry a TCR composed of a γ- and a δ-chain. These chains are very similar to α- and β-chains regarding all structural aspects. However, the variability between different γ/δ-TCRs seems to be reduced as compared to α/β-TCRs, suggesting that the ligands for these receptors are invariant and conserved (Hayday, 2000).

1.5 T CELL DEVELOPMENT

The major site of T cell maturation is the thymus, which provides a special microenvironment. T cell maturation follows sequential stages consisting of somatic recombination and expression of TCR genes, cell proliferation, antigen-induced selection, and acquisition of mature phenotypes and functional capabilities (Fig. 2).

T lymphocytes originate from precursor cells that arise in the fetal liver and adult bone marrow and seed the thymus. Developing T cells in the thymus are called thymocytes. They are found in the subcapsular sinus and outer cortical region of the thymus. From here the thymocytes migrate into and through the cortex, where most of the subsequent maturation events occur. As the thymocytes undergo the final stages of maturation, they migrate to the medulla and then exit the thymus through the circulation. Many of the stimuli that are required for these steps come from cells in the thymus. These include thymic epithelial cells, bone-marrow derived macrophages and dendritic cells, providing MHC molecules, that are important for the selection of the mature T cell repertoire, and also cytokines like IL-7, which are important for the proliferation and survival of immature T cells (Abbas, 2003).

The genes encoding the TCR α- and β-chain are encoded in separate loci. Each germline TCR locus includes V and J, in the case of the β-chain V, D and J, gene segments. At the 5′ end of the locus, there is a cluster of several V gene segments (≈50). At varying distances 3′ of the TCR V genes are the TCR C genes (two for β, one for α). Between the V and C genes, there are several J segments, and also D segments in case of the β-chain. Each TCR C gene segment has its own cluster of J (and D) segments. The process of somatic recombination

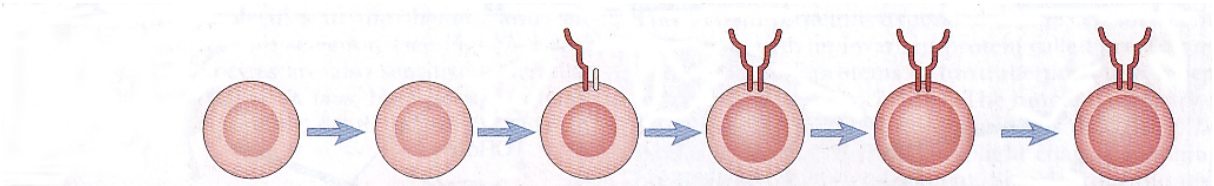

Stage of maturation	Stem cell	Pro-T	Pre-T	Double positive	Single positive (immature T cell)	Naive mature T cell
Proliferation						
RAG expression						
TdT expression						
TCR DNA, RNA	Unrecombined (germline) DNA	Unrecombined (germline) DNA	Recombined β chain gene [V(D)J-C]; β chain mRNA	Recombined β, α chain genes [V(D)J-C]; β and α chain mRNA	Recombined β, α chain genes [V(D)J-C]; β and α chain mRNA	Recombined β, α chain genes [V(D)J-C]; β and α chain mRNA
TCR expression	None	None	Pre-T receptor (β chain/pre-T α)	Membrane αβ TCR	Membrane αβ TCR	Membrane αβ TCR
Surface markers	c-*kit*$^+$ CD44$^+$ CD25$^-$	c-*kit*$^+$ CD44$^+$ CD25$^+$	c-*kit*$^+$ CD44$^+$ CD25$^+$	CD4$^+$CD8$^+$ TCR/CD3^{lo}	CD4$^+$CD8$^-$ or CD4$^-$CD8$^+$ TCR/CD3^{hi}	CD4$^+$CD8$^-$ or CD4$^-$CD8$^+$ TCR/CD3^{hi}
Anatomic site	Bone marrow	Thymus				Periphery
Response to antigen	None	None	None	Positive and negative selection	Negative selection	Activation (proliferation and differentiation)

Fig. 2 *Stages of T cell maturation. Events corresponding to each stage of T cell maturation from a bone marrow stem cell to a mature T cell are illustrated. (Abbas, 2003)*

involves selecting one V, one J and one D gene (when present) in each developing T cell and bringing these gene segments together to form a single V(D)J gene that will encode for the variable region of a TCR chain. The C segment remains separate from the V(D)J gene in the DNA and in the primary RNA transcript. The primary transcript is then processed so that the V(D)J gene becomes contiguous with the C gene, forming an mRNA that is translated to produce one of the TCR chains. Different T cell clones use different combinations of V, (D) and J genes. In addition, during V(D)J recombination nucleotides are added or removed from the joint regions. These processes generate the huge diversity of different TCRs. The region of the greatest variability is at the site of V(D)J recombination, the region that forms the third hypervariable region or CDR3 in the completed TCR chain. The enzymes involved in these processes are collectively called V(D)J recombinase. They include the RAG-1 and RAG-2 recombinases, the DNA-dependent protein kinase and the terminal deoxynucleotidyl transferase (TdT) (Abbas, 2003).

The most immature thymocytes contain TCR genes in their germline configuration and do not express TCR, CD3, ζ chain or CD4 or CD8. These cells are called double-negative thymocytes, and the stage of maturation is called the pro-T cell stage. The majority of double-negative thymocytes will ultimately give rise to αβ TCR-expressing, MHC-restricted $CD4^+$ or $CD8^+$ T cells. RAG-1 and RAG-2 are first expressed at this stage, and D_β to J_β rearrangements occur. The next stage of maturation is called the pre-T cell stage, where V_β to DJ_β rearrangements occur. The DNA segments between the rearranged elements are deleted during this process. The primary transcript of the TCR β gene is 3′ polyadenylated, and noncoding regions between VDJ and C are spliced out. Translation of this mRNA gives rise to a full-length C_β protein. This protein is expressed on the cell surface in association with an invariant protein called pre-Tα and with ζ and CD3 to form the pre-T cell receptor. Signals from this pre-TCR stimulate proliferation of the pre-T cells, recombination of the α-chain locus, transition from the double-negative to the double-positive stage (see later) and inhibit further β-chain rearrangements. This latter process ensures that mature T cells express only one β-chain allele. At the next stage of T cell maturation, thymocytes express both CD4 and CD8. Rearrangement of the TCR α-chain occurs in this double-positive stage very similar to β-chain rearrangement. Because there are no D segments, only V and J segments are joined. The large number of J_α segments permits multiple attempts at productive V-J joining on each chromosome, increasing the probability that a functional αβ TCR will be produced. Unlike in the β-chain locus, there is no allelic exclusion in the α-chain locus. Therefore, productive

rearrangements may occur on both chromosomes, and if this happens, the T cell will express two different α-chains. In fact, up to 30% of mature peripheral T cells express two different TCRs, with different α-chains but the same β-chain. In both the α- and β-chain loci, if productive rearrangements fail to occur, the thymocyte will die by apoptosis.

TCR α-chain expression in the double-positive stage leads to the formation of the complete αβ TCR in association with CD3 and ζ chain. The expression of RAG genes and further TCR gene recombination ceases after this stage of maturation. By virtue of their expression of complete TCR complexes, double-positive cells become responsive to antigens and are subjected to positive and negative selection (Abbas, 2003).

The selection of developing T cells is stimulated by recognition of antigen (peptide-loaded MHCs) in the thymus, and is responsible for preserving useful cells and eliminating useless or potentially harmful ones (Fig. 3). The immature T cell repertoire consists of cells that may recognize any peptide antigen (self or foreign) displayed by any MHC (self or foreign). In addition, receptors may be expressed that do not recognize any pMHC complex at all. The only useful cells are those that recognize foreign peptide displayed by self MHC molecules.

T cells now receive indispensable survival signals through weak interactions with self-MHC molecules of thymic epithelial cells and thymic antigen-presenting cells. These interactions are a prerequisite for antigen recognition in the periphery, because antigen is always presented in the context of self-MHC. Lack of these survival signals leads to apoptosis, a process that is called positive selection. This ensures, that all mature T cells are self-MHC restricted. Positive selection also fixes the MHC class I or class II restriction, ensuring that $CD8^+$ T cells are specific for peptides displayed by MHC I and $CD4^+$ T cells specific for peptides displayed by MHC II.

T cells that cannot interact with self-MHC molecules at all also go into apoptosis ("death by neglect"), as well as T cells that have a very high affinity for self-MHC, because these cells are potential autoreactive cells. The latter process is called negative selection. The net result of these selection processes is that the repertoire of mature T cells that leave the thymus is self-MHC restricted and tolerant to self-antigens (Jameson et al., 1995; Sprent and Kishimoto, 2002; Zinkernagel and Doherty, 1974).

After selection in the thymus, the mature T cells are released into the blood and lymphatic system. They circulate here as naïve T cells until a possible antigen contact. Only through antigen contact, naïve T cells develop into effector T cells and take part in an adaptive immune response. Very few T cells from the naïve repertoire can react to a given

antigen in a highly specific manner, expand clonally and generate an efficient effector response and immunological memory.

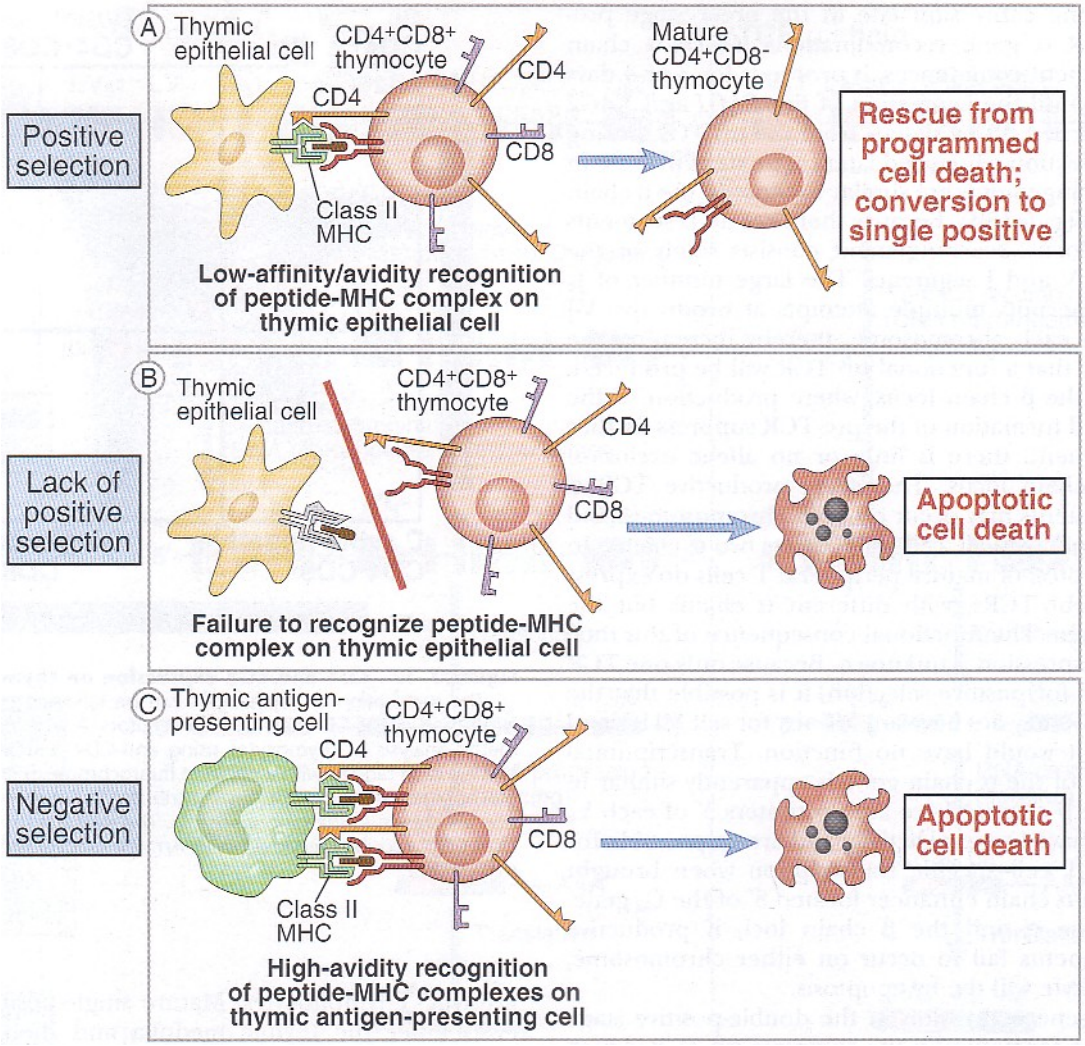

Fig. 3 *Positive and negative selection in the thymus. If during positive selection a developing T cell interacts weakly with self-MHC molecules it is rescued from apoptosis (A, B). T cells that have a too high affinity for self-MHC are deleted by apoptosis during negative selection (Abbas, 2003).*

1.6 T CELL RECEPTOR – LIGAND INTERACTIONS

During the last years, more than a half-dozen of complexes between αβ TCR and pMHC complexes have been visualized by X-ray crystallography (Fig. 4) (Hennecke and Wiley, 2001; Rudolph et al., 2006). These molecular complexes precisely describe the common recognition component of cell-cell encounters that activate T cells both during the development and effector stages.

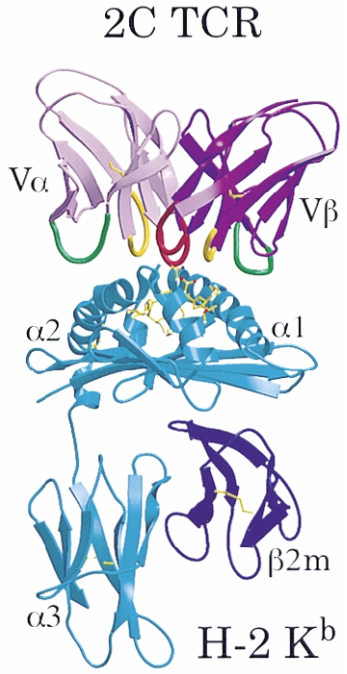

Fig. 4 *Structure of the 2C TCR binding to H2-K^b. Only the V domains of the TCR (Vα/Vβ) are shown. α1/α2/α3, α-domains of H2-K^b; β2m, β2-microglobuline; CDR1, yellow; CDR2, green; CDR3, red (Bjorkman, 1997; Garcia et al., 1996).*

The TCR is a hypervariable molecule that can bind to short peptides from antigens that are presented on the cell surface of other cells by MHC class I or class II molecules. Even though some induced fitting has been observed at the TCR interface upon pMHC binding, no global conformational changes occur that could currently explain the initiation of TCR signaling. All TCRs studied have found that pMHC complexes bind in a similar way, positioned across the pMHC surface at an angle between 45° and 80° (Hennecke and Wiley, 2001). The hypervariable complementarity determining regions (CDRs) of the TCR recognize the composite antigenic surface made of the margins of the MHC molecules peptide-binding cleft and the bound peptide. The CDR2 loops of α and β contact only the MHC molecule, while CDR1 and CDR3 contact both peptide and MHC (Fig. 5). The V_α domain of the TCR is always closer to the N-terminal end of the bound peptide, and the V_β domain closer to the C-terminal end. The surface of the TCR is relatively flat, sometimes with a central cavity. In contrast, the MHC surface contains two elevations. To achieve a large surface, the TCR binds between these two highpoints on the pMHC surface (Bjorkman, 1997).

Of the 31 MHC amino acid positions forming contact points in at least one of the known TCR/pMHC structures, only about 50% of those are contacted simultaneously in each complex. Even contacts to the same pMHC complex by two different TCRs can share as few as only one conserved atomic interaction (Ding et al., 1998; Garboczi et al., 1996). Which of these residues are contacted depends on global parameters like the twist, tilt, and shift of the TCR over the pMHC surface (Teng et al., 1998), the different angles found between the V_α

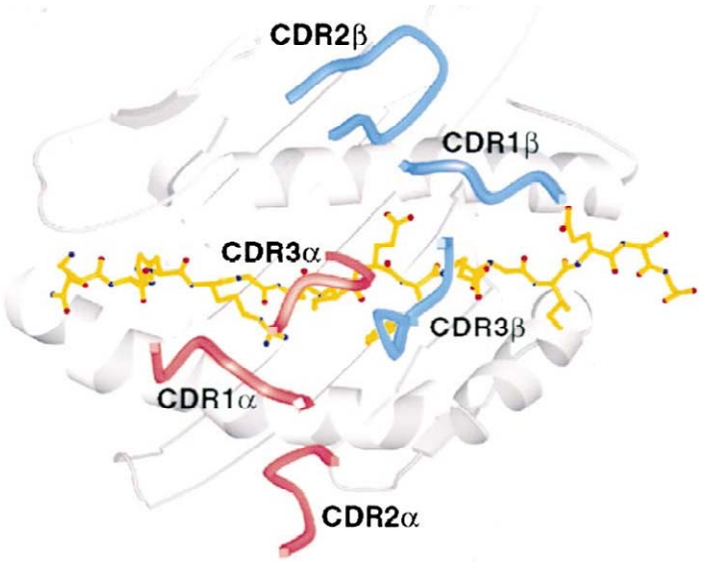

Fig. 5 *CDR placement over the pMHC molecule. CDR2 only contacts the MHC, while CDR1 and CDR3 contact the MHC plus the peptide (Hennecke and Wiley, 2001).*

and V_β domains, and the conformation and length of the CDR loops. At present, there is no simple means for predicting these global parameters or the details of binding from the sequence of a TCR and the pMHC antigen. The lack of conserved contacts between TCRs and the conserved residues on the MHC molecules poses the question how TCRs can bind similarly if contacts are not conserved. Because there are many conserved MHC residues and about 50 V_α and V_β genes, the binding mode might have been preserved by a combinatorial mechanism where different TCRs contact a different subset of MHC residues (Hennecke and Wiley, 2001). However, even TCRs with identical CDR1 and CDR2 loops in one V domain can interact very differently with MHC molecules (Ding et al., 1998; Garcia et al., 1998; Teng et al., 1998). An alternative is that the co-evolution of TCRs with MHC molecules has only selected for TCRs that can initiate a signal (e.g. during positive selection). Any binding mode consistent with signaling would have been preserved, irrespective of the conservation of particular atomic contacts (Hennecke and Wiley, 2001). Indeed, it has been shown very recently, that to escape negative selection, TCRs have to interact with many of the side chains of pMHC complexes as "hot spots" for TCR binding. Moreover, even when a side-chain did not contribute to binding affinity, some pMHC residues contributed to TCR specificity, as amino acid substitutions substantially reduced binding affinity. The presence of such "interface-disruptive" side chains helps to explain how TCRs generate specificity at low-affinity interfaces (Huseby et al., 2006).

Only one-third of the surface of peptides bound to MHC molecules is available to be recognized by contacts to a TCR. In some cases a relatively flat surface of a TCR contacts the projecting side-chains from a bound peptide (Hennecke et al., 2000), in other cases the central

peptide residue is completely surrounded by a deep pocket in the TCR surface formed primarily by the two CDR3 loops (Fig. 6) (Garboczi et al., 1996). The number of contacts

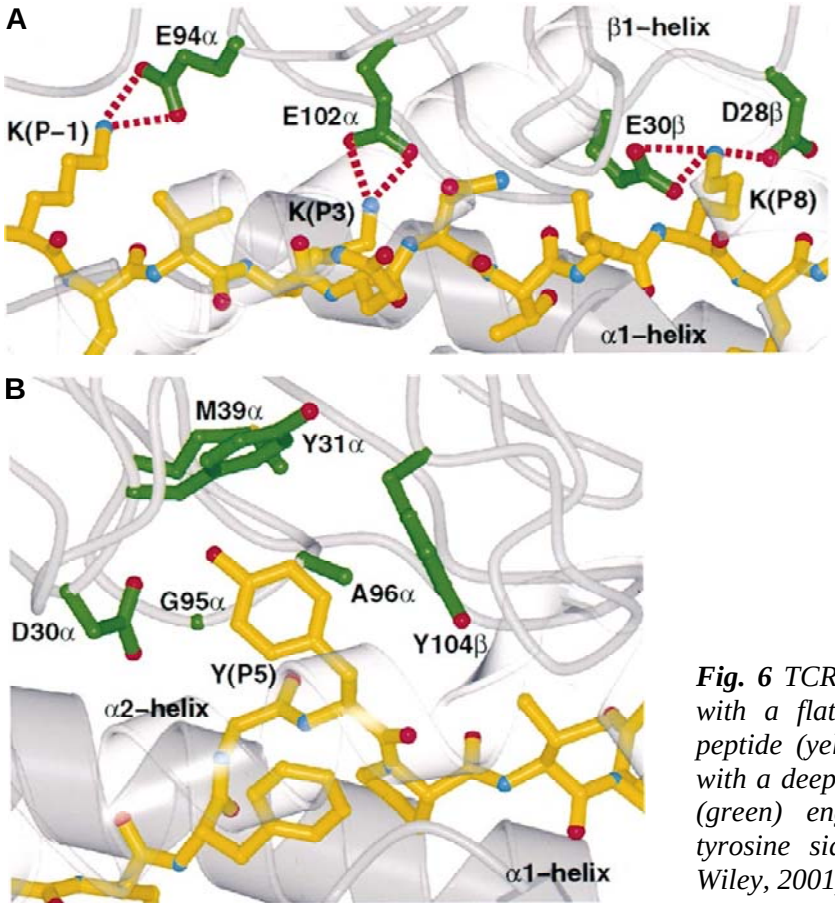

Fig. 6 *TCR – pMHC interfaces. A TCR with a flat surface (green) contacting peptide (yellow) sidechains (A). A TCR with a deep pocket between CDR3 loops (green) engulfing a peptide (yellow) tyrosine sidechain (B) (Hennecke and Wiley, 2001).*

between TCR and peptide is limited, suggesting that cross-reactivity in which more than one peptide can fit between a given TCR/MHC pair will occur. Although in cross-reactions different peptides can generate the same activation signal, in other cases TCR signaling can be very sensitive and specific to the peptide sequence. Single amino acid substitutions in peptides can convert a strong agonist pMHC ligand into a weak agonist or even an antagonist. Such peptides are called altered peptide ligands (APL) (Sloan-Lancaster and Allen, 1996). One structural study of three TCR/MHC/APL complexes showed that some amino acid substitutions could be accommodated by very minor readjustments in the TCR/peptide interface (induced fit), which did not propagate to the outer TCR surface (Ding et al., 1999). Furthermore, there was no correlation between these minor structural refittings and signaling outcome. A comparison of the structures of a weak and a strong agonist peptide also showed only minor adjustments in the TCR/pMHC interface (Degano et al., 2000). This lack of correlation between the structure and the signal generated is consistent with the hypothesis

that different signals are caused by different affinities and/or duration of TCR binding (Davis et al., 1998), not different conformations of the TCR/pMHC complex.

The affinities of the TCR to the pMHC are substantially weaker than those of antibody/antigen complexes, and are usually in the low micromolar range (Karjalainen, 1994; Matsui et al., 1991) (see next chapter for a detailed discussion of TCR avidity). Because of this, the TCR has the problem of achieving sufficient antigen specificity from the small structural differences that result from the peptide binding to the highly conserved surface of the MHC. The dominance of the MHC helices in the recognition of pMHC has been supported by an alanine scan of the 2C TCR against its alloligand H2-L^d/QL9 (Manning et al., 1998). Here, 42 single-site alanine substitutions of the 2C TCR were performed and analyzed for binding to H2-L^d/QL9 to provide an energy map of TCR recognition. From this alanine scan, the interaction surface was found to be relatively flat in energetics in that most of the TCR contact residues contributed roughly equal energies, with the total interaction energy being distributed over the entire surface area (Manning et al., 1998). These data support a "scanning" model in which there exists enough binding energy between the MHC and TCR to enable the TCR to dock on the pMHC complex and read out the peptide contents (Matsui et al., 1991; Valitutti et al., 1995). Those peptides that contribute a sufficient number of energetically favorable contacts with the TCR can provide the slight amount of additional kinetic stabilization required for signaling to occur (Valitutti et al., 1995).

In addition to their cognate TCRs, class I and class II MHCs are recognized by their respective coreceptors CD8 and CD4. The current database for CD8 coreceptor structures consists of human CD8αα/HLA-A2 (Gao et al., 1997), murine CD8αα/H2-K^b (Fig. 7) (Kern et al., 1998) and murine CD8αα/TL (Liu et al., 2003). In all complexes, the CD8αα homodimer binds primarily to the α_3 domain of the MHC molecule in an antibody-like fashion. The structure and conformation of the C-terminal stalk region of CD8, which connects the coreceptor to the T cell surface are still unclear (Rudolph et al., 2006). The determination of a crystal structure of the CD8αβ heterodimer has been elusive. This heterodimer is not simply a functional homolog of the CD8αα homodimer, as CD8αβ is the true TCR coreceptor, whereas the main function of CD8αα on intraepithelial lymphocytes is to aid in adaptation and survival in the gut (Gangadharan and Cheroutre, 2004). The crystal structure of CD4 bound to I-A^k shows how the analogous coreceptor interaction is achieved in the MHC class II system (Wang et al., 2001). Whereas both domains of CD8 cooperate to bind to class I MHCs, only one domain of CD4 makes contact with the MHC. Comparison of the CD4/MHC and CD8/MHC structures exposes a surprising structural difference of the

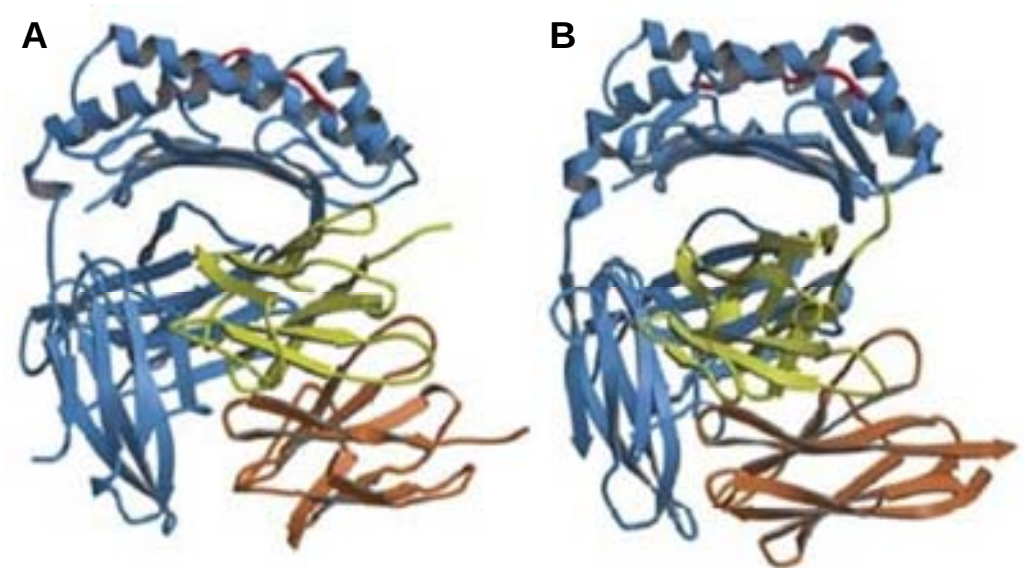

Fig. 7 *Structure of CD8αα homodimers (orange, yellow) binding to MHC I (blue). HLA-A2/hCD8aa (A). H2-K^b/mCD8αα (B). The CD8 stalk region is not shown. (Rudolph et al., 2006)*

MHC class I and class II architectures, implying profoundly different modes of organization in their respective immunological synapses (Rudolph et al., 2006).

1.7 ASSESSING T CELL AVIDITY

T cell avidity is a term that is often used in an ambiguous manner. It can be defined by functional readout systems, or as a function of T cell receptor structure and the properties of the physical interactions of the TCR and its coreceptor to their ligand pMHC.

Functional T cell avidity describes how sensitive a given T cell can detect its cognate antigen. In other words, a T cell that can detect low amounts of antigen and responds to it with activation and/or exertion of effector functions has a higher functional avidity than a T cell that needs higher amounts of antigen for the same effects (Alexander-Miller, 2005). T cells with high functional avidity have been shown to be superior regarding their *in vivo* efficacy in both viral and tumor models (Alexander-Miller et al., 1996; Dutoit et al., 2001; Sedlik et al., 2000; Yee et al., 1999; Zeh et al., 1999). There have been two mechanisms described by which T cells with high functional avidity promote increased viral clearance. First, they recognize virally infected cells at earlier time-points postinfection compared to low-avidity cells. Second, high-avidity $CD8^+$ T cells have the ability to lyse target cells with more rapid kinetics than low-avidity cells (Derby et al., 2001). The mechanisms that regulate

functional T cell avidity are manifold. They include the expression of adhesion molecules, coreceptors, and components of the T cell receptor signaling cascade. For example, analysis of CD8 coreceptor expression demonstrated that differences in functional avidity correlated with the increased expression of CD8αβ heterodimers versus CD8αα homodimers on high-avidity T cells, which promoted the increased colocalization of CD8 with the TCR (Cawthon and Alexander-Miller, 2002; Cawthon et al., 2001). In addition to CD8, other molecules certainly have the potential to impact functional avidity. These include cell-surface molecules, like LFA-1 or the TCR, as well as intracellular signaling molecules like ZAP-70 or Lck. In addition to the expression level of cell-surface molecules or components of the signal transduction cascade, the ability to localize these molecules at the contact region of the T cell with the APC is of crucial importance to the outcome of APC engagement. In this sense, high functional avidity can be determined by the optimal membrane localization of cell-surface molecules, which is mediated by compartmentalization into lipid rafts (Cawthon and Alexander-Miller, 2002). Functional T cell avidity is most often determined *in vitro* by stimulating T cells with APC that are pulsed with graded concentrations of peptide antigen and measuring T cell effector functions like IFN-γ production or lysis of peptide-pulsed target cells (Alexander-Miller et al., 1996) (see 1.7.1). The extent to which high and low functional avidity cells can be distinguished by properties other than peptide sensitivity, e.g. dependence of cytokines or costimulatory or adhesion molecules, remains largely undefined.

Structural T cell avidity is defined by the combined affinities of the CD8 or CD4 coreceptor and the T cell receptor to the peptide-loaded MHC molecule. It is an invariant parameter dependent on electrostatic forces, hydrogen bonds, van der Waals forces and hydrophobic interactions between the protein surfaces. To what extent structural T cell avidity determines the functional avidity of a cell has been discussed for a long time. However, the question has never been conclusively resolved, because until now, there was no exact method available to measure this parameter on living T cells (see 1.7.2). Nevertheless, several groups have tried to assess structural T cell avidity. Using conventional MHC tetramer-based techniques, it could be shown that TCR avidity plays an important role during T cell selection, where only T cells showing TCR avidities lying in an intermediate range are allowed to mature (Savage and Davis, 2001). In a *Listeria monocytogenes* infection model, it was shown that the dissociation rate of MHC tetramers was slower in cells from a secondary response when compared to the primary response (Busch and Pamer, 1999). A correlation between MHC tetramer staining intensity and the ability to lyse tumor cells was seen in melanoma-specific $CD8^+$ T cells (Yee et al., 1999). However, no correlation between tetramer binding

and functional avidity was seen by others (al-Ramadi et al., 1995; Echchakir et al., 2002; Palermo et al., 2001). Therefore, interpretations of MHC tetramer-based experiments for the assessment of structural T cell avidity should be taken with caution, since TCR avidity does not necessarily have to be responsible for differences in tetramer binding. The multimeric nature of tetramers allows for the possibility that factors other than TCR avidity control the level and dissociation rate of binding. For example, changes in the organization of the TCR in the cell membrane have been shown to alter tetramer binding (Drake and Braciale, 2001; Fahmy et al., 2001).

1.7.1 Functional T cell assays

1.7.1.1 ELISPOT assay

The so called ELISPOT assay (Miyahira et al., 1995) is a method to detect antigen-specific T cells directly *ex vivo*. It can also be used to determine the functional avidity of T cells.

The cells are detected via the secretion of certain cytokines, for example IFN-γ. Antibodies against the cytokine are bound to a surface, which is then covered with cells. After antigen-specific stimulation for 10-16 h the cells produce cytokines, which bind to the antibodies in their immediate proximity. The cells are washed away, and a second, labeled antibody against the cytokine is added. This allows the visualization of spots where cytokine-secreting cells were located. When titrating the amount of peptide used for stimulation, functional avidity can be determined by correlating the amount of cells that reacted with cytokine production to the amount of peptide used. The ELISPOT assay is a T cell function-dependent assay, since only cells that can react with cytokine production to *in vitro* stimulation can be detected.

Using this assay, it could be shown that the functional avidity of T cells is not a constant parameter, but is influenced by past antigen encounters of the cells (Hesse et al., 2001). Another group used a modified single-cell ELISPOT assay system to investigate the frequencies and functional avidities of T cells in a murine model of multiple sclerosis (Hofstetter et al., 2005).

1.7.1.2 Intracellular cytokine staining

The intracellular cytokine staining (ICCS) is a method that allows the detection of antigen-specific T cells after fixation and permeabilization via the staining of intracellular cytokines (Prussin and Metcalfe, 1995). The target cells are stimulated in an antigen-specific manner to induce cytokine production. After two hours the cells are treated with brefeldin A to block the transport of cytokines out of the Golgi apparatus. This leads to an enrichment of cytokines in the stimulated T cells. After additional 3 h of stimulation, the cells can be stained with fluorescence-labeled surface antibodies, fixed, permeabilized and then stained intracellularly with fluorescence-labeled antibodies against the cytokine of interest. After the staining procedure, the cells are analyzed by flow cytometry. Again, when titrating the amount of peptide used for stimulation, functional avidity can be determined by correlating the amount of cells that reacted with cytokine production to the amount of peptide used. The peptide concentration that is needed to stimulate IFN-γ production in 50% of the cells is normally defined as IC_{50} and serves as a quantitative parameter of functional avidity.

The detection of cytokine production in response to titrated peptide stimuli has been widely used to quantify the functional avidity of T cells. For example, several groups have tried to correlate functional avidity, as determined with this assay, to structural TCR avidity using MHC tetramers (Slifka and Whitton, 2001) or surface plasmon resonance measurements (al-Ramadi et al., 1995) (see 1.7.2). In both cases it could be shown that, while there was a certain correlation between functional and structural avidity in many cases, T cells seem to undergo also extensive functional maturation during the early stages of an infection, possibly due to the optimization of the signal transduction machinery (Slifka and Whitton, 2001). However, the data for structural TCR avidity in these studies have to be interpreted with caution, since both tetramer-based avidity assays and surface plasmon resonance measurements have inherent limitations and disadvantages that can easily lead to misinterpretations and false conclusions (see 1.7.2).

1.7.1.3 ^{51}Chromium release assay

The ^{51}Cr release assay is a method to detect antigen-specific T cells via their ability to lyse peptide-loaded target cells (Brunner et al., 1968). The target cells are labeled with the γ-radiating isotope ^{51}Cr and loaded with peptide. Defined amounts of target and effector cells

are incubated together for 4-5 h, which leads to lysis of the target cells and release of ^{51}Cr into the supernatant. The amount of released radioactivity is measured and correlates to the extent and efficiency of killing by the T cells. When titrating the peptide used to load the target cells, functional avidity of the effector cells can be defined as that amount of peptide that leads to 50% specific lysis of the target cells.

The ^{51}Cr release assay has also been widely used to quantify the functional avidity of T cells. It could been shown with this assay for example that the amount of peptide that is used to elicit cytotoxic T cells inversely correlates with the functional avidity of those cells (Alexander-Miller et al., 1996), an important finding for the development of effective adoptive cellular immunotherapy. In the *Listeria monocytogenes* infection model it was shown that the functional avidity of antigen-specific T cells is higher in a secondary infection compared to a primary infection, and that this correlated with an increase in TCR affinity in recall populations due to a focusing of the TCR repertoire (Busch and Pamer, 1999).

1.7.2 Measuring structural avidity

1.7.2.1 MHC tetramer-based techniques

Tetrameric complexes of peptide-loaded MHC molecules (MHC tetramers) are able to stably bind to T cells via the T cell receptor in an antigen-specific manner (Altman et al., 1996). They are therefore potential reagents for the analysis of the structural binding avidity of the TCR. Two types of MHC tetramer-based techniques have been introduced to assess T cell avidity (Wang and Altman, 2003). In the first type of experiment, several groups have shown a correlation between MHC tetramer staining intensity and T cell avidity (Crawford et al., 1998; Dutoit et al., 2001; Fahmy et al., 2001; Rees et al., 1999; Yee et al., 1999). In contrast, other investigators have used tetramer dissociation kinetics to characterize differences in T cell avidities (Amrani et al., 2000; Blattman et al., 2002; Busch and Pamer, 1999; Dutoit et al., 2002; Rubio-Godoy et al., 2001; Savage et al., 1999; Valmori et al., 2002).

The determination of MHC tetramer staining intensities is a straightforward experimental procedure with relatively few complicating variables. However, a missing correlation between tetramer staining intensity and T cell avidity has been found by several investigators, questioning this readout as a reliable measure for T cell avidity (al-Ramadi et al., 1995; Echchakir et al., 2002; Lawson et al., 2001; Palermo et al., 2001).

Regarding MHC tetramer dissociation experiments, there is a considerable variation in the way these experiments have been performed. The principle variable that distinguishes the methods used is whether specific reagents are used to block rebinding of labeled MHC tetramers during the dissociation phase of the experiment, and if so, what is the nature of the blocking reagent. Several options have been used: No blocking reagents (Busch and Pamer, 1999; Rubio-Godoy et al., 2001), intact anti-MHC antibodies (Amrani et al., 2000; Savage et al., 1999), unlabeled MHC tetramers (Dutoit et al., 2002; Valmori et al., 2002) and Fab fragments (Blattman et al., 2002). One problem when using normal anti-MHC antibodies to block rebinding of MHC tetramer is that bivalent antibodies might crosslink tetramers together, or crosslink tetramers to MHC molecules on the surface of the labeled cell. Using monovalent Fab fragments or forgoing blockade of rebinding altogether can solve these problems, however tetramer dissociation without a blocking agent is very slow or even not detectable at all in some cases (Wang and Altman, 2003).

Furthermore, the first three of the described methods can potentially generate artifacts, since the tetramer dissociation kinetics are not independent of the concentration of the reagents used to block rebinding of the labeled tetramer. This proves that the tetramer dissociation seen in these experiments results from the tetramer dissociation rate and the rate of association of the blocking agent with the free tetramers, resulting in multifactorial and hard to interpret tetramer dissociation kinetics. Since this problem was not observed when using Fab fragments in high concentrations, these seem to be the more appropriate blocking reagents for tetramer dissociation experiments (Wang and Altman, 2003).

One further caution in the interpretation of tetramer-based experiments for the determination of the structural component of T cell avidity is that the underlying assumption that TCR affinity is responsible for differences in tetramer binding might be wrong. The multimeric nature of MHC tetramers allows for the possibility that factors other than TCR affinity control the level and dissociation rate of binding (Alexander-Miller, 2005). It has been shown for example that changes in the organization of the TCR in the membrane can alter MHC tetramer binding (Drake and Braciale, 2001; Fahmy et al., 2001).

All in all, the multimeric nature of MHC tetramers alone makes the results obtained with tetramer-based TCR avidity studies very difficult to interpret. The dissociation of MHC tetramers from a T cell is likely to proceed through multiple steps. The first step does not result in decreased fluorescence on the cell but only represents dissociation of one of the four “arms” of the tetramer. This step is reversible, and the MHC might rebind to the cell. The difficulty is that since the tetramer is still bound to the T cell through other attachment points,

the effective local concentration of the newly dissociated MHC subunit is extremely high (Wang and Altman, 2003). This effect might lead to quite complicated higher order dissociation kinetics. Although some reports claim that MHC tetramer dissociation follows first order kinetics (Amrani et al., 2000; Savage et al., 1999; Savage and Davis, 2001), others have reported more complicated higher order dissociation kinetics, especially when blocking tetramer rebinding (Wang and Altman, 2003). This leaves the need for an improved assay system for TCR avidity measurements, ideally using monomeric pMHC – TCR interactions.

1.7.2.2 Surface plasmon resonance

Surface plasmon resonance (SPR) is an optical phenomenon that allows the real-time analysis of biospecific interactions using biosensors (Fagerstam et al., 1992; Liedberg et al., 1983). The phenomenon arises in connection with total internal reflection of light at a metal film-liquid interface. Normally, light traveling through an optically denser medium, for example a glass prism, is totally reflected back into the prism when reaching an interface to an optically less dense medium, for example a buffer. A component of the light called the evanescent wave penetrates a distance of the order of one wavelength into the buffer. If the light is polarized and monochromatic and the interface is coated with a thin metal film, the evanescent wave will interact with free oscillating electrons (plasmons) in the metal film surface under certain conditions. When surface plasmon resonance occurs, light energy is lost to the metal film and the reflected light intensity is decreased. The resonance phenomenon will only occur for light incident at a sharply defined angle which, when all else is kept constant, is dependent on the refractive index in the buffer close to the surface. Changes in the refractive index out to about 1 μm from the metal film surface can thus be followed by continuous monitoring of the resonance angle. The biospecific interface is a sensor chip where the metal film is covered with a hydrogel matrix. One component of the interaction to be studied is immobilized covalently to the hydrogel and the other interactant is passed over the chip in solution. The changes of the refractive index at the sensor surface, reflecting the progress of the interaction studied, are monitored in real-time (Fig. 8 A) (Fagerstam et al., 1992).

The most widely used technical implementation of these principles is the Biacore system. The instrument consists of a processing unit, reagents for ligand immobilization, exchangeable sensor chips and a computer for control and data analysis. The processing unit

contains the SPR monitor and an integrated microfluidic cartridge that, together with an autosampler, controls the delivery of sample plugs into a transport buffer that passes continuously over the sensor chip surface (Fig. 8 B).

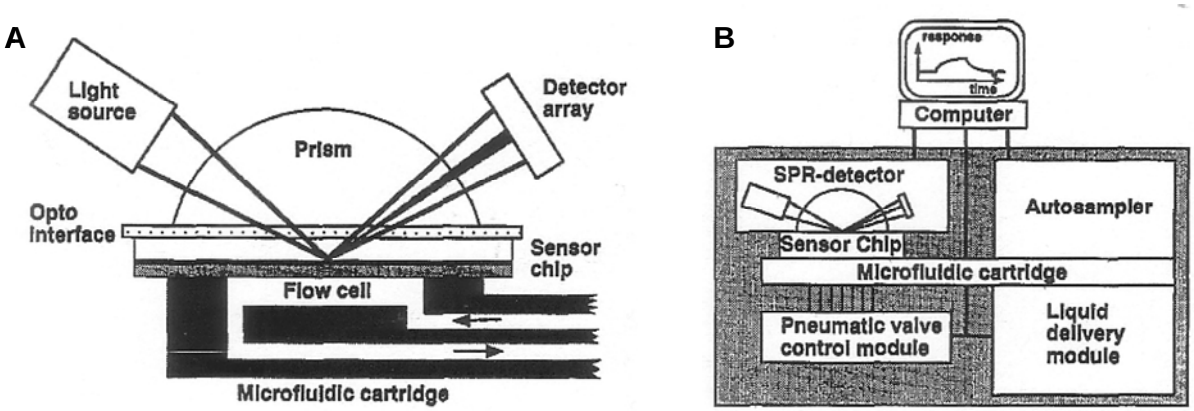

Fig. 8 *Surface plasmon resonance. SPR detector, sensor chip and flow cell are shown. Light is coupled to the chip via a prism. The resonance angle is monitored continuously by a photodiode array (A). The processing unit of a Biacore machine containing the SPR detector and an integrated microfluidic cartridge that, together with an autosampler, controls the delivery of the sample to the sensor chip surface (B) (Fagerstam et al., 1992).*

By continuously monitoring the refractive index and plotting this value against time a so called sensorgram is obtained. Here, time is plotted against so called resonance units (RU); 1000 RU correspond to a 0.1° shift in the SPR angle, which for an average protein corresponds to a surface concentration change of about 1 ng/mm^2 (Fagerstam et al., 1992). This results in a remarkable sensitivity to weak macromolecular interactions. Mathematical analysis of the sensorgram allows the calculation of the on- and off-rates and thus of a K_d value for the interaction studied.

Since the first application of SPR for biosensing more than 20 years ago (Liedberg et al., 1983), the method has been constantly improved and used for the analysis of a wide spectrum of biomolecular interactions, including measurements to quantify T cell receptors in interaction with syngenic or allogenic ligands. One of the most extensively characterized T cell receptors is the 2C TCR. Consequently, the earliest studies done using SPR analysis of TCR-pMHC interactions used this receptor. Half-life times for the dissociation of the 2C TCR and its allogenic ligand H2-L^d/p2Ca were found to be lying in the range of about 30 seconds, with an equilibrium K_d of about 10^{-7} M (Corr et al., 1994). Similar studies analyzing the binding of the 2C TCR to its syngenic ligand H2-K^b/dEV8 and syngenic derivatives thereof showed K_d values of 10^{-4} M to 10^{-6} M (Garcia et al., 1997). When substituting single amino acids of the p2Ca peptide, SPR analysis of the 2C TCR binding to these altered L^d/p2Ca ligands revealed a good correlation between TCR affinity and T cell function as measured by

intracellular cytokine staining in most cases. There was however one remarkable exception to this correlation, indicating that TCR affinity is not always a single critical determinant of T cell activation (al-Ramadi et al., 1995). SPR studies have also been done to find differences in the binding of T cell receptors to agonist and antagonist ligands. These studies could show that agonist ligands are bound with higher affinity, and thus slower dissociation rates, than antagonist ligands (Alam et al., 1999; Lyons et al., 1996). During selection in the thymus, T cells have to recognize self-MHC molecules to be rescued from apoptosis (positive selection), but are sent into apoptosis at a later stage if they recognize self-peptides in the context of self-MHC (negative selection). Using positively and negatively selecting ligands in SPR measurements, it could be shown that there exists a window of affinity for selection, with T cells lying below this window being deleted during positive selection, and cells lying above this window being deleted during negative selection (Alam et al., 1996). These results could later be confirmed by a group using MHC tetramer dissociation as a measure of TCR affinity (Savage and Davis, 2001).

Although some very important findings have been made using SPR measurements to determine TCR affinity, the method suffers from several drawbacks. For every interaction to be analyzed, not only the pMHC has to be generated recombinantly, but also each individual TCR. Expression of active soluble forms of TCR has been solved in a variety of ways, including replacing the transmembrane regions with signal sequences for glycolipid linkage (Lin et al., 1990), deleting the transmembrane regions (Garcia et al., 1996; Gregoire et al., 1996), cystein mutation and *Escherichia coli* expression (Garboczi et al., 1996), or other methods. Unfortunately, not one method is working for all TCRs, making TCR production difficult and time-consuming. Another difficulty pertains to the data analysis in SPR experiments. Although the measurements are relatively easy to perform, the interpretation of kinetic data can be difficult because of the complexity of diffusion near the immobilized binding partner. It could be shown that under conditions that may apply to many published experimental studies, diffusion within the hydrogel matrix was found to decrease the overall ligand transport significantly. For relatively rapid reactions strong inhomogenities of ligands within the gel occurred before establishment of an equilibrium (Schuck, 1996). If not carefully taken into account, such effects can lead to false conclusions. Last but not least, SPR measurements require a very artificial, unphysiological setting for the molecular interaction, with one binding partner immobilized on a surface, and the other in solution. This differs greatly from the circumstances in a physiological cell-cell interaction, where both binding partners are allowed to move in two dimensions (as opposed to no movement for one, and

movement in three dimensions for the other in the SPR setting) and where coreceptors and complex cell surfaces are involved. Garcia *et al*. examined the enhancement of binding of pMHC complexes with the 2C TCR using an artificial CD8 molecule. They observed an apparent stabilization of the complex, resulting in a half-life time of MHC dissociation of 184 seconds with CD8, and 25 seconds in the absence of CD8 (Garcia et al., 1996).

All in all, although SPR measurements have been a valuable tool in the past, there is still a need for a fast and easy assay system for the determination of TCR affinities, especially since the very complex setting of a living cell surface can not be modeled in the currently available SPR systems.

1.8 T CELL THERAPY

Provided they can recognize an antigen in the context of MHC class I on a given target cell, most so-called "cytotoxic T cells" have the inherent ability to lyse target cells with high efficiency. Therefore, $CD8^+$ T cells have been very interesting candidates for a wide range of clinical applications making use of such cells. The *in vitro* activation and expansion of antigen-specific T cells for therapeutic purposes has yielded impressive results in the context of prophylaxis and treatment of virus-associated infection and disease (Leen et al., 2006).

CMV-specific $CD8^+$ T cell clones have been infused into recipients of allogenic hematopoetic stem cell transplants (HSCT). The cells were found to be safe and capable of restoring CMV-specific CTL responses (Walter et al., 1995). Einsele and colleagues (Einsele et al., 2002) infused polyclonal CMV-specific CTL lines into eight HSCT recipients who had persisting or recurring CMV infection despite the prolonged use of antiviral medications. Following T cell therapy, viral load, as determined by quantitative PCR, showed significant reductions in seven of seven evaluable patients. This reduction was persistent in five and transient in two patients. The results of adoptive immunotherapy for the prophylaxis and treatment of EBV-associated post-transplant lymphoproliferative disease (PTLD) were similarly successful. After infusion of donor-derived polyclonal EBV-specific T cell lines into more than 60 HSCT recipients, none of the patients in the prophylaxis group developed PTLD, in contrast to an incidence rate of 11.5% in an untreated control group (Rooney et al., 1995). Analysis of EBV-DNA levels post-infusion showed direct evidence of antiviral activity, as DNA levels decreased up to four logs within three weeks of the first T cell

infusion. Furthermore, adoptively transferred T cells were able to persist and sustain long-term protection against viral reactivation (Heslop et al., 1996).

Thus, adoptive immunotherapy for the prevention and treatment of virus-associated diseases in immunocompromised patients is safe, effective and protective *in vivo*. These successes prompted the extension of this method for the treatment of tumors in immunocompetent individuals. Initial approaches for the treatment of patients with metastatic melanoma by infusion of highly active tumor-specific T cell clones failed to demonstrate engraftment and persistence of the transferred cells (Dudley et al., 2001; Dudley et al., 2002). In the case of EBV-associated Hodgkin´s disease and nasopharyngeal carcinoma, infused EBV-specific CTLs were shown to persist *in vivo*, traffic to tumor-sites, and produce antitumor responses. However, in patients with bulky disease, responses were limited and transient (Bollard et al., 2004; Straathof et al., 2005). Therefore, it appears that the cellular immunity directed against viruses that cause disease in immunocompromised individuals can easily be reconstituted by the transfer of antigen-specific T cells, whereas malignancies that arise in immunocompetent individuals are significantly more complicated to treat.

Tumors have evolved numerous mechanisms to evade both innate and adaptive immunity. These include downregulation of MHC and costimulatory molecules, expression of proapoptotic molecules on the cell surface (Niehans et al., 1997; Song et al., 2001), production of inhibitory factors like TGF-β (Newcom and Gu, 1995) and IL-10 (Suzuki et al., 1995) or the recruitment of regulatory T cells (Marshall et al., 2004). These enable tumor cells to persist and proliferate even in the presence of large numbers of tumor-specific T cells (Rosenberg et al., 2005). Any adoptive immunotherapy protocol must take these factors into consideration and either engineer T cells to make them resistant to tumor evasion strategies or modify the tumor environment to make it less inhibitory to T cell activation and effector function.

With the development of new gene transfer technologies, it is now possible to modify T cells with genes that increase their proliferation, survival, and resistance to tumor-derived inhibitory molecules or that alter their receptor specificity. A first step in this latter approach is the identification of tumor-associated antigens (TAAs) that are ectopically expressed or overexpressed in tumor cells relative to normal tissue (Boon and Old, 1997; Rosenberg, 2001). However, despite aberrant expression of TAAs in tumor cells, many of these proteins are also expressed at some level in nonmalignant tissues (Engelhard et al., 2002). Because of this, the immune system may recognize TAAs as self-antigens and limit the T cell immune response through normal mechanisms of tolerance, including clonal deletion and anergy

(Ochsenbein et al., 1999; Speiser et al., 1997). Because T cells with high avidity for self may be deleted during negative selection, isolated TAA-specific T cells may possess low avidity TCRs and be less effective at killing tumor cells (Teague et al., 2006). This limits the number of TAA-specific T cells that could be isolated from patient blood and affects the ability of TAA-specific T cells to expand *in vitro* following stimulation with cognate antigen. To circumvent these practical limitations, T cells can be genetically modified with receptors capable of specifically recognizing TAAs.

Several investigators have cloned genes that encode TCR α- and β-chains from tumor-reactive T cells found in patients and then introduced them into recipient T cells to endow them with the specificity of the donor TCR (Dembic et al., 1986). This procedure allows the rapid production of antigen-specific T cells by inserting a tumor-specific TCR into bulk T cells. This promising approach has been applied to melanoma antigens (Clay et al., 1999; Morgan et al., 2003; Schaft et al., 2003; Zhao et al., 2005) or common oncoproteins (Cohen et al., 2005; Stanislawski et al., 2001; Xue et al., 2005). *In vitro* experiments show that following gene transfer, redirected T cells acquire the antigen specificity of the parent T cell, including production of IFN-γ in response to antigen stimulation and lysis of tumor cells in coculture assays. Additionally, murine studies have shown that infusion of T cells transduced with antigen-specific TCRs can eliminate tumors *in vivo* (Kessels et al., 2001; Xue et al., 2005). The feasibility of this new approach has recently been demonstrated for the treatment of metastatic melanoma (Morgan et al., 2006). In this study, patients were infused with T cells genetically modified with TCRs recognizing a melanoma antigen. Prolonged persistence of CTL and objective tumor regression of metastatic lesions was observed in two patients.

Obviously, high avidity TCRs would be best suited for this kind of approach. However, it might not be possible to find endogenous high avidity human TCRs for all malignancies or antigens, and therefore other approaches for isolating tumor-specific TCR genes might involve the use of transgenic mice that express human MHC molecules and/or human TCRs (Kuball et al., 2005; Stanislawski et al., 2001). In this approach, human TAAs are seen as foreign by the mouse immune system, and high avidity TCRs can be generated that are specific for peptides associated with human MHC molecules. Combining this with a method to easily measure TCR avidity and identify the α- and β-chain sequences of high avidity TCRs could make T cell therapy with genetically enhanced T cells a highly efficient tool for the treatment of various forms of cancer.

Despite the promising preclinical data, there are problems with current strategies for TCR gene transfer that may limit its use in the clinic. The primary concern is that transferred

α- and β-chains cross-pair with endogenous TCR chains, form hybrid TCRs with unintended autoimmune reactivity, and reduce correct pairing. These problems may be solved through modification of transmembrane association domains to eliminate dimerization with endogenous chains (Willemsen et al., 2000).

1.9 THE *LISTERIA MONOCYTOGENES* INFECTION MODEL

In order to investigate the complex regulation and mechanisms of an effective innate and/or adaptive immune response, immunological research frequently uses live pathogens in experimental mouse infection studies. One of the most widely used organisms is the Gram-positive, facultative intracellular bacterium *Listeria monocytogenes* (*L.m.*) (Kaufmann, 1995), which is also a human pathogen that can cause disease mainly in immunocompromised individuals and pregnant women, often with deleterious consequences for the fetus (Gellin and Broome, 1989). Besides the importance of early antigen-independent immune responses, like the crucial function of neutrophils in controlling replicating, intracellular pathogens (Conlan and North, 1991) or the essential role of TNF receptor signaling for the early immune response (Plitz et al., 1999), *L.m.* is mostly applied in the study of antigen-specific T cell responses. Many antigenic peptides derived from *L.m.* proteins are known, which are presented on murine MHC molecules and induce detectable frequencies of *Listeria*-specific T cells (Busch and Pamer, 1998). With the help of MHC I tetramers (Altman et al., 1996; Busch et al., 1998) or Streptamers (Knabel et al., 2002), these antigen-specific $CD8^+$ T cells can be visualized and analyzed in detail. Thus, major advances in contemporary T cell research, like the kinetics of primary and secondary T cell responses (Busch et al., 1998) or the importance of $CD8\alpha^+$ DC for the entry of intracellular bacteria into the spleen (Neuenhahn et al., 2006) are based on results generated in the murine *L.m.* infection model. Furthermore, after primary infection, mice develop very effective protection against reinfection with *L.m.* that is mediated by $CD8^+$ memory T cells (Harty and Bevan, 1992). For this reason, *L.m.* is also used extensively for the analysis of the generation and maintenance of memory T cells. Important findings in this field, like the changed TCR repertoire composition and TCR affinity maturation during recall responses (Busch and Pamer, 1999; Busch et al., 1998), or the distinction of effector, effector memory and central memory T cells by the surface markers CD62L and CD127 (Huster et al., 2004), are rooted in *L.m.* infection experiments.

Even though to a large extent dependent on $CD8^+$ T cells (Mombaerts et al., 1993), the relevance of the structural TCR avidity for the expansion, function and maintenance of antigen-specific T cells in this model system has never been examined.

1.10 AIM OF THIS PHD WORK

Interactions of the T cell receptor (TCR) and its coreceptor with their ligand, the peptide-loaded MHC molecule (pMHC), represent a central event in T cell physiology. This starts with T cell maturation and selection in the thymus, followed by T cell activation upon antigen encounter in the periphery, and ends with T cell fate decisions after antigen-recognition and subsequent exertion of distinct effector functions. The structural avidity of the TCR to its ligand has always been thought of as a major determinant for the outcome of these interactions.

For this reason, several different attempts to measure this important parameter have been made in the past. Unfortunately, due to experimental limitations, all of these suffered from more or less severe drawbacks, especially since none of them was able to model the physiological situation of TCR/coreceptor binding to monomeric pMHC on the surface of a living T cell to a satisfying degree.

With this thesis work, the attempt was made to develop a novel assay system for the determination of TCR avidities of individual T cells. It was tried to get as close as possible to the level of singular TCR/coreceptor – pMHC interactions on living T cell surfaces, which would be a major improvement over the existing experimental approaches.

Conceptually the novel method should be based on the recently established MHC-Streptamer technology (Knabel et al., 2002), which should allow to accumulate TCR-bound pMHC on the T cell surface and follow their subsequent dissociation upon monomerization. Specific goal of this thesis work was to generate the necessary molecular tools for such a novel assay system and to find experimental platforms that would allow real time analysis of MHC dissociations on single T cells. After definition of optimized assay conditions, the affinity-associated parameters should be validated by analysis of TCR-transgenic T cells for which affinity data are already available. Once established, the assay should be used to answer the following questions concerning basic T cell biology:

1) In what way does functional T cell avidity correlate with the structural avidity of the TCR?
2) To what degree is functional T cell avidity dependent on the structural avidity of the TCR?
3) Do T cells with higher structural avidity confer better protection against pathogens?

Finally, the experiences and insights gained to that point should be used to envision potential new clinical applications for adoptive T cell therapy, and to provide first evidence for the feasibility of such new applications in preclinical model systems.

2 MATERIAL AND METHODS

2.1 MATERIAL

2.1.1 Chemicals and reagents

The reagents used in the experimental procedures of this thesis were purchased from the following companies:

Reagent	Supplier
Alexa-488-maleimide	Molecular Probes, Leiden, The Netherlands
α-Methylmannopyranoside (α-MM)	Calbiochem, Darmstadt, Germany
Ammoniumchloride (NH_4Cl)	Sigma, Taufkirchen, Germany
Ampicillin	Sigma, Taufkirchen, Germany
BCA assay reagents	Interchim, Montlucon, France
β-Mercaptoethanol	Sigma, Taufkirchen, Germany
Biocoll Ficoll solution	Biochrom, Berlin, Germany
Bovine serum albumin (BSA)	Sigma, Taufkirchen, Germany
Carbenicillin	Roth, Karlsruhe, Germany
Chromium-51 (^{51}Cr)	Amersham, Munich, Germany
Cytofix/Cytoperm	BD Biosciences, Heidelberg, Germany
d-Biotin	Sigma, Taufkirchen, Germany
Dimethylformamid (DMF)	Sigma, Taufkirchen, Germany
Ethanol	Klinikum rechts der Isar, Munich, Germany
Ethidium-monazide-bromide (EMA)	Molecular Probes, Leiden, The Netherlands
Fetal calf serum (FCS)	Biochrom, Berlin, Germany
Gentamycin	GibcoBRL, Karlsruhe, Germany
Gluthathione (oxidized)	Sigma, Taufkirchen, Germany
Gluthathione (reduced)	Sigma, Taufkirchen, Germany
Golgi-Plug	BD Biosciences, Heidelberg, Germany
Guanidine-HCl	Sigma, Taufkirchen, Germany
HCl	Roth, Karlsruhe, Germany

Reagent	Supplier
HEPES	GibcoBRL, Karlsruhe, Germany
IPTG	Sigma, Taufkirchen, Germany
L-Arginine	Roth, Karlsruhe, Germany
L-Glutamine	GibcoBRL, Karlsruhe, Germany
Leupeptin	Sigma, Taufkirchen, Germany
Lysozym	Sigma, Taufkirchen, Germany
NaOH	Roth, Karlsruhe, Germany
Paraformaldehyde	Sigma, Taufkirchen, Germany
Penicillin	Roth, Karlsruhe, Germany
Pepstatin	Sigma, Taufkirchen, Germany
PermWash	BD Biosciences, Heidelberg, Germany
pET3a, pET27b expression vectors	Novagen, Darmstadt, Germany
Phosphate buffered saline (PBS)	Biochrom, Berlin, Germany
RPMI 1640	GibcoBRL, Karlsruhe, Germany
Sodiumacetate	Sigma, Taufkirchen, Germany
Sodiumazide (NaN_3)	Sigma, Taufkirchen, Germany
Sodiumchloride (NaCl)	Roth, Karlsruhe, Germany
Sodium-EDTA (Na-EDTA)	Sigma, Taufkirchen, Germany
Streptomycin	Sigma, Taufkirchen, Germany
Streptactin-PE (ST-PE)	IBA, Göttingen, Germany
Tris-hydrochloride (Tris-HCl)	Roth, Karlsruhe, Germany
Triton X-100	Biorad, Munich, Germany
Trypan Blue solution	Sigma, Taufkirchen, Germany
T-Stim culture supplement	BD Biosciences, Heidelberg, Germany

2.1.2 Buffers and media

All buffers were filtered using a Stericup 0.22 µm vacuum filter system (Millipore, Bedford, USA) shortly before use. Adjustment of the proper pH was done with NaOH or HCl.

Buffer	Composition	
FACS staining buffer	1x	PBS
	0.5% (w/v)	BSA
	0.02% (w/v)	NaN_3
	pH 7.45	
$RP10^+$ cell culture medium	1x	RPMI 1640
	10% (w/v)	FCS
	0.025% (w/v)	L-Glutamine
	0.1% (w/v)	HEPES
	0.001% (w/v)	Gentamycin
	0.002% (w/v)	Streptomycin
	0.002% (w/v)	Penicillin
Ammoniumchloride-Tris	0.17 M	NH_4Cl
	0.17 M	Tris-HCl
	mix NH_4Cl and Tris-HCl at a ratio of 9:1	
Refolding buffer	100 mM	Tris-HCl
	400 mM	L-Arginin
	2 mM	NaEDTA
	0.5 mM	ox. Gluthathione
	5 mM	red. Gluthathion
	ad 1 L H_2O, pH 8.0	
Guanidine solution	3 M	Guanidine-HCl
	10 mM	NaAcetate
	10 mM	NaEDTA
	ad 100 ml H_2O, pH4.2	
FPLC buffer	20 mM	Tris-HCl
	50 mM	NaCl
	ad 1 L H_2O, pH 8.0 or pH 7.3	

Buffer	Composition
d-biotin 10 M stock solution	244.31 g d-biotin ad 100 ml H_2O, pH was brought to ≈ pH 11 to facilitate solution of d-biotin, then back down to pH 7

2.1.3 Peptides

All peptides were purchased from Biosyntan GmbH, Berlin, Germany.

LLO_{91-99}: GYKDGNEYI
$Ova_{257-264}$: SIINFEKL
dEV8: EQYKFYSV
p2Ca: LSPFPFDL
$m164_{257-265}$: AGPPRYSRI

2.1.4 Antibodies

Antibody	clone	supplier
$F_c$block (rat anti-mouse CD16/CD32)	2.4 G2	BD Bioscience, Heidelberg, Germany
Rat anti-mouse CD3 APC	145-2C11	BD Bioscience, Heidelberg, Germany
Rat anti-mouse CD8α Alexa-488	CT-CD8α	Caltag Laboratories, Hamburg, Germany
Rat anti-mouse CD8α FITC	CT-CD8α	Caltag Laboratories, Hamburg, Germany
Rat anti-mouse CD8α PE	CT-CD8α	Caltag Laboratories, Hamburg, Germany
Rat anti-mouse IFNγ FITC	XMG1.2	BD Bioscience, Heidelberg, Germany
Rat anti-mouse TCRβ FITC	H57-597	BD Bioscience, Heidelberg, Germany

2.1.5 MHC tetramers

Conventional MHC I tetramers for the detection of Ag-specific $CD8^+$ T cells were routinely produced in our laboratory according to well established protocols (Busch et al., 1998). Depending on the respective MHC allele, the following peptide-loaded MHC I tetramers were used:

H2-K^d#45/mβ_2m/LLO_{91-99} Streptavidin-PE
H2-K^b#45/mβ_2m/$Ova_{257-264}$ Streptavidin-PE

2.1.6 MHC Streptamers

MHC I Streptamers were generated as described (see 2.2.3). The following MHC I Streptamers were used:

H2-K^d StreptagIII/mβ_2m-cys67 Alexa-488/LLO_{91-99} Streptactin-PE
H2-K^b StreptagIII/mβ_2m-cys67 Alexa-488/$Ova_{257-264}$ Streptactin-PE
H2-K^b StreptagIII/mβ_2m-cys67 Alexa-488/dEV8 Streptactin-PE
H2-L^d StreptagIII/mβ_2m-cys67 Alexa-488/p2Ca Streptactin-PE
H2-D^d StreptagIII/mβ_2m-cys67 Alexa-488/$m164_{257-265}$ Streptactin-PE

2.1.7 Gels

SDS-PAGE running gel:	7 ml	dH_2O
	4.38 ml	1.5 M Tris-HCl pH 8.8
	5.8 ml	30% Acrylamide 1% Bisacrylamide
	170 µl	10% SDS
	8.8 µl	TEMED
	170 µl	10% APS

SDS-PAGE stocking gel:	6.2 ml	dH_2O
	2.5 ml	0.5 M Tris-HCl pH 6. 8
	1.2 ml	30% Acrylamide 1% Bisacrylamide
	100 µl	10% SDS
	5 µl	TEMED
	100 µl	10% APS
Agarose gel:	0.45 g	Agarose
	40 ml	TBE buffer
	1 µl	Ethidium bromide

2.1.8 Mice

Inbred mouse strains BALB/c and C57BL/6 were purchased from Harlan-Winkelmann (Borchen, Germany) and mice were used for primary infection experiments at 6-8 weeks of age. Mice were housed in a specific pathogen free (SPF) animal facility at the Institute of Medical Microbiology, Immunology and Hygiene at the Technical University Munich.

2.1.9 Microscope and equipment for bulk TCR avidity measurements

Zeiss LSM 510	confocal microscope (Zeiss, Jena, Germany)
Leica SP5	confocal microscope (Leica, Bensheim, Germany)
Zeiss temperable insert P	cooling device (Zeiss, Jena, Germany)
Huber Minichiller	peltier cooler (Huber Kältemaschinenbau, Offenburg, Germany)
Metal inserts for cooling device	(Locksmithery, Klinikum rechts der Isar, Munich, Germany)
Polycarbonate membranes, pore size 5 µm	(Millipore, Bergisch-Gladbach, Germany)
Metal shims	(Schneider + Klein, Landscheid, Germany)

2.1.10 Evotec Cytocon400 System

Evotec Cytocon400 generator	(Evotec, Berlin, Germany)
WPI SP 260 PZ syringe pumps	(WPI, Berlin, Germany)
WPI SP 210 IWZ syringe pump	(WPI, Berlin, Germany)
Evotec Cytocon microscope adapter for Zeiss LSM510	(Evotec, Berlin, Germany)
Evotec Cytocon400 Loader4++ chip	(Evotec, Berlin, Germany)
Evotec Cytocon400 electrical adapter Loader4++	(Evotec, Berlin, Germany)
Evotec Cytocon fluidic block	(Evotec, Berlin, Germany)
Cooling block for Evotec Cytocon fluidic block	(Locksmithery, Klinikum rechts der Isar, Munich, Germany)
Evotec Cytocon injector	(Evotec, Berlin, Germany)
Evotec Cytocon injector holder	(Evotec, Berlin, Germany)
Evotec Cytocon dual injector holder	(Evotec, Berlin, Germany)
Evotec Cytocon 4-way valve and holder	(Evotec, Berlin, Germany)
Evotec Cytocon objective extension for Zeiss LSM510	(Evotec, Berlin, Germany)
Evotec Cytocon fluidic case	(Evotec, Berlin, Germany)
Evotec Cytocon rack	(Evotec, Berlin, Germany)
Precision syringes	(Hamilton, Bonaduz, Switzerland)
Evotec Cytocon BufferII	(Evotec, Berlin, Germany)
Lenovo Thinkpad R50	(Lenovo, Paris, France)
VsCom Quaid serial adapter	(VsCom, Norderstedt, Germany)
Creative USB GamePad	(Creative Labs, Dublin, Ireland)
Evotec Cytocon Switch software	(Evotec, Berlin, Germany)

2.1.11 Equipment

Zeiss LSM 510, confocal microscope	Zeiss, Jena, Germany
Leica SP 5, confocal microscope	Leica, Bensheim, Germany
Evotec Cytocon400	Evotec, Berlin, Germany
FACSCalibur flow cytometer	BD Bioscience, Heidelberg, Germany
FPLC System	Amersham, Munich, Germany
OB29/B02-1 ^{137}Cs γ-ray source	Buchler, Braunschweig, Germany

Packard CobraII Auto-Gamma γ-counter	Perkin-Elmer, Wellesley, USA
Varifuge 3.0RS centrifuge	Thermo, Schwerte, Germany
Multifuge 3S-R centrifuge	Thermo, Schwerte, Germany
Biofuge fresco table top centrifuge	Thermo, Schwerte, Germany
Biofuge 15 table top centrifuge	Thermo, Schwerte, Germany
Axiovert S100 microscope	Zeiss, Jena, Germany
RC26 Plus ultra-centrifuge	Sorvall, Langenselbold, Germany
HE33 agarose gel casting system	Hoefer, San Francisco, USA
Mighty Small SE245 gel casting system	Hoefer, San Francisco, USA
NanoDrop spectrophotometer	NanoDrop, Baltimore, USA
Gel Imaging System	BioRad, Munich, Germany

2.1.12 Software

FlowJo	Treestar, Ashland, USA
Microsoft Office	Microsoft, Redmond, USA
MetaMorph Offline	Molecular Devices, Downingtown, USA
Evotec Switch	Evotec, Berlin, Germany
Analyzer 2.2	Jörg Mages, Institute of Medical Microbiology, Immunology and Hygiene, Technical University Munich, Munich, Germany

2.2 METHODS

2.2.1 Generation of T cell lines

Epitope-specific T cell lines were generated by *in vitro* restimulation with peptide-loaded stimulator cells.

For *in vitro* expansion of responder cells, spleens of *L.m.*-infected mice at d7 after primary infection or of naïve TCR-transgenic mice were removed, washed in $RP10^{+}$ and homogenized through a steel-net. After pelleting at 460 x g for 7 min, the cells were resuspended in 5 ml ACT to lyse erythrocytes at RT for 7 min. Lysis was stopped by addition

of 5 ml $RP10^+$. The responder cells were pelleted again, 3-4 x 10^7 cells resuspended in 5 ml $RP10^+$ and put into T25 cell culture flasks.

Syngenic spleen cells were used as stimulator cells. Cells were generated from naïve mice as described above and irradiated with γ-rays at a dosis of 25 Gy. Afterwards the cells were loaded with the appropriate amounts of peptide (10^{-6} M to 10^{-9} M) in $RP10^+$ by incubation for 1 h at 37°C. The cells were then washed twice to remove unbound peptide and 3 x 10^7 cells were added to the responder cells in 5 ml $RP10^+$.

The cell lines were restimulated weekly by addition of stimulator cells generated in the same manner as described above. Starting with the second *in vitro* restimulation, the medium was supplemented with rat ConA supernatant (5% T-Stim, inactivation of ConA by addition of 5% α-MM). The peptides used were LLO_{91-99} at a concentration of 10^{-6} M or 10^{-9} M (see 3.1.1) and $Ova_{257-264}$ at a concentration of 10^{-7} M. The cell cultures were kept at 37°C/ 5% CO_2.

2.2.2 T cell staining

2.2.2.1 Antibody and MHC multimer staining for FACS analysis

For tetramer, Streptamer and/or antibody staining, 5 x 10^6 or less cells per staining were used. Usually, the stainings were performed in 96-well plates. The cells were first incubated in 50 µl F_c block (1:500, stock at 2.5 µg/µl) and EMA (1:1000, stock at 2 µg/µl) for 20 min under light, to block $F_c\gamma$ receptors and to stain dead cells. Cells were then washed once with FACS buffer in a total volume of 200 µl, pelleted for 2 min at 460 x g and resuspended in 50 µl tetramer or Streptamer solution (see *2.2.3.3*). Cells were incubated on ice in the dark for 45 min. Antibodies at the appropriate dilution were added for the last 20 min of the staining. The samples were then washed three times in FACS buffer, fixed in 1% PFA and stored in the dark at 4°C until further analysis.

2.2.2.2 FACS acquisition and analysis

For FACS analysis, at least 10^5 cells of the populations of interest were acquired on a FACSCalibur flow cytometer (Becton Dickinson, Heidelberg, Germany). Data analysis was performed using FlowJo software (Treestar, Ashland, USA).

2.2.3 Streptamers

All MHC class I molecules for the generation of the Streptamers used in this study were expressed in *E. coli*, purified, refolded *in vitro* and conjugated with fluorescent dyes.

2.2.3.1 Protein production

Expression vectors (pET3a, pET27b; Novagen, Darmstadt, Germany) encoding the murine MHC class I heavy chains H2-K^b, H2-K^d, H2-D^d, H2-L^d and H2-L^d D227K, all lacking the transmembrane region but having a C-terminal StreptagIII sequence, as well as a vector encoding the mβ_2m with a mutated cystein at position 67 to allow conjugation of fluorescent dyes, were available in the lab.

Expression of the proteins after transformation of the vectors in *E. coli* BL21 (DE3) CP (Novagen, Darmstadt, Germany) was done in 6 L cultures (LB, 0.4% Glucose, Carbenicillin 100 µg/ml). Expression was induced by addition of 0.4 mM IPTG at an OD_{600} of 0.7 for 3 h. Purification of the recombinantly expressed insoluble protein inclusion bodies was done by enzymatic and mechanic lysis (Lysozym, ultrasound, Triton X-100, freeze-thawing). The proteins were then solved in 8 M Urea.

2.2.3.2 Refolding and fluorescence conjugation of MHC class I molecules

Heavy chain and mβ_2m proteins in 8 M Urea were diluted into refolding buffer containing high concentrations of the respective synthetic peptide epitope (60µg/ml).

Aliquots of the proteins were first diluted in 3 M guanidine buffer, injected directly into 200 ml refolding buffer every 8 h while vortexing heavily and incubated under constant

agitation for 48 h at 10°C. The refolding buffer contained a gluthathion redox system to facilitate optimal formation of disulfide-bridges. After 48 h, the protein solution was concentrated to a volume of 10-20 ml over a 10 kDa membrane (Millipore, Eschborn, Germany), then further reduced to 1 ml using 10 kDa concentrator columns (Millipore, Eschborn, Germany). The flowthrough of the first concentration step still contained large amounts of peptide and could be used for a second refolding.

Correctly folded MHC I molecules were purified by gelfiltration (Superdex 200HR, Amersham, Munich, Germany) over a FPLC system (FPLC basic, Amersham, Munich, Germany), pooled and incubated over night in a buffer containing NaN_3, protease inhibitors (1 mM NaEDTA, Leupeptin, Pepstatin) and 0,1 mM DTT to keep the cystein-67 of the $m\beta_2m$ in a reduced state. The next day, the buffer was exchanged against FPLC buffer and the protein concentration determined by a standard BCA-assay. The activated fluorescent dye Alexa-488-maleimide was added to the protein in a molar ration of 10:1 and incubated at RT for 2 h. The conjugation was then stopped by addition of 1 µl 50 mM β-mercaptoethanol and the correctly conjugated MHC I molecules purified by gel filtration (Superdex 200HR). Fractions were pooled, the buffer exchanged against PBS pH 8 containing NaN_3 and protease inhibitors (1 mM NaEDTA, Leupeptin, Pepstatin) and the protein stored in liquid nitrogen after measuring its concentration.

2.2.3.3 Multimerization

For each staining (up to 5 x 10^6 cells), 1 µg of Alexa-488-conjugated MHC I and 5 µg Streptactin-PE were diluted in a final volume of 50 µl FACS buffer and incubated over night or for at least 1 h.

2.2.4 Functional avidity assays

2.2.4.1 Intracellular cytokine staining

To check for their ability to produce IFN-γ, T cells were stimulated *in vitro* with titrated amounts of peptide. For each stimulation, 5 x 10^5 T cell line cells and 5 x 10^5 P815 cells used as stimulator cells were put in a 96-well plate in 100 µl $RP10^+$. Serial dilutions of peptide

were added, resulting in peptide concentrations of 10^{-7} M to 10^{-13} M. After 2 h of incubation at 37°C, Brefeldin-A was added at a concentration of 2 µg/ml, to inhibit the transport of intracellular cytokines through the Golgi apparatus. After three additional hours of incubation the cells were spun down and stained in 50 µl F_c block/EMA mix (F_c block 1:500, stock at 2.5 µg/µl, EMA 1:1000, stock at 2 µg/µl, 20 min, under light, on ice). The cells were washed three times in FACS buffer and stained in 50 µl against the surface marker CD8α (20 min, in the dark, on ice). After washing, the cells were then fixed and permeabilized in 100 ml Cytofix/Cytoperm (BD Biosciences) (20 min, in the dark, on ice), then washed three times in PermWash buffer (BD Biosciences). After that, the cells were stained with an intracellular antibody against IFN-γ (30 min, in the dark, on ice), washed three times in PermWash, one time in FACS buffer and then fixed in 1% PFA until FACS analysis.

2.2.4.2 ^{51}Chromium release assay

To test their ability to lyse peptide-loaded target cells, we performed ^{51}Cr release assays using titrated amounts of peptide for stimulation of T cells. P815 target cells were labeled with 18.5 MBq ^{51}Cr for 1 h at 37°C. After washing, 10^4 of these target cells in 100 µl were put in each well of a 96-well plate and serial dilutions of peptide were added, resulting in peptide concentrations of 10^{-7} M to 10^{-13} M. Effector cells were added in 100 µl at an E/T-ratio of 10:1. To determine the spontaneous and maximal lysis, PBS or 0.1% Triton X-100 were used respectively instead of effector cells. Each stimulation was performed in triplicates. The cells were incubated for 4-5 h at 37°C, spun down and the supernatants transferred to counting tubes. The amount of radioactivity in the supernatants was measured in a γ-counter and the specific lysis for each sample was calculated.

2.2.4.3 Listeria monocytogenes infection and adoptive cell transfer

For infection experiments of BALB/c mice, the isolate *L.m.* 10403s (ATCC, Rockville, USA) was used. Mice were infected at 6-8 weeks of age. Infections were performed intravenously (i.v.) with the indicated dosage of bacteria in 200 µl PBS. For infection, 20 µl glycerol stock of bacteria were pre-cultured in 5 ml BHI medium at 37°C until the bacteria entered the exponential growth phase as determined by OD measurement ($OD_{600} \approx 0.1$). The amount of

bacteria was calculated using standard curves. The exact infection dose was further controlled by plating out dilutions of the *L.m.* suspension used on BHI plates, incubating over night, counting CFU and calculating the original bacteria concentration.

T cells for adoptive transfer were counted using a Neubauer counting chamber, excluding dead cells by Trypan blue staining. About 1 h prior to *L.m.* infection, the indicated amount of T cells was transferred i.v. in 200 µl PBS.

2.2.4.4 Measurement of bacterial load

As an indicator of the protective capacity of the transferred T cells, numbers of live bacteria in spleens and livers of infected animals were determined.

The organs were harvested at d 3 after infection with 2 x 10^4 bacteria, homogenized and resuspended in 5 ml sterile PBS. 100 µl of the cell suspensions were diluted 1:10, 1:100 and 1:1000 in 0.1% Triton X-100 to release the intracellular bacteria from the cells. Aliquots of 10 µl per dilution were plated out in triplicates on BHI plates and incubated over night at 37°C. CFU were counted on the following day, and the amounts of *L.m.* per organ were calculated according to the respective dilutions.

2.2.5 Measuring structural avidity

2.2.5.1 Streptamer staining for structural avidity assays

Between 10^5 and 10^6 T cells were stained for the structural avidity assay. Cells from T cell lines were first purified over a Ficoll gradient to deplete dead cells. The cells were allowed to rest in a 96-well plate on ice for at least 1 h before staining, to minimize side effects of MHC multimer staining like internalization of the reagents. After that, the cells were spun down, resuspended in 50 µl Streptamer solution and stained for 30 min on ice. The cells were washed three times in ice-cold FACS buffer, resuspended in 100 µl FACS and transferred to pre-cooled 1.5 ml tubes. The whole staining procedure was performed on ice or in a cooled centrifuge at all times.

2.2.5.2 Bulk analysis of T cell receptor avidity

All TCR avidity measurements were performed on a Zeiss LSM 510 confocal laser scanning microscope or a Leica SP5 confocal laser scanning microscope. The microscope was equipped with a Zeiss cooling device and a peltier cooler (Huber Kältemaschinenbau). To ensure optimal cooling of the cells during the assay, we manufactured steel inserts for this cooling device that constituted the lateral boundary for the reservoir in which the assay was performed. These steel inserts were sealed from the bottom with cover slip glass (0.1 mm) using a sealing compound. Into this reservoir, 1800 µl of ice-cold FACS buffer were added, and a small aliquot of Streptamer stained cells were pipetted very slowly and carefully into the middle of the reservoir, directly above the cover slip glass. The cells were allowed to subside to the bottom of the reservoir for five minutes. To prevent the cells from moving around during the course of the measurement, a polycarbonate membrane (pore size 5 µm; Millipore) was put on top of the cells. A small metal shim was put on top of the membrane very slowly and carefully, to help the membrane sink down onto the cells and to keep it in place. After this procedure, the cells were again allowed to settle down for five minutes. Image acquisition was started, with one picture taken every ten seconds. After the first image, 1800 µl of ice-cold 2 mM d-biotin were carefully added to the rim of the reservoir to disrupt the Streptamers and initiate MHC I dissociation. Usually between 80 and 160 images were taken, depending on the expected dissociation rates. Bleaching measurements were conducted the same way without addition of d-biotin.

2.2.5.3 T cell receptor avidity assay and subsequent single cell sorting

The TCR avidity assay for subsequent cell sorting was performed with the help of an Evotec Cytocon400 system that was mounted to a Zeiss LSM510 confocal laser scanning microscope. All experimental procedures were performed according to the manufacturers instructions. In brief, the Evotec Cytocon400 system was mounted to the microscope stage in its dual injector configuration. One injector was used to add Streptamer stained cells, the other to add 1 mM d-biotin to the system. Transport of the cells and the d-biotin to the microfluidic Cytocon Loader4++ chip was controlled by high precision syringe pumps. All actions of the pumps and the electrical elements of the chip were controlled with the Evotec Cytocon Switch software and a gamepad as controlling device. To ensure optimal cooling of the system, a

custom-made water-cooled cooling block was mounted onto the microfluidic chip. The whole system was flushed thoroughly with Evotec Cytocon BufferII before start of the experiment. The same buffer was used as running buffer for the cells.

Once a Streptamer stained cell was captured in the chips field cage image acquisition was started, taking one picture every four seconds. After the first picture, addition of 1 mM d-biotin to the chip was initiated. Depending on the expected MHC dissociation rate, 60 to 300 pictures were taken. After completion of the assay, the cell was released from the field cage and flushed out of the chips outlet channel, were it could be taken up with a pipette in a volume of 1 µl and put to further use.

2.2.5.4 Data analysis

Images were analyzed using MetaMorph Offline image analysis software (Molecular Devices, Downingtown, USA). For each individual cell, integrated fluorescence intensity inside a gate containing the cell was measured over the whole time series that was acquired. The same gate was then put in close proximity to the cell, but not containing the cell, for measurement of background fluorescence intensity. Data were logged into Microsoft Excel (Microsoft, Redmond, USA). Further data analysis was done automatically by the Analyzer 2.2 software (Jörg Mages, Institute of Medical Microbiology, Immunology and Hygiene, Technical University Munich, Munich, Germany) according to the following scheme. Background intensities were subtracted from absolute fluorescence intensities, and data were corrected for bleaching effects (see 3.2.3). These corrected data sets were fit to the equation $y = ae^{-kt} + y_0 + c$. This allowed us to exactly determine the minimum of the curve. The minimum was defined as the endpoint of MHC dissociation, because from this point on, correction for bleaching resulted in over-compensation of the bleaching of the cells autofluorescence and a seeming increase in fluorescence intensity. The start-point of MHC dissociation was defined as the first data-point equal or below 80% of the maximum value. Data-points between start- and endpoint were singled out and fit to the equation $y = ae^{-k_{off}t} + y_0$. The dissociation constant k_{off} was calculated and the half-life time of MHC dissociation determined according to the formula $t_{½} = \ln(2)/k_{off}$. All graphs and regressions for each cell are put out by the software graphically. All dissociation constants and half-life times for each cell are put out in list form.

3 RESULTS

3.1 T CELLS WITH HIGHER FUNCTIONAL AVIDITY CONFER BETTER PROTECTION

3.1.1 Two different LLO_{91-99}-specific T cell lines show differing functional avidities

The amount of peptide used for *in vitro* restimulation of polyclonal T cells inversely correlates with the functional avidity of subsequently generated T cell lines (Alexander-Miller et al., 1996). In order to examine a possible correlation between functional and structural avidity (see 3.3), we generated two different polyclonal T cell lines specific for the *Listeria monocytogenes* epitope LLO_{91-99} by long-term restimulation with high and low amounts of peptide (10^{-6} M LLO_{91-99}, cell line A; 10^{-9} M LLO_{91-99}, cell line B) (Fig. 9). Both cell lines consisted of more than 95% antigen-specific cells after five rounds of restimulation (R5) as determined by tetramer staining (Fig. 9 A). Expression of TCR β-chain was similar in both cell lines. Interestingly, cell line B lost most of its expression of CD8α over the time (Fig. 9 A and B).

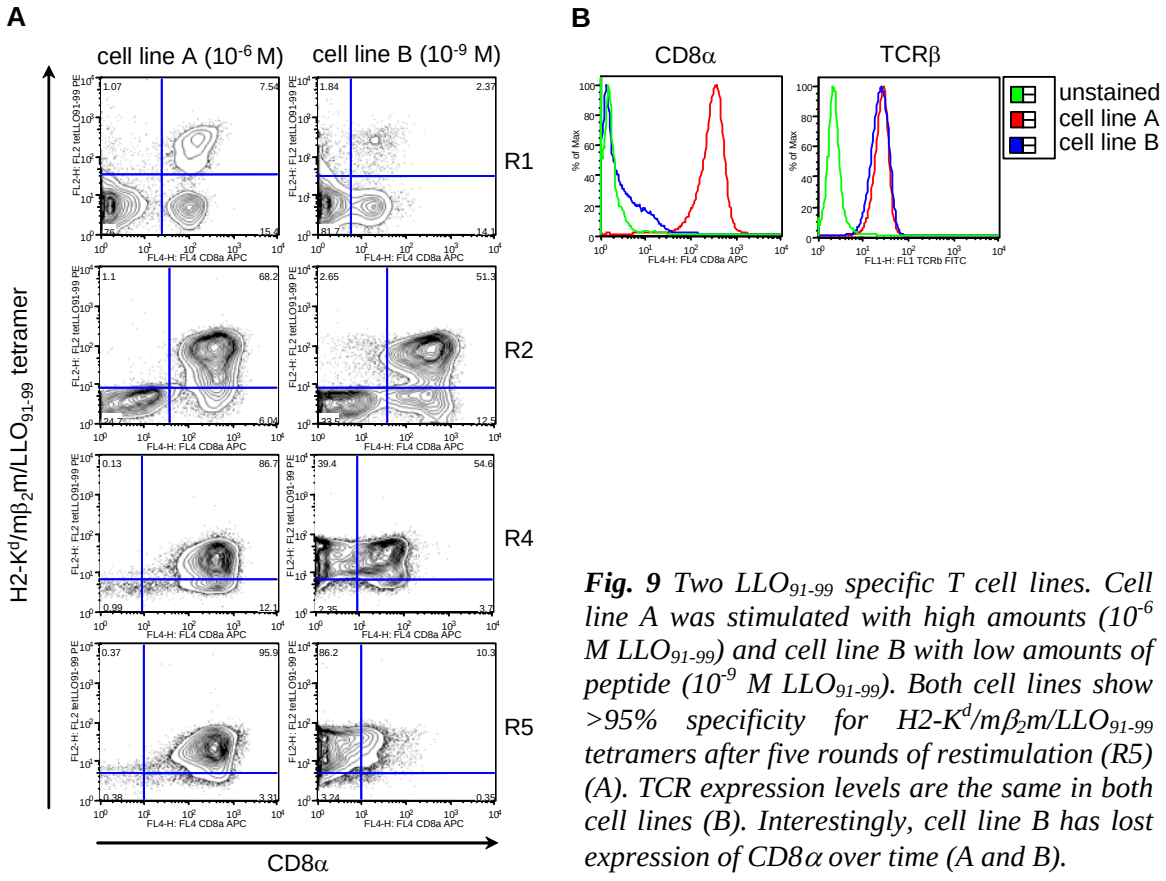

Fig. 9 *Two LLO_{91-99} specific T cell lines. Cell line A was stimulated with high amounts (10^{-6} M LLO_{91-99}) and cell line B with low amounts of peptide (10^{-9} M LLO_{91-99}). Both cell lines show >95% specificity for H2-K^d/mβ_2m/LLO_{91-99} tetramers after five rounds of restimulation (R5) (A). TCR expression levels are the same in both cell lines (B). Interestingly, cell line B has lost expression of CD8α over time (A and B).*

To measure the functional avidities of the two cell lines, we performed intracellular cytokine staining and ^{51}Chromium release assay using titrated amounts of peptide for restimulation. In intracellular cytokine staining assays, cell line B showed increased responsiveness compared to cell line A, with cells producing IFN-γ already when stimulated with 10^{-12} M peptide. A hundred-fold higher peptide concentration was needed to stimulate IFN-γ production in cell line A (Fig. 10 A). The difference in the amount of peptide needed to stimulate IFN-γ production in 50% of the cells (IC_{50}) was not as large, with an IC_{50} of 5.0 x 10^{-10} M for cell line A, and an IC_{50} of 1.6 x 10^{-10} M for cell line B (Fig. 10 B). Still, a significant difference in the functional avidities of the two cell lines could be demonstrated with this experiment.

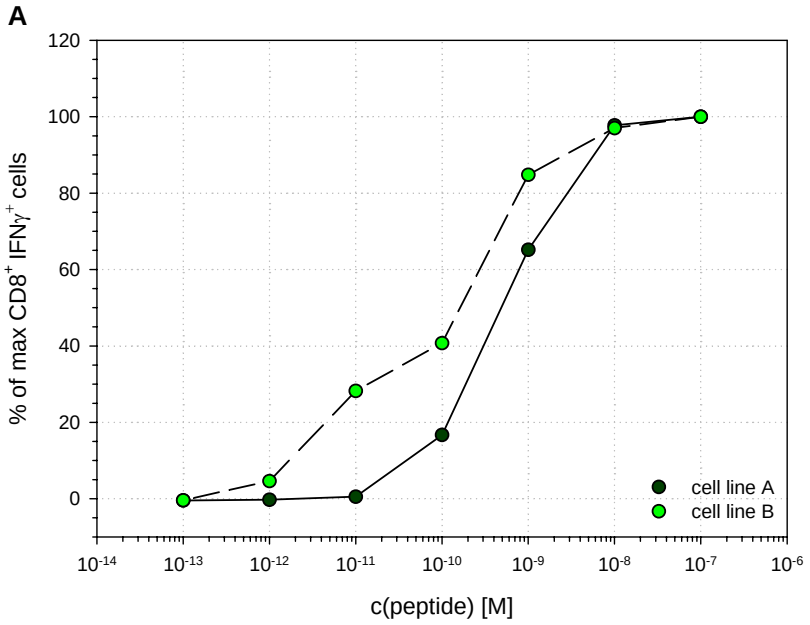

Fig. 10 *Functional avidity of two LLO_{91-99}-specific T cell lines measured by intracellular cytokine staining. Percentage of $CD8^+$ IFN-γ^+ cells is plotted against the peptide concentration used for stimulation of the cells. Cell line B responds more readily to lower peptide concentrations than cell line B (A). The IC_{50} for both cell lines is shown (B).*

In ^{51}Chromium release assays, cell line B was again more responsive to peptide stimulation, with about 70% specific lysis at 10^{-12} M peptide. Cell line A did not show any specific killing at this low concentration, reaching a similar degree of killing only at hundred- to thousand-fold higher peptide concentration (Fig. 11 A). The peptide concentrations where 50% specific lysis was observed were 5.0 x 10^{-13} M for cell line B, and 8.7 x 10^{-12} M for cell line A (Fig. 11 B).

A

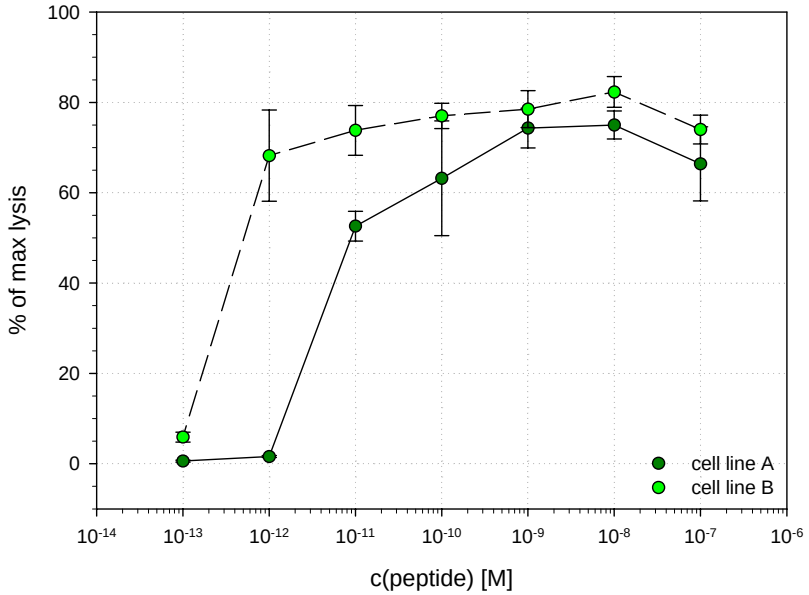

B

	50% spec. lysis
cell line A	8,7 * 10^{-12} M
cell line B	5,0 * 10^{-13} M

Fig. 11 *Functional avidity of two LLO_{91-99} specific T cell lines as measured in ^{51}Chromium release assay. Specific lysis is plotted against the peptide concentration used for stimulation of the cells. Cell line B responds more readily to lower peptide concentrations than cell line A (A). The peptide concentrations needed to reach 50% specific lysis for both cell lines is shown (B). Stimulations were performed in triplicates with standard deviations shown.*

The two cell lines we generated were both polyclonal T cell lines specific for the *Listeria monocytogenes* epitope LLO_{91-99}. Restimulation of the cell lines with high and low amounts of peptide clearly resulted in populations with distinct functional avidities as measured by intracellular cytokine staining and ^{51}Chromium release assay. As expected, the cell line that was restimulated with the lower amount of peptide displayed the higher functional avidity. The loss of CD8 in this cell line (Fig. 9 A and B) makes this difference even more striking, since CD8 is described to not only stabilize the TCR/pMHC complex, but also to functionally enhance TCR signaling (Rudolph et al., 2006). So even with a reduced expression level of the CD8 coreceptor, cell line B still showed a higher functional avidity.

3.1.2 Differing functional avidities translate into differing protective capacities

In order to see whether the differences in both cell lines regarding functional avidity would translate into differences regarding protective capacity of the cell lines *in vivo*, we performed adoptive transfer experiments. BALB/c mice were injected i.v. with 5 x 10^6 cells from one or the other cell line, or with PBS as a negative control. One hour later, the mice were infected i.v. with a dose of 2 x 10^4 *Listeria monocytogenes* (*L.m.*). Three days later the mice were

sacrificed and numbers of viable *L.m.* were determined in the spleen and liver by plating out dilutions of the respective organ homogenates. Mice that received cells from cell line A, the lower functional avidity cell line, showed large numbers of L.m. CFU in the spleen and liver, almost indistinguishable from the control group that did not receive any cells at all. In sharp contrast, mice that received cells from cell line B, the high functional avidity cell line, showed a hundred-fold reduction of viable bacteria in the spleen and no detectable bacteria in the liver (Fig. 12).

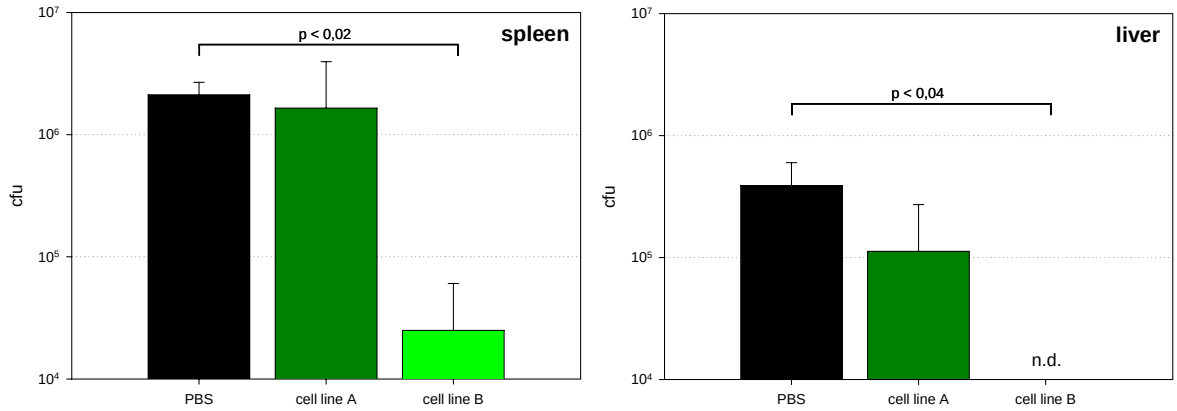

Fig. 12 *Protective capacity of two LLO_{91-99}-specific T cell lines. 5 x 10^6 cells from the indicated cell lines were transferred into BALB/c mice. Mice were then infected with 2 x 10^4 L.m.. At day 3, dilutions of homogenates of spleen and liver were plated out in triplicates to check for viable bacteria. Control mice did receive PBS instead of any cells. Numbers of L.m. CFU are shown as mean of three mice per group. Statistical significance as determined in unpaired Student´s t-test is shown. Error bars show standard deviation. (n.d. – not detectable).*

The results shown here clearly demonstrate that the functional avidity of T cells is a very important determinant of the protective capacity of the cells. Two different polyclonal T cell lines specific for the same epitope but differing in their functional avidity can exhibit very good protection in adoptive T cell transfer, as is the case for cell line B in our experiments, or almost no or only very weak protection, as is the case for cell line A.

3.2 A NOVEL ASSAY SYSTEM FOR THE ASSESSMENT OF STRUCTURAL TCR AVIDITY

3.2.1 Principle

Previous results generated in our lab had shown that MHC multimers can be used to track the dissociation of MHC molecules from T cell surfaces (Fig. 13) (Knabel et al., 2002). These so called Streptamers of an earlier generation consisted of MHC molecules that carried two StreptagII sequences, one on the heavy chain and one on the β_2-microglobuline, and a HSV-epitope-tag on the β_2-microglobuline. The MHC molecules were multimerized using a streptavidin derivative that binds StreptagII and the resulting reagents were used to stain T cells in an antigen-specific manner. Addition of d-biotin to the cells lead to the disruption of the reagents and subsequent MHC dissociation (Fig. 13). The accumulation and dissociation of MHC molecules could be monitored by antibody-staining against the HSV-epitope-tag. Unfortunately, MHC dissociation assays using these reagents had several severe drawbacks. First of all, the indirect detection of the MHC molecules by antibody-staining and subsequent FACS analysis restricted the system to the level of whole T cell populations and did neither allow for the measurement of single individual cells nor for real-time monitoring of MHC dissociation. Furthermore, interference of the epitope-tag with MHC binding could not be excluded, and recovery of live cells after MHC dissociation measurements was not possible since the cells had to be fixed in PFA.

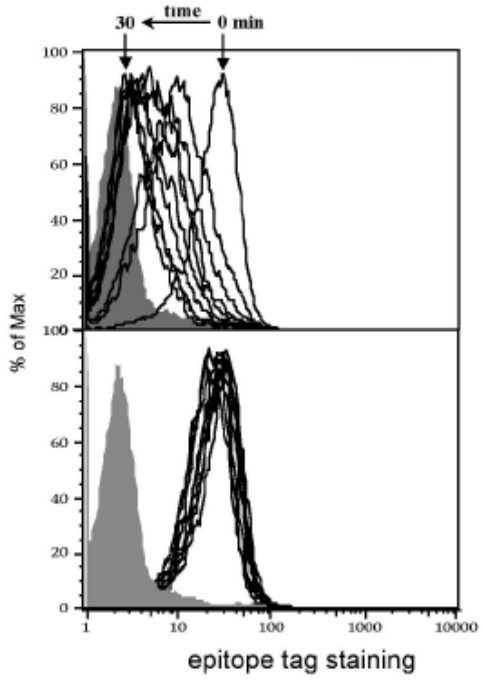

Fig. 13 *Early MHC dissociation experiment using early generation Streptamers. LLO_{91-99}-specific T cells were stained with H2-K^d StreptagII/mβ_2m StreptagII HSV-epitope-tag/LLO_{91-99} Streptactin multimers, briefly washed and incubated in the presence (upper panel) or absence (lower panel) of 1 mM d-biotin. Cell aliquots were collected at different time intervals (indicated above histograms), fixed with 1% PFA and stained for remaining HSV-epitope-tag on the cell surface (x axis). Filled gray histograms show unstained control. Addition of d-biotin leads to time-dependent loss of MHC-molecules from the cell surface (Knabel et al., 2002).*

For these reasons, we sought to develop a new assay system for the real-time measurement of MHC off-rates based on the dissociation of monomeric MHC molecules from the surface of individual living T cells. The key to this approach is how to get monomeric MHC molecules onto the T cell surface, since the binding strength of MHCs to the TCR is usually too weak to allow stable staining when using monomers. Therefore, we made use of a new generation of modified multimeric MHC reagents, so called Streptamers, that were based on a recently described reversible staining approach (Knabel et al., 2002). An important modification to that approach is the direct conjugation of fluorochromes to the MHC molecules. We changed the amino acid at position 67 of the mβ_2m to a cystein. This cystein lies at the surface of the mβ_2m and can serve as an acceptor for the chemical conjugation of activated fluorescent dyes.

Such fluorochrome-labeled MHC I molecules (Fig. 14 A) were multimerized using fluorochrome-labeled Streptactin, a streptavidin derivative that binds StreptagIII, a short

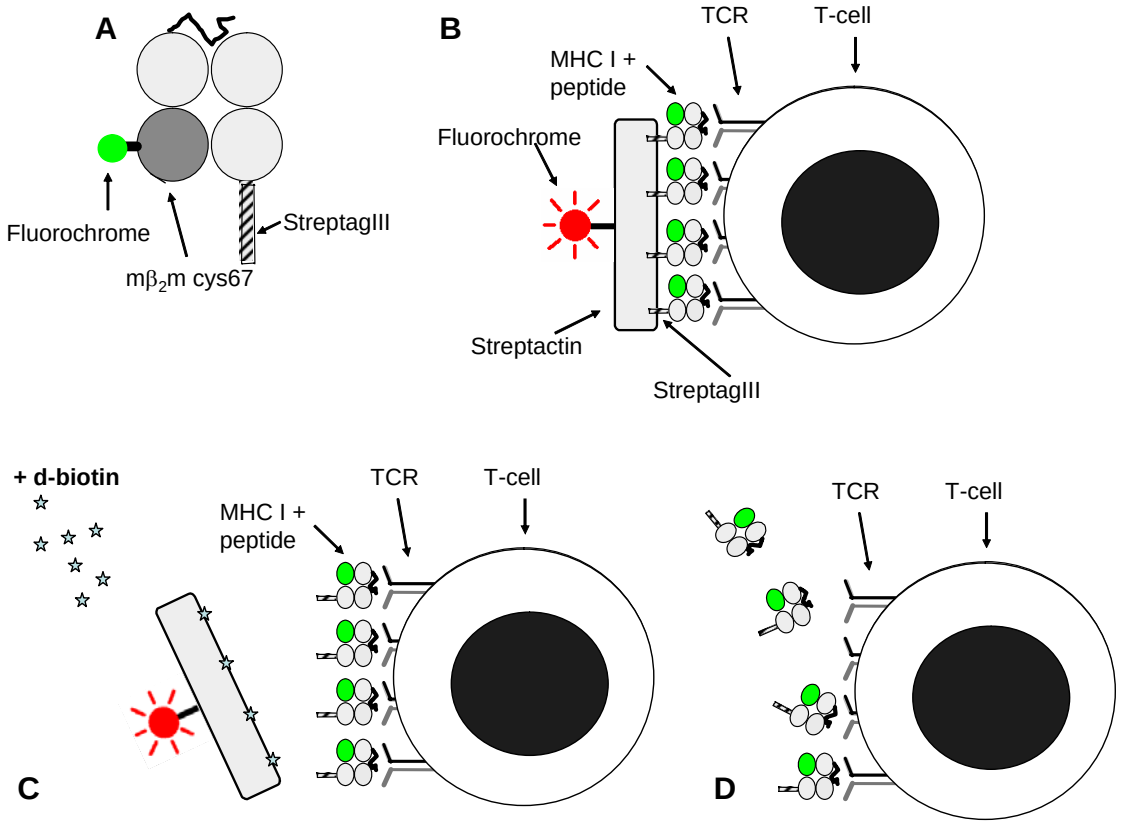

Fig. 14 *Principle of a novel Streptamer-based T cell avidity assay. A cysteine mutated into the β_2-microglobuline of recombinantly produced MHC I molecules allows chemical conjugation of single fluorochrome molecules (A). Fluorescence-labeled MHC I molecules are multimerized with fluorescence-labeled Streptactin. The resulting bichromatic MHC multimers stain T cells in a stable and antigen-specific manner (B). Addition of d-biotin disrupts the multimers. The Streptactin-backbone dissociates away fast (C). Monomeric MHC I molecules dissociate from the T cell surface (D). All this is done at 4° C.*

peptide sequence at the C-terminus of the MHC heavy chain. The fluorochromes used were Phycoerythrin (PE) on the Streptactin and Alexa-488 on the MHC molecules, a very small molecule that is unlikely to interfere sterically with MHC binding and which is highly resistant to bleaching. These multimer reagents were used to stain T cells in an antigen-specific manner (Fig. 14 B and Fig. 15). The cys67 mutation and the conjugation of Alexa-488 did not negatively interfere with staining intensity or efficiency, which was as good as that of conventional MHC tetramers or of conventional unlabeled MHC Streptamers (Fig. 15). The slightly higher staining intensity of the Alexa-488 conjugated reagents in the PE channel (Fig. 15) could be observed in some, but not all cases, indicating a slight variability of the

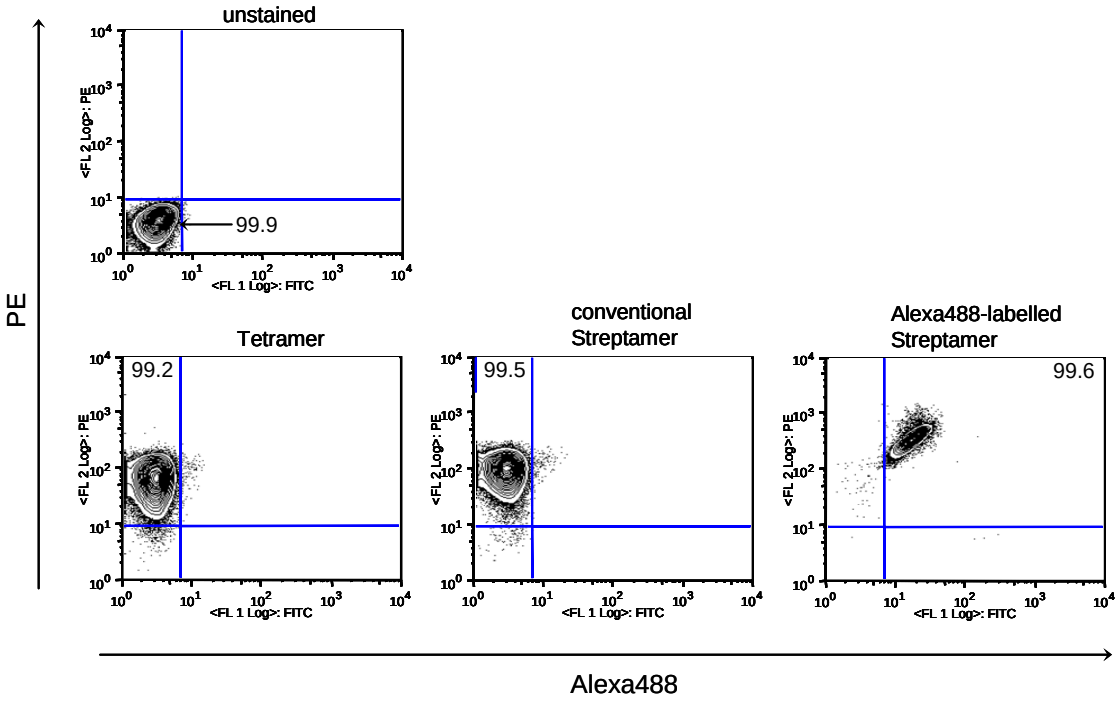

Fig. 15 *Staining of T cells with Alexa-488 labeled Streptamers and comparison to staining with conventional tetramers and conventional unlabeled Streptamers. LLO_{91-99} specific T cells were stained with conventional H2-K^d#45/mβ_2m/LLO_{91-99} Streptavidin-PE tetramers, conventional H2-K^b StreptagIII/mβ_2m/LLO_{91-99} Streptactin-PE Streptamers or fluorochrome-labeled H2-K^b/mβ_2m-cys67 Alexa-488/LLO_{91-99} Streptactin-PE Streptamers. All reagents stain >99% of the cells. No negative influence of the cys67-mutation or the conjugated Alexa-488 on the staining efficiency can be seen.*

Alexa-488 conjugated Streptamers regarding PE staining intensity. We did however never find lower PE staining intensities when comparing Alexa-488 conjugated to unconjugated Streptamers. With the Streptactin heaving a much higher affinity for d-biotin than for the StreptagIII, addition of d-biotin leads to very rapid disruption of the multimers and fast dissociation of the Streptactin backbone (Fig. 14 C). This procedure leaves T cells that are

still covered with monomeric MHC I molecules bound to their TCR, which subsequently dissociate from the cell surface with rates depending on their binding avidity (Fig. 14 D). This dissociation is monitored microscopically at 4° Celsius and the off-rate and half-life time of MHC dissociation can be calculated.

3.2.2 T cell receptor avidity assay for bulk measurements

Cooling is very critical when working with MHC multimers, because the ligation of the TCRs natural ligand combined with TCR crosslinking leads to partial activation of the T cells. This can lead to unwanted effects like T cell anergy, apoptosis or internalization of the multimers. For this reason, we chose inverse confocal laser scanning microscopes (Zeiss LSM 510; Zeiss, Jena, Germany or Leica SP5; Leica Microsystems, Bensheim, Germany) as the microscopic platform for our T cell avidity assay, since an inverse microscope allows for the easy equipment of the experimental setup with a cooling device. Additionally, the confocal laser scanning technology allows for the exact adjustment of the optical planes thickness. This gave

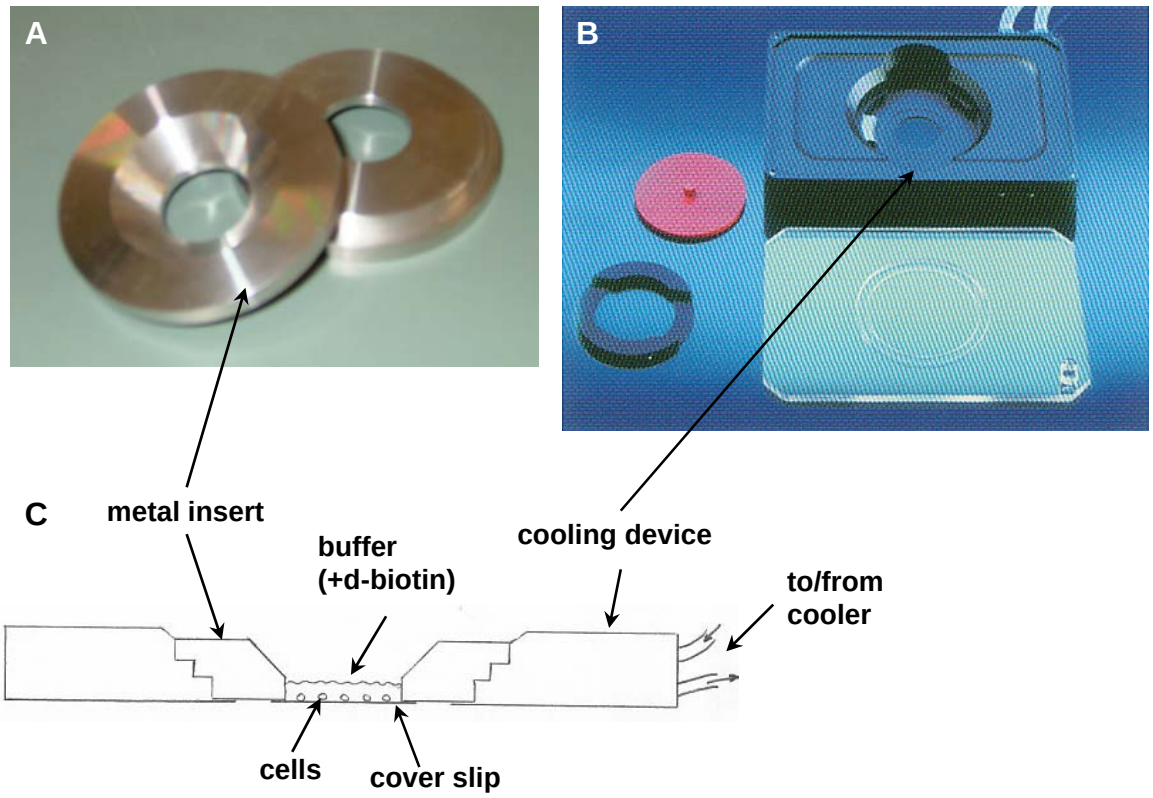

Fig. 16 *Cooling strategy for the TCR avidity assay on bulk level. Metal inserts were designed (A) that fit exactly into the cooling device (Zeiss Temeperable Insert P, Zeiss, Jena, Germany) (B). The metal inserts were sealed with cover slip glass from the bottom using a sealing compound and the buffers and cells added into the resulting reservoir (C).*

us the possibility to acquire fluorescent light from a defined optical plane containing whole individual cells.

For cooling, the microscope was equipped with a water-cooling device (Zeiss Temperable Insert P; Zeiss, Jena, Germany) in combination with a peltier cooler (Huber Minichiller; Huber Kältemaschinenbau, Offenburg, Germany). Since we wanted to perform the assay in an ideally cooled reservoir, we designed stainless steel inserts (Locksmithery; Klinikum rechts der Isar, Munich, Germany) to fit into the cooling device. These inserts were sealed from the bottom with 0.1 mm cover slip glass using a d-biotin free sealing compound. Into this reservoir buffer was added and the cells to be analyzed were pipetted directly onto the glass surface. This setup allowed for optimal cooling and easy monitoring of the cells (Fig. 16, 18). Unfortunately, addition of d-biotin to this system resulted in great disturbance of the cells, which were even flushed out of the observation field. To circumvent this problem, a polycarbonate membrane (pore size 5 µm; Millipore; Bergisch-Gladbach, Germany) was carefully put on top of the cells, which in turn was held in place by a small metal shim (Schneider + Klein; Landscheid, Germany) (Fig. 17, 18). To further reduce movement during the course of the measurement, the cells were allowed to rest for five minutes before and after application of the membrane and metal shim. This setup prevented disturbance of the cells by the addition of d-biotin, but did not hinder the diffusion of the d-biotin to the cells.

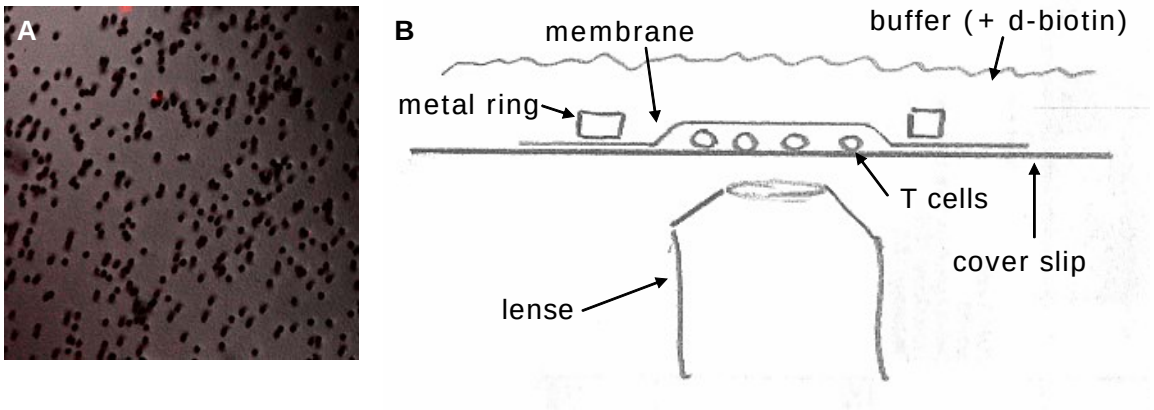

Fig. 17 *A polycarbonate membrane with a pore size of 5 µm (Millipore, Bergisch-Gladbach, Germany) (A) keeps the cells in place. The membrane is held in place by a small metal ring (B).*

With this experimental setup we had in our hands a fast and easy system to analyze up to 40 cells in one measurement. For the exact experimental procedure see 2.2.5.2.

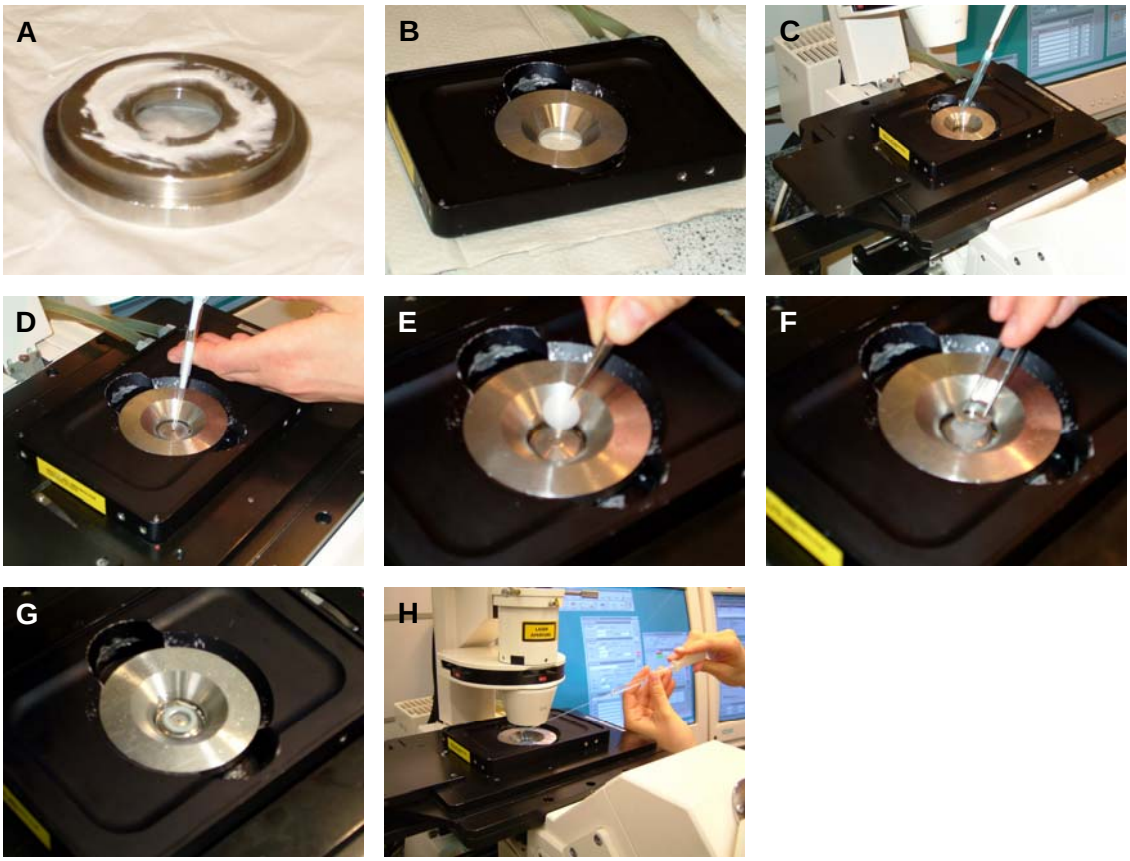

Fig. 18 *Conduction of the TCR avidity assay on bulk level. A metal insert is sealed from the bottom with cover slip glass using a sealing compound (A) and fit into the cooling device (B). The cooling device is mounted onto the microscope stage and buffer as well as the cells are added (C, D). To keep the cells in place, a polycarbonate membrane is put on top of the cells, which is in turn held in place by a small metal ring (E, F, G). After image acquisition is started, d-biotin is added to the system to trigger MHC dissociation (H).*

3.2.3 Data analysis

Data analysis of the movies acquired during the MHC dissociation assay was performed as follows. Fluorescence intensity of each individual cell was measured using MetaMorph image analysis software (Molecular Devices, Downingtown, USA). Here, a gate was drawn around each cell to be analyzed and the cells fluorescence intensity over the whole stack of pictures measured. Background fluorescence intensity in the same gate in close proximity to the cell was acquired as well (Fig. 19). The intensity data were logged into an Excel sheet. Further data analysis from this point on was done automatically with the help of the Analyzer 2.2 software (Jörg Mages, Institute of Medical Microbiology, Immunology and Hygiene, Technical University Munich, Munich, Germany). Here, background fluorescence intensity is subtracted from the fluorescence intensity values measured for the cell. The resulting intensity values plotted against the time resemble an exponential decay, as is expected for MHC

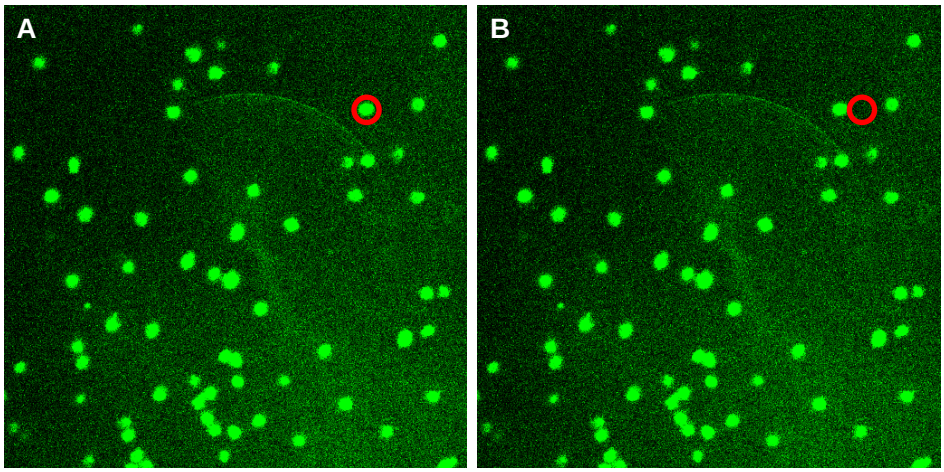

Fig. 19 *Measurement of an individual cells fluorescence intensity. A gate is drawn around the cell to be analyzed (A) and fluorescence intensity is measured over the whole stack of pictures. Background fluorescence intensity in the same gate is measured as well (B).*

dissociation (Fig. 20 A). A small part of the decrease in fluorescence intensity seen is not due

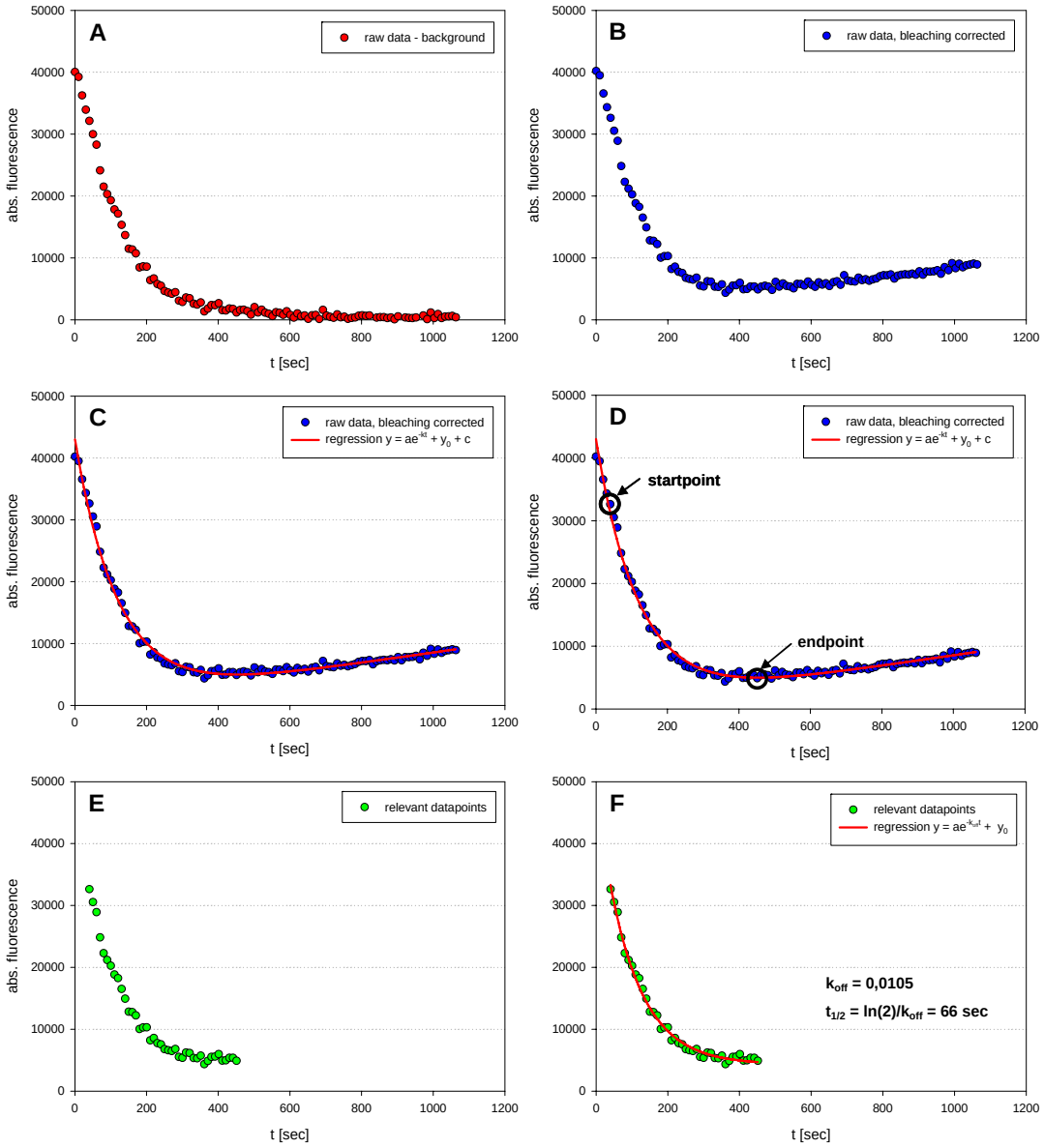

Fig. 20 *Data analysis of the TCR avidity assay shown for Alexa-488 fluorescence. Fluorescence intensity values of each cell and background fluorescence intensity are subtracted from each other (A). Data are corrected for bleaching (B) and data are fit to* $y = ae^{-kt} + y_0 + c$ *(C). The minimum of this regression is defined as endpoint of MHC dissociation and the first value equal or below 80% of the maximum value is defined as start-point (D). Those data-points are singled out (E), fit to* $y = ae^{-k_{off}t} + y_0$ *and the dissociation constant and half-life time are calculated (F).*

to MHC dissociation, but to bleaching of the fluorescent dyes used in the Streptamers. To

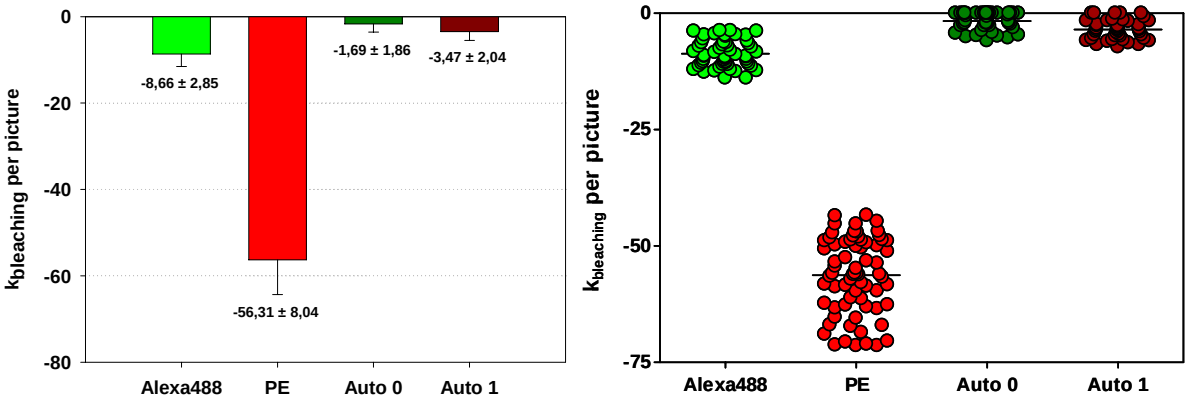

Fig. 21 *Bleaching of fluorescent dyes and of autofluorescence on the Leica SP5 confocal microscope. Cells were stained with anti-CD8α Alexa-488 (N=56), anti-CD8α PE (N=70) or left unstained (N=45). The T cell avidity assay was conducted as usual without the addition of d-biotin and the cells analyzed for loss of fluorescence intensity. Right panel shows bleaching rates per picture taken for individual cells, left panel shows mean bleaching rates per picture taken. Auto 0/ Auto 1: bleaching of autofluorescence in green and red detection channel respectively.*

be able to correct our data for this bleaching effect, we did extensive measurements of the bleaching rates of Phycoerythrin (PE), the dye that is conjugated to the Streptactin backbone of the Streptamers, and of Alexa-488, the dye that is conjugated to the MHC molecules. We found bleaching rates to be very consistent, with PE bleaching moderately fast and Alexa-488 being very resistant to bleaching. The rates measured for PE were -71.38 fluorescence intensity units per picture taken on the Zeiss LSM510 confocal microscope (data not shown) and -56.31 fluorescence intensity units per picture taken on the Leica SP5 confocal microscope (Fig. 21). The rates measured for Alexa-488 were -7.87 fluorescence intensity units per picture taken on the Zeiss LSM510 (data not shown) and -8.66 fluorescence intensity units per picture taken on the Leica SP5 (Fig. 21). The intensity data generated are corrected for these bleaching rates (Fig. 20 B). Since cells in general always display a certain amount of autofluorescence, we never reach fluorescence intensity values of zero with the MHC

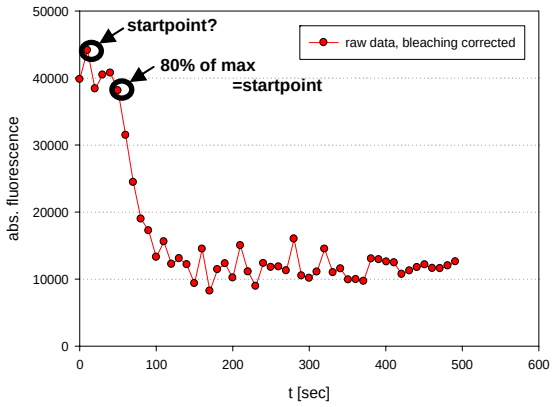

Fig. 22 *Delay in onset of MHC dissociation. Because of this experimental artifact, for automatic data analysis the start-point of MHC dissociation is defined as the first value equal or below 80% of the maximum value.*

dissociation, but reach a certain plateau value which is the level of autofluorescence of the respective cell. From this point onwards, we over-compensate for bleaching, since autofluorescence does bleach much slower, with rates of -1.69 fluorescence units per picture taken in the red detection channel (Auto 0) and -3.47 fluorescence unites per picture taken in the green detection channel (Auto 1) (Fig. 21). This explains the seeming increase in fluorescence intensity (Fig. 20 B), and lets us define the minimum of the graph as the time-point when MHC dissociation is completed. To exactly identify this minimum, we fit the data to the equation $y = ae^{-kt} + y_0 + c$ (Fig. 20 C) and define the x-value of the minimum of this regression as the endpoint of the MHC dissociation. The start-point of MHC dissociation is defined as the first value that is equal or below 80% of the maximum value (Fig. 20 D). The reason for this is the fact that we sometimes saw a certain delay in the onset of the MHC dissociation. This delay was most likely due to differences in the diffusion of d-biotin to the cells. In such cases, defining the maximum fluorescence intensity value as the start-point of MHC dissociation would result in the wrong data-point, as can be seen in figure 22. The data-points between start- and endpoint are now selected out (Fig. 20 E) and fit to the equation $y = ae^{-k_{off}t} + y_0$. The dissociation constant k_{off} is calculated, and the half-life time of the MHC dissociation determined according to the formula $t_{½} = \ln(2)/k_{off}$ (Fig. 20 F). All these steps are done automatically and the graphs, regressions, dissociation constants and half-life times put out by the Analyzer 2.2 software. An example of this output can be seen in Figure 23.

A

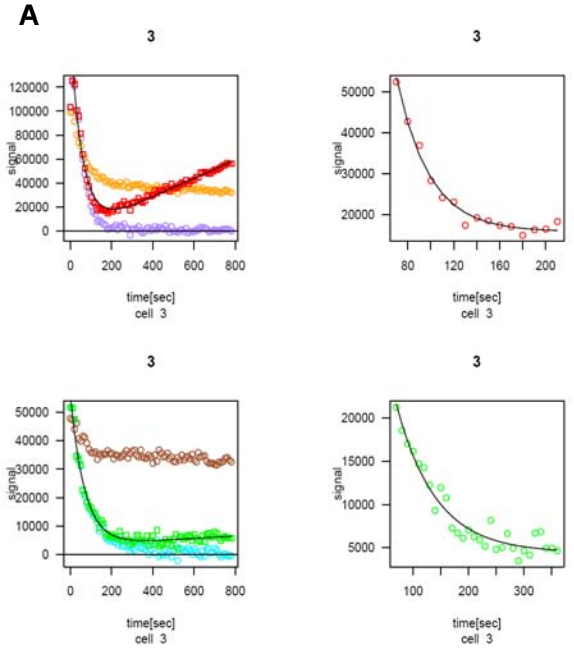

B

cells	cell.names	k(PE)	t1/2(PE)	k(Alexa)	t1/2(Alexa)
1	1	0.0654	10.59	0.0416	16.67
2	2	0.0411	16.87	0.0382	18.16
3	3	0.035	19.82	0.014	49.42
4	4	0.0396	17.52	0.0239	28.94
5	5	0.0207	33.53	0.0183	37.97
6	6	0.0446	15.53	0.0133	51.96
7	7	0.0259	26.78	0.0305	22.72
8	8	0.0603	11.5	0.0159	43.64
9	9	0.016	43.44	0.0094	73.56
10	10	0.0811	8.55	0.0119	58.11
11	11	0.0427	16.22	0.0277	25.02
12	14	0.036	19.25	0.0056	124
13	15	0.0455	15.24	0.0345	20.11
14	16	0.0411	16.86	0.0089	77.66
15	17	0.0812	8.54	0.0212	32.66
16	18	0.0394	17.6	0.0176	39.49
17	19	0.0662	10.46	0.0108	64.2
mean	NA	0.046	18.135	0.02	46.135
sd	NA	0.019	9.092	0.011	27.658

Fig. 23 *Output of the Analyzer 2.2 software. Graphs and regressions for one cell (A) and dissociation constants and half-life times for all cells are shown (B).*

3.2.4 Evaluation and validation of the assay

A reliable and robust assay system for the measurement of MHC off-rates should be able to give uniform results for different T cells that possess the same T cell receptor. To test whether our assay can fulfill this requirement, we sought to analyze TCR-transgenic T cells because these exclusively express identical TCRs. To do this, we chose two different TCR-transgenic models, the OT-1 mouse which is transgenic for a TCR that recognizes H2-K^b/SIINFEKL (Hogquist et al., 1994), and the 2C mouse (Saito et al., 1984; Sha et al., 1988) which is transgenic for a TCR that recognizes its native epitope H2-K^b/dEV8 and also the allogenic epitope H2-L^d/p2Ca with a much higher avidity. The OT-1 system is a very wide-spread model system for the analysis of $CD8^+$ T cell responses in the mouse, and the 2C TCR is probably the most well characterized TCR available regarding its structure, as well as its binding avidity that has been measured using other assay systems (see 1.7.2) allowing us to compare these results with the results generated in our novel assay system.

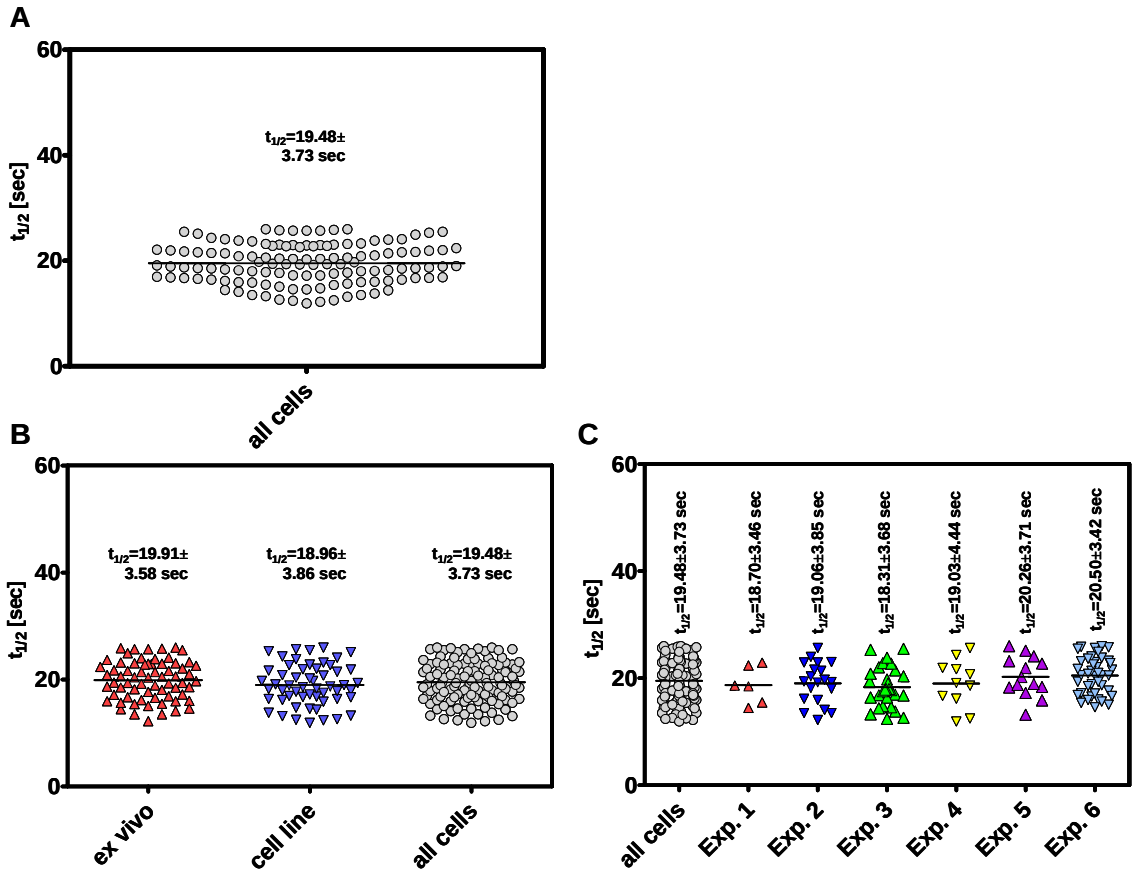

Fig. 24 *TCR avidity assay on TCR-transgenic OT-1 cells. The 121 cells analyzed show half-life times of MHC dissociation in a very narrow range (A). Comparing naïve ex vivo cells (N=67) and activated cells from a T cell line (N=54) shows independence from the cells activation status (B). Data from six independent experiments (N=6, 20, 29, 11, 14, 41) show good reproducibility of the system (C).*

We analyzed 121 individual OT-1 cells in six independent experiments that all showed half-life times of MHC dissociation in a very narrow range around a median of 19.48 seconds with a standard deviation of 3.73 seconds (Fig. 24 A). Of these 121 cells, 67 cells were *ex vivo* isolated cells, and 54 cells came from *in vitro* stimulated cell cultures. The rationale behind this was that *ex vivo* isolated cells have a naïve phenotype, while *in vitro* stimulated T cell lines have an activated phenotype. This important difference in cell physiology, which might affect functional avidity, should not influence the outcome of our assay if the assay really measures pure TCR/coreceptor binding strength. As expected, the half-life times of MHC dissociation for different activation stages were very similar, with 19.91±3.58 seconds for naïve, and 18.96±3.86 seconds for activated OT-1 cells (Fig. 24 B). A robust and reliable assay system has to deliver reproducible results in independent experiments. In six independent experiments with OT-1 T cells, we measured half-life times of 18.70±3.46 seconds (N=6), 19.06±3.85 seconds (N=20), 18.31±3.68 seconds (N=29), 19.03±4.44 seconds

(N=11), 20.26±3.71 seconds (N=14) and 20.50±3.42 seconds (N=41) (Fig. 24 C), which proofs a very good reproducibility of the assay.

Next we analyzed TCR-transgenic 2C T cells. Unfortunately we could not achieve any Streptamer staining with the allogenic epitope H2-L^d/p2Ca, even though the interaction of the 2C TCR with this molecule is described to be of a very high avidity. We could however stain the exact same cells with the syngenic epitope H2-K^b/dEV8, which indicates that TCR expression was normal. The reason for this inability to stain 2C cells with allogenic H2-L^d/p2Ca Streptamers could never be conclusively resolved. There is however another example of TCR-transgenic T cells that cannot be stained with MHC multimers despite sufficient TCR expression in the so called DO11.10 cells that are specific for the *Listeria monocytogenes* epitope $p60_{217-225}$. 2C cells stained with syngenic H2-K^b/dEV8 Streptamers showed off-rates and half-life times of MHC dissociation that were equally uniform than those found for OT-1 T cells. We could measure 51 *ex vivo* isolated cells that showed a half-life time of 12.71 seconds with a standard deviation of only 3.76 seconds (Fig. 25).

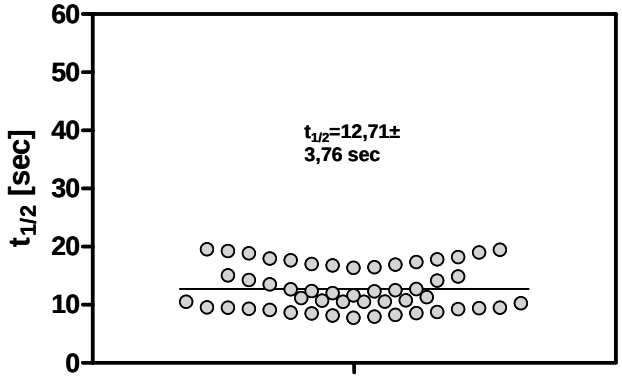

Fig. 25 *TCR avidity assay on TCR-transgenic 2C cells. The 51 cells analyzed show half-life times of H2-K^b/dEV8 dissociation in a very narrow range around a mean value of 12.71 seconds.*

All in all, our results using TCR-transgenic T cells show very uniform off-rates and half-life times of MHC dissociation. This is true for two different cell types, for independent experiments and for cells with different activation status. This proves that our novel assay system can generate meaningful and highly reproducible data.

3.3 HIGHER FUNCTIONAL AVIDITY CORRELATES WITH HIGHER STRUCTURAL AVIDITY

In 3.1 we showed two different LLO_{91-99} specific $CD8^+$ T cell lines that exhibit different functional avidities and have different protective capacities *in vivo*. To see whether these differences in functionality correlate with different MHC off-rates and half-life times of MHC dissociation, we analyzed both cell lines in our TCR avidity assay.

We measured 54 cells from cell line A (restimulated with 10^{-6} M peptide) and 84 cells from cell line B (restimulated with 10^{-9} M peptide). Of cell line A, 89% showed a relatively fast MHC dissociation, with half-life times ranging from 6 to 27 seconds with a maximum at 11 to 12 seconds. 9% of the cells showed a half-life time around 40 seconds and 2% a relatively slow MHC dissociation with a half-life time of over 160 seconds. In sharp contrast, we find only 44% of the cells from cell line B in the range of 6 to 29 seconds half-life time for MHC dissociation. 18% of the cells show a half-life time from 40 to 100 seconds, and 38% half-life times above 100 seconds up to almost 340 seconds (Fig. 26). Interestingly, we find also in cell line B cells with half-life times in the low range between 6 and 30 seconds. Nevertheless, we find in this cell line also a substantial proportion (56%) of cells showing a high to very high structural avidity, with half-life times of MHC dissociation ranging from 40 up to 340 seconds.

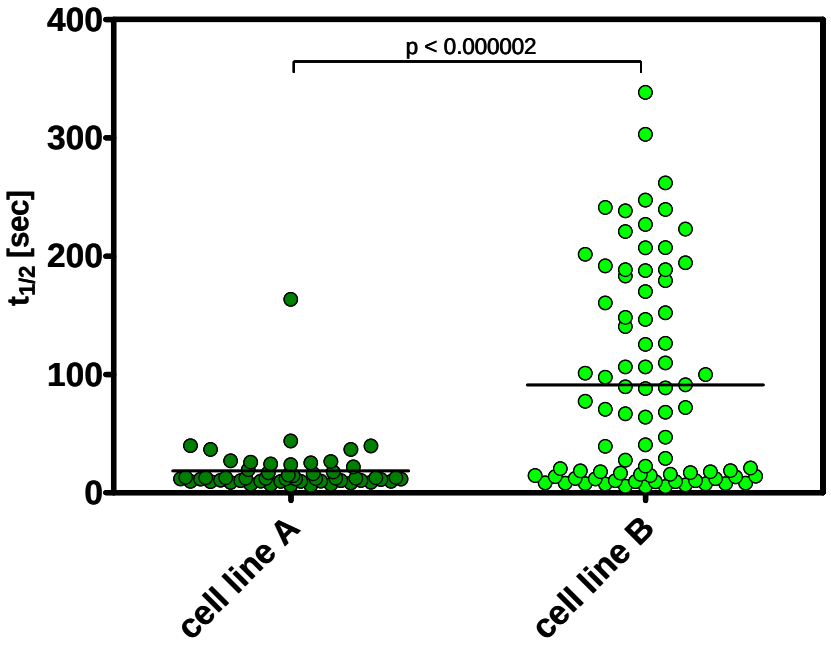

Fig. 26 *Structural avidity of two LLO_{91-99} specific T cell lines. 89% of the cells from cell line A show a fast half-life time of MHC dissociation below 30 seconds. A few cells show half-life times around 40 seconds, and one a half-life time of 160 seconds. In sharp contrast, 56% of the cells from cell line B show a half-life time above 40 seconds and up to 340 seconds, revealing a substantial proportion of high structural avidity cells in cell line B. Statistical significance as determined in Wilcoxon-Mann-Whitney test is shown.*

These results support the interpretation that the differences regarding functional avidity as well as protective capacity are a consequence of the different prevalence of high and low avidity TCRs in the two cell lines. This assumption is further strengthened by the fact that both cell lines were generated from the same *Listeria monocytogenes* infected mouse, and treated in the same manner except for the different peptide concentrations used for restimulation. It is well possible that the protective effect of cell line B (see 3.1.2) is preferentially mediated by the 55% of the cells that show a slow to very slow MHC dissociation alone, making the difference in protective capacity even more striking.

To support the results we generated with the LLO_{91-99} specific T cell lines described above in a clinically more relevant system, we obtained two T cell lines specific for the murine cytomegalovirus (mCMV) epitope $m164_{257-265}$ (Holtappels et al., 2002) from the laboratory of Prof. M. Reddehase at the Institute for Virology, University of Mainz. Murine CMV infection serves as a model system for CMV infection in humans, which is a major cause of complications in immunocompromised patients or patients that received hematopoetic stem cell transplants.

Just like the LLO_{91-99} specific T cell lines, the two $m164_{257-265}$ specific cell lines were restimulated with high and low amounts of peptide (10^{-8} M $m164_{257-265}$, cell line A; 10^{-10} M $m164_{257-265}$, cell line B). The functional avidity of these cell lines had been determined in the laboratory of Prof. Reddehase, using ELISPOT (data not shown) and ^{51}Chromium release assays (Fig. 27 A). In the ^{51}Chromium release assay, cell line B showed the higher functional

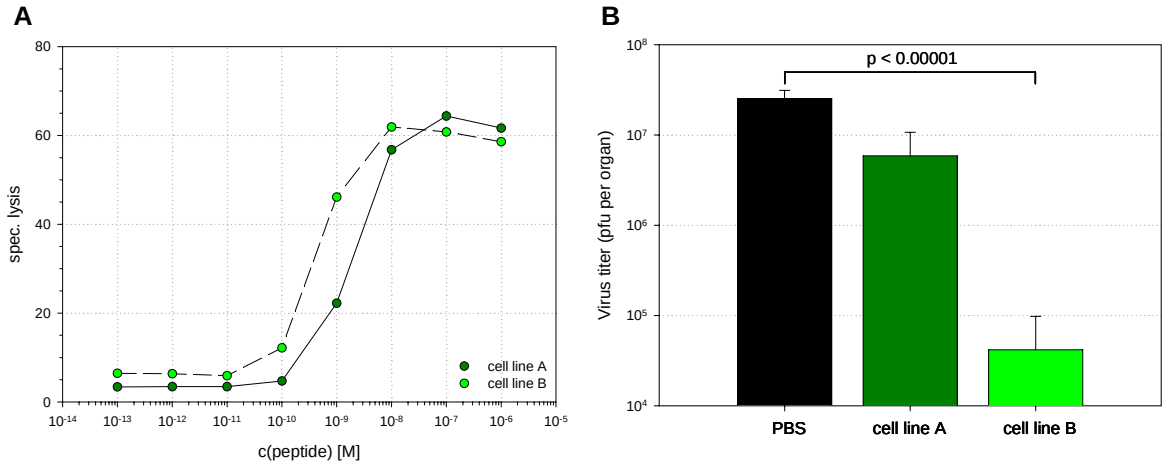

Fig. 27 *Functional avidity and protective capacity of two $m164_{257-265}$ specific T cell lines. In a ^{51}Chromium release assay cell line B responds more readily to lower peptide concentrations than cell line A. Specific lysis is plotted against the peptide concentration used for stimulation of the cells. The peptide concentrations needed to reach 50% specific lysis for both cell lines is shown (A). Protective capacity was determined after transfer of 10^6 cells of the respective cell line and intrafoodpad infection with 10^5 PFU of mCMV. The number of mCMV PFU in the spleen was determined at d12 postinfection. Control mice received PBS instead of cells. Statistical significance as determined in unpaired Student´s t-test is shown. Error bars show standard deviation (B).*

avidity with 1.7 x 10^{-9} M peptide needed for 50% specific lysis compared to 6.5 x 10^{-9} M peptide for cell line A. A similar difference was found in the ELISPOT assay. The protective capacity of the two cell lines was determined as well. BALB/c mice were given 10^6 cells from cell line A or cell line B i.v. and infected by intrafoodpad injection with 10^5 PFU mCMV. At day 12 postinfection, the number of mCMV PFU was determined in the liver, lung (data not shown) and spleen (Fig. 27 B). Mice that had received cells from cell line A showed almost no reduction of mCMV PFU compared to mice that received PBS only. In sharp contrast, mice that received cells from cell line B showed a 100-fold reduction in mCMV PFU, demonstrating the very good protective capacity of the high functional avidity cell line B.

Again, we analyzed both cell lines in our TCR avidity assay to see whether the differences in T cell functionality would correspond to differences in MHC off-rates and half-life times of MHC dissociation. We measured 34 cells from cell line A (restimulated with 10^{-8} M peptide) and 78 cells from cell line B (restimulated with 10^{-10} M peptide). In cell line A, 76% of the cells showed a relatively fast MHC dissociation, with half-life times between 10 and 40 seconds with a maximum around 30 seconds. 7% of the cells showed half-life times ranging from 50 to 100 seconds and only 3% showed a relatively slow MHC dissociation with a half-life time of 160 seconds. Cell line B in contrast showed only 14% of the cells in the fast MHC dissociation region with half-life times between 10 and 40 seconds. 67% of the cells were lying in the region between 50 and 100 seconds, 10% between 100 and 140 seconds, and 9% of the cells showed a very slow MHC dissociation with half-life times of 150 seconds and more, with some exceeding 200 seconds (Fig. 28). Like in the LLO_{91-99} specific T cell lines described above, we find also in cell line B cells that show a fast MHC dissociation with half-life times between 10 and 40 seconds, but find also a quite substantial proportion (86%) of cells with slow to very slow MHC dissociation.

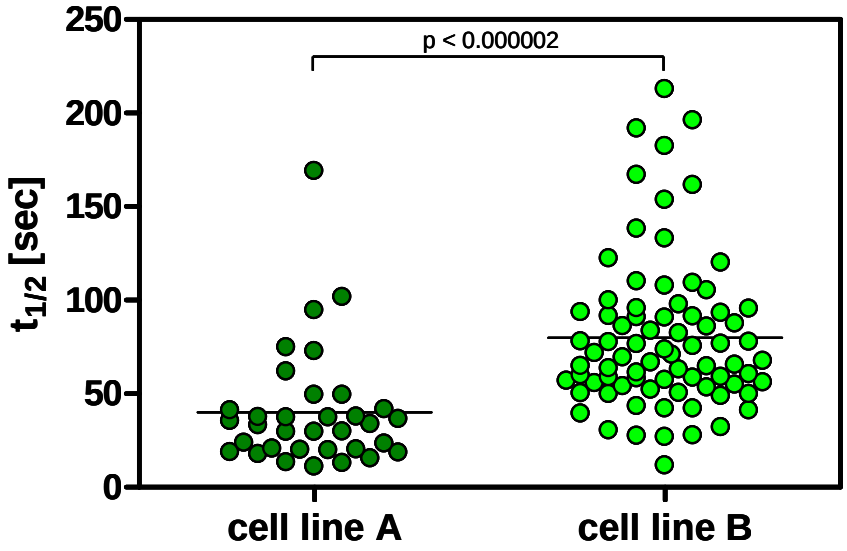

Fig. 28 *Structural avidity of two m164$_{257-265}$ specific T cell lines. 76% of the cells from cell line A show a fast half-life time of MHC dissociation below 40 seconds. A few cells show a half-life time between 50 and 100 seconds and one cell a half-life time of 160 seconds. In sharp contrast, 86% of the cells from cell line B show a half-life time above 50 seconds and up to more than 200 seconds, revealing a substantial proportion of high structural avidity cells in cell line B. Statistical significance as determined in Wilcoxon-Mann-Whitney test is shown.*

These results confirm the results we generated using LLO$_{91-99}$ specific T cell lines and further support the interpretation that differences in functional avidity and protective capacity between different T cell lines are a consequence of the different prevalence of high and low avidity TCRs. Also here it is very well possible that the strong protective effect of cell line B is preferentially mediated by the 86% of cells that show a slow to very slow MHC dissociation alone.

To further elucidate the role of those cells that were characterized by a slow to very slow MHC dissociation for protective effects, we tried to generate clones out of the LLO$_{91-99}$ specific cell line B by limiting dilution and long-term peptide restimulation. By this procedure, we were only able to establish one LLO$_{91-99}$ specific clone (clone B) for further analysis, demonstrating the difficulties in the generation and maintenance of murine T cell clones. The MHC dissociation rates were found to be in a range of 55 to 120 seconds, with a maximum around 80 seconds for the 23 cells analyzed for this particular clone (Fig. 29). Compared to the spectrum of MHC dissociation rates found for the parental cell line, this represents an intermediate to low avidity. This finding is in line with the observations by many other groups obtained for murine and human T cells that it is extremely difficult to establish T cell clones with high avidity for their specific ligand. Obviously, *in vitro* culture systems tend to select for T cells with low to intermediate avidity. We tested clone B for its protective capacity and found only weak protection compared to cell line B after short-term in

vitro culture (Fig. 29). This finding is in accordance with the intermediate to low MHC dissociation rates found for this clone.

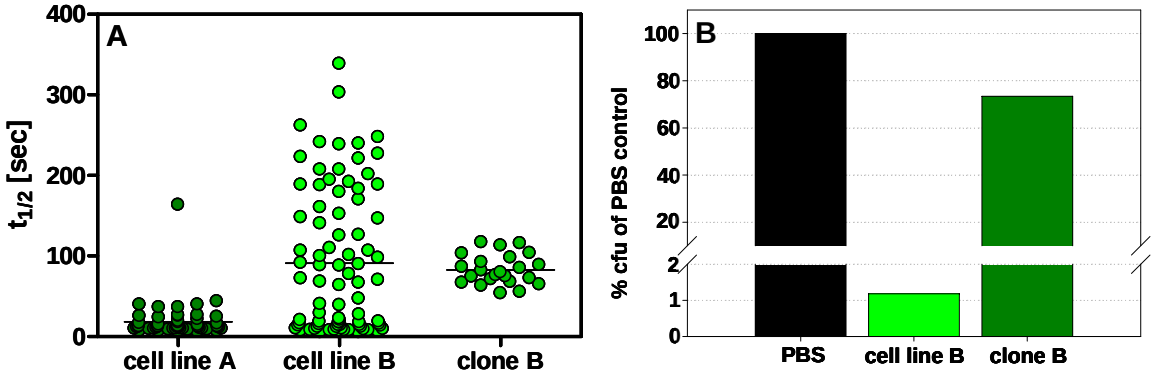

Fig. 29 *Structural avidity and protective capacity of clone B. Only cells with intermediate MHC dissociation half-life times could be kept in culture. MHC dissociation half-life times of the cell lines A and B after short-term in vitro culture are shown for comparative reasons (A). Protective capacity of clone B in comparison to cell line B after short-term in vitro culture is shown as percent L.m. cfu compared to PBS control in the spleen (B).*

The heterogeneity of the high avidity cell lines after short-term *in vitro* culture, and the inability to long-term culture and clone specifically those cells that are characterized by a slow to very slow MHC dissociation lead us to the conclusion that for potential therapeutical applications we had to find a way to sort selectively cells with distinct k_{off} values out of a heterogeneous high functional avidity cell line.

3.4 TCR AVIDITY ASSAY FOR SINGLE CELL MEASUREMENTS AND SUBSEQUENT SORTING

Our analysis of different T cell lines showed that cell lines with a high functional avidity are characterized by a broad spectrum of half-life times of MHC dissociation, comprising cells with relatively fast half-life times, but also a substantial proportion of cells with slow to very slow half-life times. It is reasonable to assume that the good protective effect of such cell lines is preferentially mediated by the cells that show slow to very slow MHC dissociation, making these cells the ideal candidates for potential therapeutical applications. This might be the adoptive transfer of such cells, either directly or after *in vitro* expansion, which might be difficult as we have seen before, or the identification and sequencing of the cells´ TCR to genetically generate high avidity T cells. Since high functional avidity T cell lines still contain substantial proportions of cells with fast MHC dissociation rates, and the cell culture of cells

with slow to very slow MHC dissociation rates proved to be difficult, we were trying to find a way to recover cells after the measurement of their MHC off-rates and dissociation half-life times to facilitate research into such potential therapeutical applications.

In our search for an experimental system that would allow the conduction of our assay and the subsequent recovery of analyzed cells, we found the Evotec Cytocon400 system. The core element of this system is a micro channel flow-through device, the so called CellProcessor chip (Fig. 30 A), which is equipped with dielectrophoretic elements for contact-free cell guidance and trapping within a detection window. Individual cells can be trapped in a field cage (Fig. 30 B), floated with a reagent, imaged, sorted, and deposited into micro titer plates (Fig. 30 C) or other reaction tubes, while maintaining cell viability (Fiedler et al., 1998;

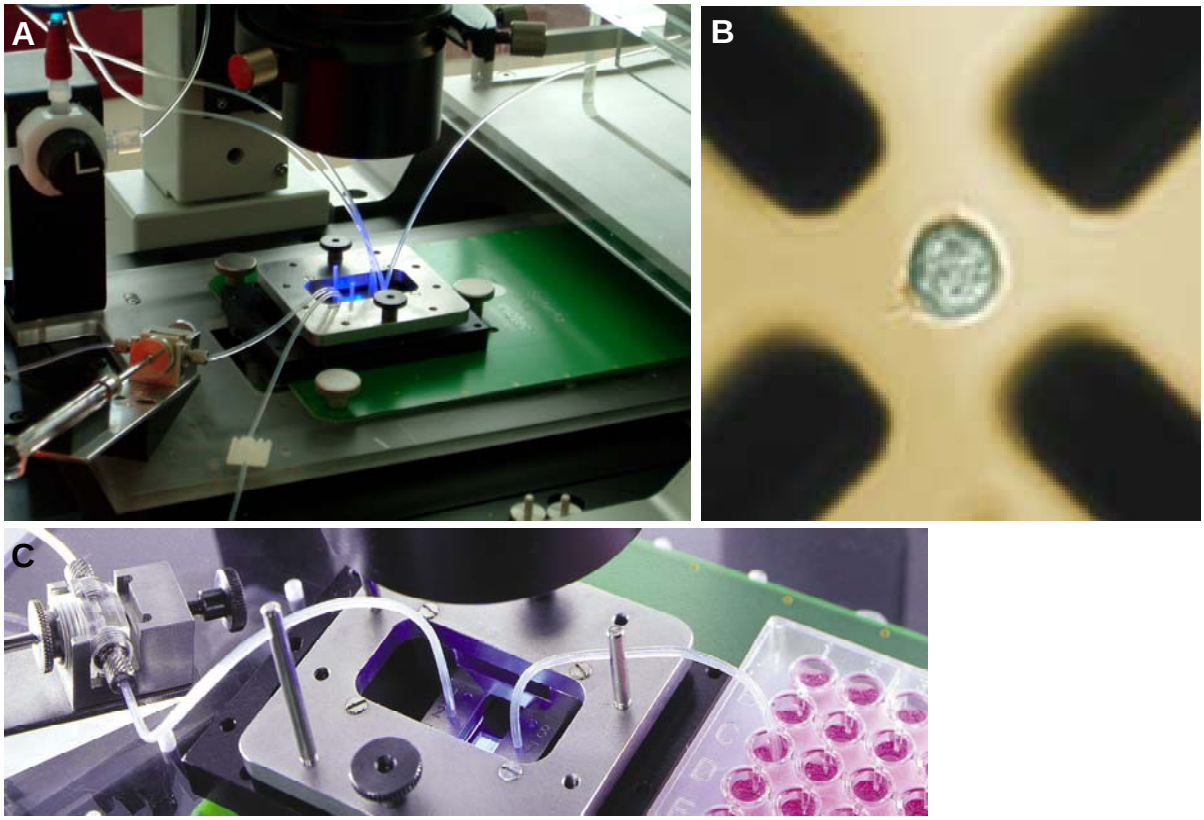

Fig. 30 *Evotec Cytocon400 system. CellProcessor chip mounted to the microscope stage. Tubing leading cells and buffers into and out of the chip can be seen (A). Single cell trapped inside the field cage (B). Sorting of individual cells into a 96-well plate (C).*

Kentsch et al., 2003). Streptamer stained cells are loaded into the chip with the help of high precision syringe pumps, a single cell is trapped in the field cage and our assay started under microscopic control by the addition of d-biotin into the chip, again with the help of a high precision syringe pump. After complete dissociation of the MHC molecules, the cell is

released from the field cage and flushed out of the chip, where it can be picked with a pipette and deposited in a reaction tube for further analysis.

We tested whether the results generated in this new system were similar to the ones generated in the bulk measurement setup by comparing half-life times of MHC dissociation from OT-1 T cells measured in the single cell sorting setup using the Evotec Cytocon400 to cells measured in the bulk setup. The half-life times measured were 19.48±3.73 seconds (N=121) for bulk analysis and 14.97±3.54 seconds (N=8) for analysis using the Evotec system (Fig. 31). The slightly faster half-life times seen in the Evotec system are not unexpected and very likely due to the fact that here the assay is performed under a constant buffer flow that actively transports dissociated MHC molecules away from the cell. This result shows again the robustness and good reproducibility of our MHC dissociation assay. Furthermore, it opens up the possibility to not only identify high avidity T cells that exhibit slow to very slow MHC dissociation, but to also recover such cells after completion of the assay for further use as therapeutic agents.

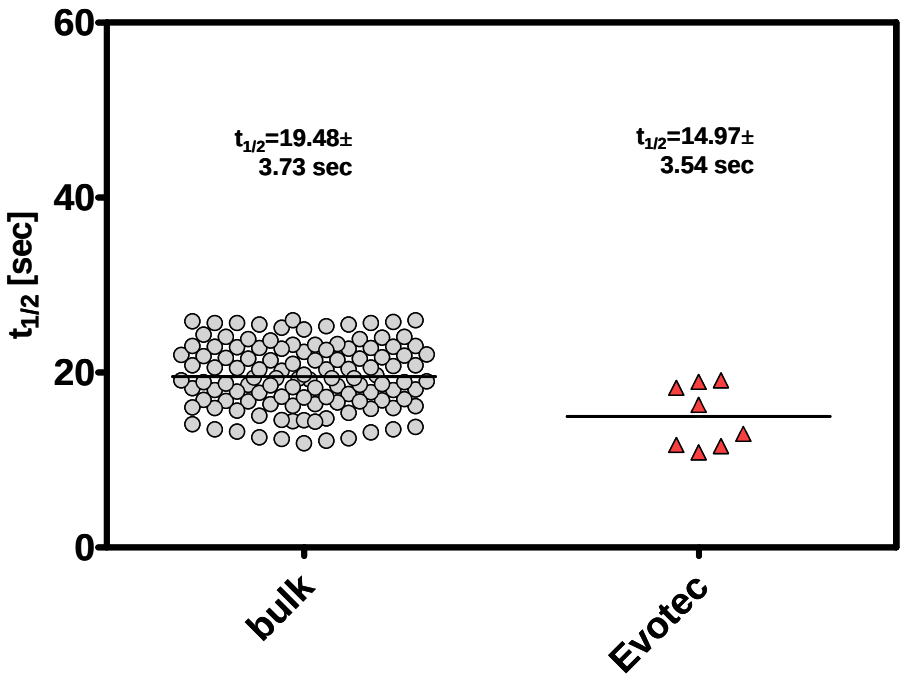

Fig. 31 *Comparison of TCR-transgenic OT-1 cells analyzed in the bulk setup or the Evotec system. Half-life times of MHC dissociation in the Evotec system are slightly faster because dissociated MHC molecules are actively transported away from the cell in this setup.*

4 DISCUSSION

With this PhD work, a novel method for the measurement of MHC off-rates and half-life times of MHC dissociation on the level of single cells was established. This novel assay is based on the dissociation of monomeric MHC molecules from the surface of living T cells, which clearly distinguishes the assay from other MHC multimer-based approaches for the measurement of structural T cell avidity. Using this novel assay, we could show that the functional avidity of T cells can directly correlate with their MHC off-rate. We could also show that T cells with a higher structural avidity are superior regarding their protective capacity upon *in vivo* transfer. Combination with a new technique that allows capturing and sorting of single cells gave us the possibility to recover T cells of defined structural avidities after conduction of the assay. In first experiments, we could show that the TCR sequences of such cells can be identified. This opens up fascinating new possibilities for the rapid identification and use of high avidity T cells as a therapeutic agent.

4.1 A NEW WAY TO DETERMINE STRUCTURAL T CELL AVIDITY

T cell avidity can be best described as the efficiency by which a T cell can react to antigen encounter. Since the readout systems to measure this parameter most often measure aspects of T cell function, this efficiency is often termed the ´functional avidity` of a T cell. Functional avidity is influenced by several factors. These are on the one hand functional factors like expression levels of TCR, expression of CD8αβ heterodimers (Cawthon and Alexander-Miller, 2002; Cawthon et al., 2001), efficiency of downstream signaling events and others, and on the other hand structural factors, that is, the strength of the physical interaction between the TCR, its coreceptor and their ligand, the peptide-loaded MHC molecule. This latter parameter is termed the structural avidity of a T cell.

T cells with a high functional avidity have been shown in different model systems to be superior regarding their *in vivo* efficacy for protection against viruses or tumors (Alexander-Miller et al., 1996; Derby et al., 2001; Dutoit et al., 2001; Sedlik et al., 2000; Yee et al., 1999; Zeh et al., 1999). Therefore, we, among others, reasoned that T cells with a high functional avidity should be better suited for adoptive T cell therapies. However, the central question in this field has always been how to generate and/or to identify T cells with a high functional avidity. While the classic functional assays like intracellular cytokine staining or ^{51}Chromium

release assay can identify high avidity T cells in a multi-cell fashion, these assays do not work on the level of single cells and do not allow for the isolation or generation of T cells with a distinct functional avidity. This intrinsic problem could so far only be overcome by laborious T cell cloning by limiting dilution and long-term *in vitro* restimulation. Unfortunately, T cell culture is often very difficult, time consuming and not very reliable.

For these reasons, we tried to pursue another way to reach our ultimate goal of identifying high avidity T cells for use as a therapeutic agent. We suggested that there might be a direct correlation between functional T cell avidity and the structural avidity of an antigen-specific T cell. In the meantime we have evidence that this is truly the case from our own data (see 3.3), as well as from a recent publication where it could be shown that gene transfer of tumor-reactive TCRs confers both similar functional avidity and tumor-reactivity to PBMCs as it was characteristic for the parental cell (Johnson et al., 2006). Therefore, we reasoned that an elegant way to generate high avidity T cells would be to identify such cells via their structural avidity on the level of single cells. Once identified, cells with a high structural, and therefore also high functional avidity could be used for further experiments, for direct adoptive transfer or for the identification of high avidity TCR sequences. Unfortunately, the existing methods available to measure structural T cell avidity suffered from more or less severe drawbacks. Surface plasmon resonance measurements require the expression of active, soluble TCR. Although this has been achieved for several TCRs (Garboczi et al., 1996; Garcia et al., 1996; Gregoire et al., 1996; Lin et al., 1990), not one method of expression works for all TCRs, making TCR production difficult. Also, study of the contribution of the CD8 coreceptor to structural avidity is currently impossible using surface plasmon resonance, since the purification of active CD8αβ heterodimers has never been achieved. Conventional MHC multimer-based techniques for the determination of structural T cell avidity are not the ideal tools either. First of all, there seems to be no correlation between tetramer staining intensity and structural avidity (al-Ramadi et al., 1995; Echchakir et al., 2002; Palermo et al., 2001). Second, assays that are based on the dissociation of MHC tetramers always require the blocking of the rebinding of tetramers to the cells. This results in very complicated and slow dissociation kinetics that are very hard to interpret and are unlikely to solely reflect TCR binding strength (Alexander-Miller, 2005; Wang and Altman, 2003). In our eyes, the ideal experimental setup for the measurement of structural T cell avidity can only be a setup that allows to get as close as possible to singular TCR/coreceptor – pMHC interactions, preferably on a living T cell surface. To be able to do this, we decided to develop a novel assay system for the measurement of MHC off-rates and

half-life times of MHC dissociation based on the dissociation of monomeric MHC molecules from living T cell surfaces.

Formally we do not measure avidity with this assay, which is defined as the quotient between on- and off-rate, because MHC on-rate measurements are not possible in this system. We and others (Alam et al., 1996; Lyons et al., 1996) do however strongly believe that MHC off-rate is the major determinant of structural T cell avidity. This belief is supported by the fact that MHC on-rates have been found to be very uniform between different TCRs, between identical TCRs binding to different epitopes and most importantly between identical TCRs that exhibit very different MHC off-rates for different MHC molecules (Garcia et al., 1997; Lee et al., 2004). Furthermore, it seems very reasonable to assume that a T cells ability to get activated or to exert distinct effector functions is mainly determined by the length of time that the contact to an APC or a target cell is existent and not by the speed with which this contact is established. This assumption is supported by a study that examined the influence of TCR – pMHC dwell-time on the outcome of TCR engagement and could show that an optimal dwell-time is needed for efficient T cell activation (Kalergis et al., 2001). For these reasons, the terms high/low structural T cell avidity and slow/fast MHC off-rate are used in a loosely synonymous way throughout this thesis.

The novel assay is based on the so called MHC Streptamer technique (Knabel et al., 2002). These MHC multimers can be specifically disrupted by the addition of d-biotin resulting in the monomerization of the MHC molecules. We generated fluorochrome-labeled MHC molecules for multimerization with fluorochrome-labeled Streptactin resulting in dichromatic Streptamers. Conjugation of the fluorochrome to the MHC molecule was done at a reactive cysteine in position 67 of the mβ_2m that was exchanged against the native tyrosine. The amino acid at position 67 has been shown to lie at the surface of the mβ_2m (Parker and Strominger, 1983). The exchange of the native amino acid against a cysteine has been shown to be unproblematic concerning the refolding, function and binding of the MHC molecule (Walter et al., 1998). We could also show that the cys67 mutation and the conjugation of the fluorochrome Alexa-488 to this cystein does not alter multimer binding to the cells. Whether the mutation affects the dissociation of the MHC molecules has never been formally examined. However, given the position of the cys67 in the three-dimensional structure of the MHC, this seems to be highly unlikely. An alternative approach for the conjugation of fluorochromes to the MHC could be the insertion of a peptide-sequence at the C-terminus of the MHC heavy chain that serves as target-sequence for the enzymatic conjugation of fluorochromes. This approach is currently under investigation in our laboratory.

The mβ_2m/Alexa-488 conjugated reagents were used to stain T cells in an antigen-specific manner. Upon addition of d-biotin the Streptamers were disrupted and the cells left with monomeric fluorochrome-labeled and TCR-bound MHC molecules. The subsequent dissociation of the MHC molecules was monitored microscopically and an off-rate and a half-life time of the dissociation calculated.

Staining T cells with MHC multimers at physiological temperatures can result, among other effects, in the internalization of the multimers (Knabel et al., 2002). For this reason, optimal cooling of the cells during performance of the assay was of great importance for the technical implementation of this principle. We achieved this by using custom-made metal inserts that were fit into a water-cooled cooling device. These inserts constituted the lateral boundaries of the reservoir in which the assay was performed. Conduction of the assay in this reservoir in a relatively large volume of buffer allowed for the best and most constant cooling possible. One major technical problem occurred when we realized that the addition of d-biotin to the reservoir resulted in great disturbances of the cells, which in most cases were simply flushed out of the observation window. To solve this problem, we first tried to aspirate single cells to a micro-pipette. Unfortunately this proved to be technically difficult, very time-consuming and cumbersome. Furthermore, this approach would have allowed for the analysis of only one cell at a time. We then found a very simple and elegant solution to the problem of cell disturbance by putting a polycarbonate membrane (pore size 5 μm) on top of the cells. This membrane was in turn held in place by a small metal ring. The membrane did not touch the cells directly, but constituted a barrier for the micro-currents in the reservoir preventing disturbance of the cells. Diffusion of d-biotin to the cells was not hindered.

The amount of raw data generated by our new assay turned out to be extensive, which made manual data analysis quite time-consuming. Therefore, we defined clear-cut criteria that would allow automation of data analysis. First of all we tried to find criteria for the exact definition of the end-point of MHC dissociation. This was necessary because we never reach fluorescence intensity values of zero, but values that correspond to the level of autofluorescence of the individual cell. Since autofluorescence bleaches only very slowly, the compensation factor that we use to correct the raw data for bleaching of the fluorescent dyes leads to a virtual increase in fluorescence intensity beginning at the point where only autofluorescence of the cell is left, in other words the point where MHC dissociation is complete. This allowed us to define the end-point of MHC dissociation as the minimum of the dataset. Since individual data-points always scatter, we decided to fit each dataset to the equation $y = ae^{-kt} + y_0 + c$, reflecting an exponential decay with a linear component, which is

the bleaching of the dye. The minimum of this regression is defined as the end-point of MHC dissociation. The bleaching rates of the fluorescent dyes under the experimental conditions of the T cell avidity assay were carefully determined beforehand. The experimental setup to do this was exactly the same as in the assay, except for the lack of d-biotin. Bleaching rates were found to be very consistent, moderately fast for PE, and very slow for Alexa-488, a dye that is known for its high bleaching resistance.

Next we tried to find criteria for the exact definition of the start-point of MHC dissociation. Simply choosing the maximum value of fluorescence intensity sometimes yielded obviously wrong results. This was due to the fact that in some cases we saw a certain delay of the onset of MHC dissociation. During this delay, fluorescence intensity values scattered wildly, resulting in the selection of a wrong start-point when choosing the point of maximum fluorescence intensity. This delay was most likely due to differences in the diffusion of d-biotin to the cells, maybe in some cases to unspecific adhesion of the Streptactin backbone or to initial cell movements. To circumvent these problems, we decided to use the first fluorescence intensity value that is equal or below 80% of the maximum value as the start-point of MHC dissociation. This posed no problem for accuracy of the data analysis, since the data very closely reflect the model of an exponential decay, so that the range of values used for the determination of the off-rate and the half-life time of MHC dissociation is not critical. The data-points lying between the start- and end-point of MHC dissociation were now singled out and fit to the equation $y = ae^{-k_{off}t} + y_0$, which describes an exponential decay with an offset y_0, the level of autofluorescence. From this regression, the off-rate of MHC dissociation k_{off} and the half-life time $t_{1/2}$ could easily be calculated.

All this was implemented in a software analysis tool (Jörg Mages; Institute of Medical Microbiology, Immunology and Hygiene, Technical University Munich, Munich, Germany) that made rapid analysis of large amounts of raw data possible.

At this point, we had in our hands an assay system that was fast, easy to perform and which was based truly on the dissociation of monomeric MHC molecules from the surface of living T cells. With this system a tool was available for the first time that could measure MHC off-rates on the single cell level and in real-time. To validate the assay system and to proof that the data we generate with it are meaningful and reproducible, we chose to analyze two different types of TCR-transgenic T cells. Since structural T cell avidity is solely dependent on the structure of the TCR, cells that carry the same TCR should display the same off-rates and half-life times in our assay. Our analysis of OT-1 T cells, which are transgenic for a TCR that recognizes H2-K^b/SIINFEKL, demonstrated half-life times in a very narrow range around

19.48 seconds with a standard deviation of only 3.73 seconds for 121 cells. This result was consistent when comparing naïve to activated cells and was also consistent during six independent experiments, proving the good reproducibility of our assay. There is one publication that looked at the interaction between the OT-1 TCR and H2-K^b/SIINFEKL in the Biacore system (Alam et al., 1999). Alam and colleagues find a half-life time of the interaction of 31.5 seconds at 25°C, lacking the contribution of CD8 binding. We measure a half-life time of 19.48 seconds at 4°C including the contribution of CD8 binding. This discrepancy seems illogical since basic thermodynamic theory would suggest faster MHC dissociation at higher temperatures and because the CD8 molecule is described to have a stabilizing effect on TCR – pMHC binding (Wooldridge et al., 2005). The reason for it may be found in the differences between the Biacore setting and our assay, especially in the fact that in our setting the MHC dissociation takes place in the context of the very complex surface of a living T cell, which might influence MHC dissociation in hard to quantify ways. Furthermore, it is described that TCR affinities can increase with increasing temperatures for some TCR/pMHC complexes (Schlueter et al., 1996). To our knowledge, this may very well be the case for the specific interaction studied here. Still, our results lie in a similar range as the results in the Biacore system, underlining the validity of our assay.

Likewise, our analysis of 2C T cells, which are transgenic for a TCR that recognizes the syngenic H2-K^b/dEV8 and the allogenic H2-L^d/p2Ca, demonstrated half-life times for the dissociation of H2-K^b/dEV8 in a very narrow range around 12.71 seconds with a standard deviation of only 3.76 seconds, again proving the validity of our assay system. Also here there is one publication that looked at the interaction of the 2C TCR with H2-K^b/dEV8 in the Biacore system (Garcia et al., 1997). Garcia and colleagues find a half-life time of 3.7 seconds at 25°C, again lacking the contribution of CD8 binding. Our measured half-life time of 12.71 seconds is determined at 4°C and includes CD8 binding. In this case, the longer half-life time at 4°C is consistent with thermodynamic theory.

The difference between the two values for the 2C TCR – H2-K^b/dEV8 interaction allows us to speculate about the contribution of CD8 binding to MHC dissociation rates. Wooldridge et al. had a look at this contribution using various MHC I binding mutants that reduce or completely abrogate CD8 binding in tetramer dissociation assays (Wooldridge et al., 2005). By mathematical analysis they found that CD8 binding to MHC decreases MHC dissociation rates by a factor of 1.7 to 2.2. When comparing the MHC dissociation rates we found with H2-K^b/dEV8 dissociation from 2C T cells that include CD8 binding to the rates found in the Biacore system that lack CD8 binding we find a 3.4-fold decrease. The

comparison between this value and the ones found by Wooldridge et al. however has to be made with caution. First of all, the Biacore experiments and ours were conducted at different temperatures, with dissociation rates decreasing at lower temperatures according to thermodynamic theory. Furthermore, the experimental setups are quite different as we have described in 1.7.2.2. Last but not least, tetramer dissociation experiments have inherent limitations (see 1.7.2.1), aggravating the comparability of tetramer dissociation rates to dissociation rates found in the Biacore system as well as to those found in our system. Keeping these precautions in mind, the 3.4-fold decrease in MHC dissociation rates found between the Biacore experiments and ours seems to fit very well to the range of a 1.7- to 2.2-fold decrease that was found by Wooldridge et al.

In future experiments our novel assay could be the ideal tool to further elucidate the structural aspects of coreceptor – MHC binding using wildtype and mutant MHC molecules that have reduced or completely abrogated CD8 binding capacities.

4.2 STRUCTURAL AVIDITY AS A MAJOR DETERMINANT OF T CELL FUNCTION

T cells with a high functional avidity have been shown to have superior function over low avidity cells in $CD8^+$ T cell mediated immunity against tumors and viral infections (Alexander-Miller et al., 1996; Dutoit et al., 2001; Lyman et al., 2005; Nugent et al., 2000; Sedlik et al., 2000; Speiser et al., 1992; Yee et al., 1999; Zeh et al., 1999). Many factors contribute to functional avidity *in vivo*, like the numbers and synapse clustering of TCR – pMHC interactions (Cawthon and Alexander-Miller, 2002; Fahmy et al., 2001; Krogsgaard et al., 2005; Krogsgaard et al., 2003), coreceptor – MHC interactions (Cawthon and Alexander-Miller, 2002; Wooldridge et al., 2005), expression of adhesion molecules and of components of the TCR signaling cascade. While TCR – pMHC binding is known to determine the specificity of the interaction (Davis and Bjorkman, 1988), the contribution of the structural avidity of the TCR to functional T cell avidity has been unclear, especially because of the lack of a ´clean` method for the measurement of structural T cell avidity. Nevertheless, a link between structural avidity and functional avidity has been suggested by others before (Gronski et al., 2004; Holler and Kranz, 2003; Holler et al., 2001). The most impressive proof of this link comes from a recent publication, where it could be shown that transfer of tumor-reactive TCR genes confers tumor reactivity and functional avidity similar to parental cells to otherwise nonreactive PBMC and tumor infiltrating lymphocytes (Johnson et al., 2006),

suggesting strongly that functional T cell avidity is to a large degree dependent on the structural avidity of the TCR.

To test for a correlation between functional and structural T cell avidity using our novel T cell avidity assay, we generated two polyclonal T cell lines specific for the immunodominant *Listeria monocytogenes* (*L.m.*) epitope LLO_{91-99}. The cell lines were generated from the same *L.m.* infected BALB/c mouse, but were restimulated once a week using high amounts of peptide (10^{-6} M LLO_{91-99}) for the one cell line and low amounts of peptide (10^{-9} M LLO_{91-99}) for the other. The rationale behind this was that limiting the amount of peptide used for restimulation should select for high avidity T cells (Alexander-Miller et al., 1996). After six rounds of restimulation we analyzed the cell lines for their functional avidity in an intracellular cytokine staining (ICCS) for IFNγ and in ^{51}Chromium release assays. The differences in functional avidity found in these assays were striking, with the cell line that got restimulated with the lower amounts of peptide displaying the much higher functional avidity. This difference was also reflected in the cell lines´ protective capacity, the ultimate test of T cell function. The high functional avidity cell line conferred about 100-fold better protection against *L.m.* infection compared to the low functional avidity cell line. When looking at the MHC off-rates and half-life times of MHC dissociation of both cell lines with our novel assay, the differences in T cell function clearly correlated with differences in MHC off-rates. 90% of the low functional avidity cells displayed a fast MHC dissociation with half-life times around 15 seconds. In sharp contrast, about 55% of the high functional avidity cells displayed a slow MHC dissociation, with half-life times from 60 up to more than 300 seconds. It is possible that the protective effect was mediated by these 55% high avidity cells alone, making the difference in protective capacity between the two cell lines even more striking. Still, restimulation of a T cell line with limited amounts of peptide seems not to be able to exclusively generate high avidity T cells. Since the two cell lines were generated from the same mouse, and were kept under the exact same culture conditions except for the different amounts of peptide used for restimulation, we can strongly suspect that the differences in functional avidity seen are due to the differences in the structural avidity of the respective TCRs.

We could confirm these results in a clinically more relevant setting using T cell lines specific for the mCMV epitope $m164_{257-265}$. These T cell lines were also restimulated with high (10^{-8} M $m164_{257-265}$) or low amounts of peptide (10^{-10} M $m164_{257-265}$). The functional avidity of the cell lines was determined in the laboratory of Prof. M. Reddehase, Institute for Virology, University of Mainz, who kindly provided the cell lines for analysis in our MHC

off-rate assay. The cell line that got restimulated with the lower amount of peptide showed higher functional avidity in ELISPOT and ^{51}Chromium release assays. In mCMV infection experiments, the cell line also showed a 100-fold better protective capacity compared to the lower functional avidity cell line. This gave us the great possibility to confirm our findings with the LLO_{91-99} specific T cell lines by analyzing the mCMV specific cell lines in our MHC dissociation assay and to further support the interpretation that differences in functional avidity are due to differences in the structural avidity of the respective TCRs. These differences could indeed also be found in the mCMV specific cell lines. 76% of the low functional avidity cells displayed a relatively fast MHC dissociation with half-life times around 30 seconds. In sharp contrast, 86% of the high functional avidity cells showed a slow to very slow MHC dissociation, with half-life times of 50 seconds and more, up to over 200 seconds. Also in this cell line it is very well possible that the good protective effect is preferentially mediated by these cells alone.

The consistency of the results we generated in these two quite different experimental systems is striking, and allows us to strongly argue for the interpretation that T cell function is to a large extent dependent on the structural avidity of the TCR. This interpretation is further supported by the results of other groups (Gronski et al., 2004; Holler and Kranz, 2003; Holler et al., 2001; Johnson et al., 2006). With our novel assay system to measure MHC dissociation, we present for the first time a tool that allows the identification of highly functional T cells via their structural avidity on the level of single cells.

4.3 PERSPECTIVES IN T CELL THERAPY

Cytotoxic T cells have the ability to lyse target cells with high efficiency provided they recognize MHC-bound antigen. For this reason $CD8^+$ T cells have been interesting candidates for the use as a therapeutic agent for a long time. A lot of work in this field has been done in recipients of allogenic hematopoetic stem cell transplants (HSCT) that often develop complications with latent chronic viral infections like CMV or EBV (Einsele et al., 2002; Heslop et al., 1996; Rooney et al., 1995; Walter et al., 1995) and in the field of anti-tumor immunity, mostly in melanoma patients (Clay et al., 1999; Dudley et al., 2002; Dudley et al., 2005; Johnson et al., 2006; Morgan et al., 2003; Zhao et al., 2005). However, T cells as a therapeutic agent are by far not limited to these applications, but may be beneficial against a

wide range of intracellular pathogens, a wide range of tumors and, when expanding the idea also to $CD4^+$ T cells, against a wide range of infectious diseases in general.

We and others have shown that T cells with a high functional avidity are superior over low avidity cells in $CD8^+$ T cell mediated immunity against intracellular bacteria, viral infections (Alexander-Miller et al., 1996; Sedlik et al., 2000; Speiser et al., 1992) and tumors (Dutoit et al., 2001; Lyman et al., 2005; Nugent et al., 2000; Yee et al., 1999; Zeh et al., 1999). This makes T cells with a high functional avidity the ideal candidates for therapeutic applications. We and others could furthermore show that functional T cell avidity is to a large degree dependent on structural T cell avidity (Gronski et al., 2004; Holler and Kranz, 2003; Holler et al., 2001; Johnson et al., 2006). With our novel TCR avidity assay we have for the first time a tool available that allows the direct measurement of MHC off-rates and half-life times of MHC dissociation on the level of single living T cells. With this tool and the knowledge we gained in using and evaluating this tool, we propose an elegant solution to the long debated question of how T cells with a high functional avidity can be generated for the use as a therapeutic agent in adoptive cell transfer applications. We can for the first time identify high avidity T cells out of a complex T cell population. This could be *ex vivo* material, for example tumor infiltrating lymphocytes that mediated tumor regression or were able to control an infection, *in vitro* expanded T cell lines or T cell clones, cells that were generated by allogenic stimulation, or cells from mice that express human MHC molecules and human TCRs (Kuball et al., 2005; Stanislawski et al., 2001). This latter approach may be a source for high avidity T cells against human tumor-associated antigens (TAAs) in the context of human MHCs carrying human TCRs because, in contrast to the human situation where high avidity TCRs against TAAs are often deleted during negative selection, these TAAs are seen as foreign by the mouse. Out of such a T cell population, cells with a high structural avidity can be identified with our novel assay on the level of individual cells.

Obviously, further use of such cells requires the possibility to somehow recover the cell after measurement of MHC off-rates. This is especially the case since high functional avidity T cell lines are still ´contaminated´ with substantial proportions of cells that show fast MHC dissociations and which are probably quite useless regarding their protective capacities as we have shown with the low avidity $LLO_{91\text{-}99}$ and $m164_{257\text{-}265}$ specific cell lines A. We could also show that T cells with slow to very slow MHC dissociations are difficult to culture and are lost during prolonged cell culture. To be able to recover T cells after the measurement of their MHC off-rates, we transferred the assay to another experimental platform, the so called Evotec CytoCon400 system. At the core of this system is a microfluidic chip that allows

capturing an individual cell inside of an electrical field cage, exposing this cell to a different agent, and subsequently releasing the cell from the cage and flushing it out of the system where it can be picked and put to further use. We captured Streptamer-stained cells in this system, treated the cells with d-biotin to trigger MHC dissociation and after completion of the dissociation released and sorted the cells. Comparison of OT-1 T cells analyzed in this system and in the bulk measurement setup showed very similar results, with slightly faster half-life times of MHC dissociation in the Evotec system. This was very likely due to the fact that the Evotec system works under a constant buffer flow, actively transporting dissociated MHC molecules away from the cell.

Cells of defined structural avidities can this way not only be identified, but recovered after completion of the assay. Single cells with defined k_{off} can now be adoptively transferred, either after expansion *in vitro* or directly without any *in vitro* propagation. The most elegant and promising way in our eyes however would be the direct identification of the TCR α- and β-chain DNA sequences of such single high avidity T cells.

But is a high structural avidity really the optimal avidity for protection? In two recent publications working with MHC tetramer dissociation assays it could be shown that there appears to be an optimal tetramer dissociation rate specific to each TCR/tetramer combination. In a murine VSV model, TCR mutations that altered this rate below or above a certain level correlated with reduced cellular function (Kalergis et al., 2001). Another work demonstrated that HIV-specific $CD8^+$ T cells with a longer MHC tetramer dwell-time were less effective against peptide-pulsed target cells than cells with a shorter interaction (Ueno et al., 2004). Keeping in mind all the difficulties that are inherent to MHC tetramer-based T cell avidity assays, these results still hint at the fact that there might be an upper limit to structural T cell avidity for cells to be useful and that T cells with a even higher avidity can be less effective. Nevertheless, we and others have shown that T cells with a high structural avidity are superior to low avidity cells regarding their protective capacities. Should their be indeed an upper limit in structural avidity for cells to be effective as therapeutic and protective agent, cells that exceed this limit can easily be identified with our assay and excluded as potentially interesting cells just like cells with a too low structural avidity.

In first experiments in our lab, we could show that TCR sequences can be identified from single T cells (data not shown). The α- and β-chain genes of high avidity TCRs identified in this manner could now be retrovirally transduced into patient-derived T cells to generate artificial redirected high avidity T cells against a given antigen. This approach has already been explored by different groups (Clay et al., 1999; Cohen et al., 2005; Dembic et

al., 1986; Hughes et al., 2005; Johnson et al., 2006; Kessels et al., 2001; Morgan et al., 2006; Morgan et al., 2003; Schaft et al., 2003; Xue et al., 2005; Zhao et al., 2005). What has been lacking in all these studies so far however is on the one hand a robust and easy way to determine the structural avidity of the donor cells, so to be able to use the best suited cells as raw material, and on the other hand a way to identify the TCR sequences out of single cells, making difficult and time-consuming cloning steps unnecessary. Here our novel assay and a technique to identify TCR sequences out of single cells can be the crucial components in promoting this approach to a wide-spread clinical application. The use of retroviruses encoding high avidity TCRs to transduce T cells from patients, generating highly functional redirected T cells recognizing a given antigen in the context of a given MHC molecule could constitute an off-the-shelf reagent for use in the immunotherapy of patients with cancer or infectious diseases in the near future. The use of autologous cells in this setting would minimize any risk of graft versus host disease or cell rejection.

4.4 CONCLUSIONS AND OUTLOOK

Since interactions between the TCR and its ligand, the peptide-loaded MHC molecule (pMHC), represent a central event in T cell physiology, there has been long standing interest in the precise determination of the avidity of this interaction. This is not only true for questions regarding basic T cell research, but especially in the field of adoptive T cell therapy, where highly functional T cells are the main target. Functional T cell avidity is influenced by a variety of factors. To what extent it is influenced by the structural avidity of the TCR had been elusive, mainly because the possibilities to measure this parameter have been very limited in the past.

With this PhD work, we could establish a novel assay system for the measurement of MHC dissociation. This assay is fast and easy to perform, and is based on the dissociation of monomeric MCH molecules from the surface of living T cells. With this assay we have for the first time a tool available where MHC off-rates and half-life times of MHC dissociation from a T cell surface can be measured on the level of individual cells and in real-time. These parameters are the main determinant of structural T cell avidity (see 4.1). By analyzing TCR-transgenic T cells we could show that the new assay allows for exact and reproducible measurements of the off-rates of monomeric MHC molecules from living T cells. Using this assay, we could show in two different experimental systems that functional T cell avidity

correlates with structural T cell avidity, and that it is very likely to be dependent on structural avidity to a large degree. Furthermore, we could show that T cells with a higher structural avidity as measured in our assay system are superior to low structural avidity cells regarding their protective capacity.

With the transfer of our assay to the Evotec CytoCon400 system we could combine the measurement of a T cells´ structural avidity with the possibility to recover that cell after completion of the assay. This allows us to envision a very promising approach for the use of highly functional high avidity T cells as therapeutic agents in adoptive T cell therapy. The most elegant way in our eyes would be to identify the DNA sequences of high avidity TCRs out of single cells. This way patient T cells could be transduced with these TCRs and redirected to a highly efficient recognition of a given antigen. In first experiments we could show that TCR sequences can be identified out of single cells.

With this new way to determine structural T cell avidity, a lot of questions regarding T cell biology can now be answered. This could for example be the question what part the binding of the coreceptors to the MHC has for overall structural avidity. Using binding mutants of MHC molecules where coreceptor binding is abrogated, this question can now easily be addressed. Another problem that has so far been not conclusively resolved is the phenomenon of immunodominance. Structural T cell avidity might play an important role for the size of T cell populations evolving during immune responses, a hypothesis that can now be tested. But also clinically relevant questions can now be addressed by our novel assay system. This could be the question for the structural avidity of patient-derived tumor infiltrating lymphocytes and for a correlation between structural avidity and clinical outcome. Regarding a potential clinical application of our technique, we will work intensely on the approach described above. The identification of high avidity TCRs on the DNA level and the retroviral transduction of such TCRs into patient T cells for use as a therapeutic agent might result in the availability of an easy-to-use and safe off-the-shelf reagent for use in the immunotherapy of patients with cancer or infectious diseases.

5 SUMMARY

T cells are a major component of the adaptive immune system. They recognize peptide antigens in the context of MHC molecules (pMHC) via their T cell receptor (TCR) and its coreceptor CD4 or CD8. The efficiency by which a T cell can react to antigen encounter with proliferation and/or exertion of distinct effector functions is often termed “overall T cell avidity”. This parameter is dependent on a variety of functional factors like the amount of TCR surface expression, cell membrane composition or efficiency of downstream signaling, and structural factors, mainly the physical binding strength of the TCR to the pMHC. This latter parameter is called “structural avidity” of a given T cell. The ´overall T cell avidity´ is usually only defined by functional readouts, e.g. the efficiency and sensitivity of effector molecule production towards titrated stimuli, or the lysis-efficiency of peptide-loaded target cells. Therefore, these results are often described as the “functional avidity” of a T cell.

To answer questions like how the structural avidity of a T cell correlates with its functional avidity, to what extent structural avidity determines functional avidity and whether T cells with higher structural avidity are superior regarding their protective capacities was one of the main goals of this thesis work. Since the existing methods all suffer from more or less severe drawbacks, a new and improved assay system for the measurement of structural T cell avidity had to be established to be able to answer these questions.

The recently developed MHC Streptamer technology allows the accumulation of multimerized pMHCs on the T cell surface, which can subsequently be rapidly monomerized under controlled experimental conditions. Monomeric pMHCs dissociate from the TCR with distinct off-rates, which reflect the binding strength of the TCR and, since it is mainly determined by the MHC off-rate, can be used as a readout for structural avidity. Based on this concept, we were able to develop the molecular tools and experimental platform for a novel assay system that allows the real-time measurement of pMHC dissociation from living T cells on the single cell level.

A crucial component of the assay is the use of directly fluorescence-labeled pMHCs to generate MHC Streptamers. Living T cells stained with these reagents are transferred to an experimental setup based on conventional fluorescence or confocal microscopy. The disruption of the Streptamers, and thus the monomerization of the pMHCs, is initiated by addition of d-biotin, and the subsequent dissociation of the fluorescence-labeled MHC molecules can be monitored. Using straightforward fluorescence intensity measurements and

mathematics, the off-rate and half-life time of MHC dissociation can be calculated for each individual cell.

Two experimental approaches based on this principle have been established. The first one allows the analysis of many (up to 50) cells at one time, but does not allow any further experiments using selected cells. Especially when thinking about potential clinical applications, not only the knowledge about a T cells structural avidity is of interest, but also the possibility to recover such a cell for further analysis. Therefore, a second experimental approach has been established, allowing the analysis of only one cell at a time, but having the great advantage to be able to sort individual cells after measuring their structural avidity. Both experimental approaches are conducted at 4° Celsius, since otherwise MHC multimer internalization would severely interfere with data interpretation.

Using this novel assay system we could show that the functional avidity of a T cell clearly correlates with its MHC off-rates, and that T cells with a slower half-life time of MHC dissociation exhibit better protective capacity. This pointed to the fact that T cells with a high structural avidity would be superior for adoptive T cell therapy. Based on this important finding, we tried to envision a strategy for the generation of high avidity T cells for the use as therapeutic agent in adoptive immunotherapy.

This strategy is based on the identification of high avidity TCR gene sequences. In first experiments we could show that these sequences can be identified out of single T cells. Transduction of high avidity TCR sequences into patient T cells could redirect these cells to a highly efficient recognition of a given antigen in the context of a given MHC molecule. This novel strategy to identify high avidity TCR sequences and subsequently generate high avidity T cells *in vitro* opens up very promising perspectives for the treatment of a wide range of pathogens and tumors. Once the optimal TCR sequences are identified within a polyclonal T cell pool, expression vectors encoding high avidity TCR against a distinct antigen in the context of a distinct MHC molecule could represent an easy to use “off-the-shelf” reagent allowing the rapid generation of highly potent antigen-specific T cells for the treatment of disease.

In conclusion, we could establish a novel assay system that for the first time allows the fast and easy determination of MHC off-rates and half-life times of MHC dissociation on the level of single cells. This assay is not only a valuable tool for basic T cell research, but also opens up fascinating new possibilities for clinical applications in the field of adoptive T cell therapy.

6 REFERENCES

Abbas, A. K., Lichtman, A. H. (2003). Cellular and Molecular Immunology, 5th edn (Philadelphia, Elsevier Science).

al-Ramadi, B. K., Jelonek, M. T., Boyd, L. F., Margulies, D. H., and Bothwell, A. L. (1995). Lack of strict correlation of functional sensitization with the apparent affinity of MHC/peptide complexes for the TCR. J Immunol *155*, 662-673.

Alam, S. M., Davies, G. M., Lin, C. M., Zal, T., Nasholds, W., Jameson, S. C., Hogquist, K. A., Gascoigne, N. R., and Travers, P. J. (1999). Qualitative and quantitative differences in T cell receptor binding of agonist and antagonist ligands. Immunity *10*, 227-237.

Alam, S. M., Travers, P. J., Wung, J. L., Nasholds, W., Redpath, S., Jameson, S. C., and Gascoigne, N. R. (1996). T-cell-receptor affinity and thymocyte positive selection. Nature *381*, 616-620.

Alexander-Miller, M. A. (2005). High-avidity CD8+ T cells: optimal soldiers in the war against viruses and tumors. Immunol Res *31*, 13-24.

Alexander-Miller, M. A., Leggatt, G. R., and Berzofsky, J. A. (1996). Selective expansion of high- or low-avidity cytotoxic T lymphocytes and efficacy for adoptive immunotherapy. Proc Natl Acad Sci U S A *93*, 4102-4107.

Altman, J. D., Moss, P. A., Goulder, P. J., Barouch, D. H., McHeyzer-Williams, M. G., Bell, J. I., McMichael, A. J., and Davis, M. M. (1996). Phenotypic analysis of antigen-specific T lymphocytes. Science *274*, 94-96.

Amrani, A., Verdaguer, J., Serra, P., Tafuro, S., Tan, R., and Santamaria, P. (2000). Progression of autoimmune diabetes driven by avidity maturation of a T-cell population. Nature *406*, 739-742.

Berke, G. (1995). The CTL's kiss of death. Cell *81*, 9-12.

6 REFERENCES

Bevan, M. J., and Fink, P. J. (2001). The CD8 response on autopilot. Nat Immunol *2*, 381-382.

Bjorkman, P. J. (1997). MHC restriction in three dimensions: a view of T cell receptor/ligand interactions. Cell *89*, 167-170.

Blattman, J. N., Antia, R., Sourdive, D. J., Wang, X., Kaech, S. M., Murali-Krishna, K., Altman, J. D., and Ahmed, R. (2002). Estimating the precursor frequency of naive antigen-specific CD8 T cells. J Exp Med *195*, 657-664.

Bollard, C. M., Kuehnle, I., Leen, A., Rooney, C. M., and Heslop, H. E. (2004). Adoptive immunotherapy for posttransplantation viral infections. Biol Blood Marrow Transplant *10*, 143-155.

Boon, T., and Old, L. J. (1997). Cancer Tumor antigens. Curr Opin Immunol *9*, 681-683.

Brunner, K. T., Mauel, J., Cerottini, J. C., and Chapuis, B. (1968). Quantitative assay of the lytic action of immune lymphoid cells on 51-Cr-labelled allogeneic target cells in vitro; inhibition by isoantibody and by drugs. Immunology *14*, 181-196.

Busch, D. H., and Pamer, E. G. (1998). MHC class I/peptide stability: implications for immunodominance, in vitro proliferation, and diversity of responding CTL. J Immunol *160*, 4441-4448.

Busch, D. H., and Pamer, E. G. (1999). T cell affinity maturation by selective expansion during infection. J Exp Med *189*, 701-710.

Busch, D. H., Pilip, I., and Pamer, E. G. (1998a). Evolution of a complex T cell receptor repertoire during primary and recall bacterial infection. J Exp Med *188*, 61-70.

Busch, D. H., Pilip, I. M., Vijh, S., and Pamer, E. G. (1998b). Coordinate regulation of complex T cell populations responding to bacterial infection. Immunity *8*, 353-362.

Campbell, K. S., Backstrom, B. T., Tiefenthaler, G., and Palmer, E. (1994). CART: a conserved antigen receptor transmembrane motif. Semin Immunol *6*, 393-410.

Cawthon, A. G., and Alexander-Miller, M. A. (2002). Optimal colocalization of TCR and CD8 as a novel mechanism for the control of functional avidity. J Immunol *169*, 3492-3498.

Cawthon, A. G., Lu, H., and Alexander-Miller, M. A. (2001). Peptide requirement for CTL activation reflects the sensitivity to CD3 engagement: correlation with CD8alphabeta versus CD8alphaalpha expression. J Immunol *167*, 2577-2584.

Clay, T. M., Custer, M. C., Sachs, J., Hwu, P., Rosenberg, S. A., and Nishimura, M. I. (1999). Efficient transfer of a tumor antigen-reactive TCR to human peripheral blood lymphocytes confers anti-tumor reactivity. J Immunol *163*, 507-513.

Cohen, C. J., Zheng, Z., Bray, R., Zhao, Y., Sherman, L. A., Rosenberg, S. A., and Morgan, R. A. (2005). Recognition of fresh human tumor by human peripheral blood lymphocytes transduced with a bicistronic retroviral vector encoding a murine anti-p53 TCR. J Immunol *175*, 5799-5808.

Conlan, J. W., and North, R. J. (1991). Neutrophil-mediated dissolution of infected host cells as a defense strategy against a facultative intracellular bacterium. J Exp Med *174*, 741-744.

Corr, M., Slanetz, A. E., Boyd, L. F., Jelonek, M. T., Khilko, S., al-Ramadi, B. K., Kim, Y. S., Maher, S. E., Bothwell, A. L., and Margulies, D. H. (1994). T cell receptor-MHC class I peptide interactions: affinity, kinetics, and specificity. Science *265*, 946-949.

Crawford, F., Kozono, H., White, J., Marrack, P., and Kappler, J. (1998). Detection of antigen-specific T cells with multivalent soluble class II MHC covalent peptide complexes. Immunity *8*, 675-682.

Cresswell, P. (1994). Assembly, transport, and function of MHC class II molecules. Annu Rev Immunol *12*, 259-293.

Davis, M. M., and Bjorkman, P. J. (1988). T-cell antigen receptor genes and T-cell recognition. Nature *334*, 395-402.

Davis, M. M., Boniface, J. J., Reich, Z., Lyons, D., Hampl, J., Arden, B., and Chien, Y. (1998). Ligand recognition by alpha beta T cell receptors. Annu Rev Immunol *16*, 523-544.

Degano, M., Garcia, K. C., Apostolopoulos, V., Rudolph, M. G., Teyton, L., and Wilson, I. A. (2000). A functional hot spot for antigen recognition in a superagonist TCR/MHC complex. Immunity *12*, 251-261.

Dembic, Z., Haas, W., Weiss, S., McCubrey, J., Kiefer, H., von Boehmer, H., and Steinmetz, M. (1986). Transfer of specificity by murine alpha and beta T-cell receptor genes. Nature *320*, 232-238.

Derby, M., Alexander-Miller, M., Tse, R., and Berzofsky, J. (2001). High-avidity CTL exploit two complementary mechanisms to provide better protection against viral infection than low-avidity CTL. J Immunol *166*, 1690-1697.

Ding, Y. H., Baker, B. M., Garboczi, D. N., Biddison, W. E., and Wiley, D. C. (1999). Four A6-TCR/peptide/HLA-A2 structures that generate very different T cell signals are nearly identical. Immunity *11*, 45-56.

Ding, Y. H., Smith, K. J., Garboczi, D. N., Utz, U., Biddison, W. E., and Wiley, D. C. (1998). Two human T cell receptors bind in a similar diagonal mode to the HLA-A2/Tax peptide complex using different TCR amino acids. Immunity *8*, 403-411.

Drake, D. R., 3rd, and Braciale, T. J. (2001). Cutting edge: lipid raft integrity affects the efficiency of MHC class I tetramer binding and cell surface TCR arrangement on CD8+ T cells. J Immunol *166*, 7009-7013.

Dudley, M. E., Wunderlich, J., Nishimura, M. I., Yu, D., Yang, J. C., Topalian, S. L., Schwartzentruber, D. J., Hwu, P., Marincola, F. M., Sherry, R., *et al.* (2001). Adoptive transfer of cloned melanoma-reactive T lymphocytes for the treatment of patients with metastatic melanoma. J Immunother *24*, 363-373.

Dudley, M. E., Wunderlich, J. R., Robbins, P. F., Yang, J. C., Hwu, P., Schwartzentruber, D. J., Topalian, S. L., Sherry, R., Restifo, N. P., Hubicki, A. M., *et al.* (2002). Cancer regression and autoimmunity in patients after clonal repopulation with antitumor lymphocytes. Science *298*, 850-854.

Dudley, M. E., Wunderlich, J. R., Yang, J. C., Sherry, R. M., Topalian, S. L., Restifo, N. P., Royal, R. E., Kammula, U., White, D. E., Mavroukakis, S. A., *et al.* (2005). Adoptive cell transfer therapy following non-myeloablative but lymphodepleting chemotherapy for the treatment of patients with refractory metastatic melanoma. J Clin Oncol *23*, 2346-2357.

Dutoit, V., Rubio-Godoy, V., Dietrich, P. Y., Quiqueres, A. L., Schnuriger, V., Rimoldi, D., Lienard, D., Speiser, D., Guillaume, P., Batard, P., *et al.* (2001). Heterogeneous T-cell response to MAGE-A10(254-262): high avidity-specific cytolytic T lymphocytes show superior antitumor activity. Cancer Res *61*, 5850-5856.

Dutoit, V., Rubio-Godoy, V., Doucey, M. A., Batard, P., Lienard, D., Rimoldi, D., Speiser, D., Guillaume, P., Cerottini, J. C., Romero, P., and Valmori, D. (2002). Functional avidity of tumor antigen-specific CTL recognition directly correlates with the stability of MHC/peptide multimer binding to TCR. J Immunol *168*, 1167-1171.

Echchakir, H., Dorothee, G., Vergnon, I., Menez, J., Chouaib, S., and Mami-Chouaib, F. (2002). Cytotoxic T lymphocytes directed against a tumor-specific mutated antigen display similar HLA tetramer binding but distinct functional avidity and tissue distribution. Proc Natl Acad Sci U S A *99*, 9358-9363.

Einsele, H., Roosnek, E., Rufer, N., Sinzger, C., Riegler, S., Loffler, J., Grigoleit, U., Moris, A., Rammensee, H. G., Kanz, L., *et al.* (2002). Infusion of cytomegalovirus (CMV)-specific T cells for the treatment of CMV infection not responding to antiviral chemotherapy. Blood *99*, 3916-3922.

Engelhard, V. H., Bullock, T. N., Colella, T. A., Sheasley, S. L., and Mullins, D. W. (2002). Antigens derived from melanocyte differentiation proteins: self-tolerance, autoimmunity, and use for cancer immunotherapy. Immunol Rev *188*, 136-146.

Fagerstam, L. G., Frostell-Karlsson, A., Karlsson, R., Persson, B., and Ronnberg, I. (1992). Biospecific interaction analysis using surface plasmon resonance detection applied to kinetic, binding site and concentration analysis. J Chromatogr *597*, 397-410.

Fahmy, T. M., Bieler, J. G., Edidin, M., and Schneck, J. P. (2001). Increased TCR avidity after T cell activation: a mechanism for sensing low-density antigen. Immunity *14*, 135-143.

Fiedler, S., Shirley, S. G., Schnelle, T., and Fuhr, G. (1998). Dielectrophoretic sorting of particles and cells in a microsystem. Anal Chem *70*, 1909-1915.

Gangadharan, D., and Cheroutre, H. (2004). The CD8 isoform CD8alphaalpha is not a functional homologue of the TCR co-receptor CD8alphabeta. Curr Opin Immunol *16*, 264-270.

Gao, G. F., Tormo, J., Gerth, U. C., Wyer, J. R., McMichael, A. J., Stuart, D. I., Bell, J. I., Jones, E. Y., and Jakobsen, B. K. (1997). Crystal structure of the complex between human CD8alpha(alpha) and HLA-A2. Nature *387*, 630-634.

Garboczi, D. N., Ghosh, P., Utz, U., Fan, Q. R., Biddison, W. E., and Wiley, D. C. (1996). Structure of the complex between human T-cell receptor, viral peptide and HLA-A2. Nature *384*, 134-141.

Garcia, K. C., Degano, M., Pease, L. R., Huang, M., Peterson, P. A., Teyton, L., and Wilson, I. A. (1998). Structural basis of plasticity in T cell receptor recognition of a self peptide-MHC antigen. Science *279*, 1166-1172.

Garcia, K. C., Degano, M., Stanfield, R. L., Brunmark, A., Jackson, M. R., Peterson, P. A., Teyton, L., and Wilson, I. A. (1996a). An alphabeta T cell receptor structure at 2.5 A and its orientation in the TCR-MHC complex. Science *274*, 209-219.

Garcia, K. C., Scott, C. A., Brunmark, A., Carbone, F. R., Peterson, P. A., Wilson, I. A., and Teyton, L. (1996b). CD8 enhances formation of stable T-cell receptor/MHC class I molecule complexes. Nature *384*, 577-581.

Garcia, K. C., Tallquist, M. D., Pease, L. R., Brunmark, A., Scott, C. A., Degano, M., Stura, E. A., Peterson, P. A., Wilson, I. A., and Teyton, L. (1997). Alphabeta T cell receptor interactions with syngeneic and allogeneic ligands: affinity measurements and crystallization. Proc Natl Acad Sci U S A *94*, 13838-13843.

Gellin, B. G., and Broome, C. V. (1989). Listeriosis. Jama *261*, 1313-1320.

Gregoire, C., Lin, S. Y., Mazza, G., Rebai, N., Luescher, I. F., and Malissen, B. (1996). Covalent assembly of a soluble T cell receptor-peptide-major histocompatibility class I complex. Proc Natl Acad Sci U S A *93*, 7184-7189.

Griffiths, G. M. (1995). The cell biology of CTL killing. Curr Opin Immunol *7*, 343-348.

Gronski, M. A., Boulter, J. M., Moskophidis, D., Nguyen, L. T., Holmberg, K., Elford, A. R., Deenick, E. K., Kim, H. O., Penninger, J. M., Odermatt, B., *et al.* (2004). TCR affinity and negative regulation limit autoimmunity. Nat Med *10*, 1234-1239.

Harty, J. T., and Bevan, M. J. (1992). CD8+ T cells specific for a single nonamer epitope of Listeria monocytogenes are protective in vivo. J Exp Med *175*, 1531-1538.

Hayday, A. C. (2000). [gamma][delta] cells: a right time and a right place for a conserved third way of protection. Annu Rev Immunol *18*, 975-1026.

Hennecke, J., Carfi, A., and Wiley, D. C. (2000). Structure of a covalently stabilized complex of a human alphabeta T-cell receptor, influenza HA peptide and MHC class II molecule, HLA-DR1. Embo J *19*, 5611-5624.

Hennecke, J., and Wiley, D. C. (2001). T cell receptor-MHC interactions up close. Cell *104*, 1-4.

Heslop, H. E., Ng, C. Y., Li, C., Smith, C. A., Loftin, S. K., Krance, R. A., Brenner, M. K., and Rooney, C. M. (1996). Long-term restoration of immunity against Epstein-Barr virus infection by adoptive transfer of gene-modified virus-specific T lymphocytes. Nat Med *2*, 551-555.

Hesse, M. D., Karulin, A. Y., Boehm, B. O., Lehmann, P. V., and Tary-Lehmann, M. (2001). A T cell clone's avidity is a function of its activation state. J Immunol *167*, 1353-1361.

Hofstetter, H. H., Targoni, O. S., Karulin, A. Y., Forsthuber, T. G., Tary-Lehmann, M., and Lehmann, P. V. (2005). Does the frequency and avidity spectrum of the neuroantigen-specific T cells in the blood mirror the autoimmune process in the central nervous system of mice undergoing experimental allergic encephalomyelitis? J Immunol *174*, 4598-4605.

Hogquist, K. A., Jameson, S. C., Heath, W. R., Howard, J. L., Bevan, M. J., and Carbone, F. R. (1994). T cell receptor antagonist peptides induce positive selection. Cell *76*, 17-27.

Holler, P. D., and Kranz, D. M. (2003). Quantitative analysis of the contribution of TCR/pepMHC affinity and CD8 to T cell activation. Immunity *18*, 255-264.

Holler, P. D., Lim, A. R., Cho, B. K., Rund, L. A., and Kranz, D. M. (2001). CD8(-) T cell transfectants that express a high affinity T cell receptor exhibit enhanced peptide-dependent activation. J Exp Med *194*, 1043-1052.

Holtappels, R., Thomas, D., Podlech, J., and Reddehase, M. J. (2002). Two antigenic peptides from genes m123 and m164 of murine cytomegalovirus quantitatively dominate CD8 T-cell memory in the H-2d haplotype. J Virol *76*, 151-164.

Hughes, M. S., Yu, Y. Y., Dudley, M. E., Zheng, Z., Robbins, P. F., Li, Y., Wunderlich, J., Hawley, R. G., Moayeri, M., Rosenberg, S. A., and Morgan, R. A. (2005). Transfer of a TCR gene derived from a patient with a marked antitumor response conveys highly active T-cell effector functions. Hum Gene Ther *16*, 457-472.

Huseby, E. S., Crawford, F., White, J., Marrack, P., and Kappler, J. W. (2006). Interface-disrupting amino acids establish specificity between T cell receptors and complexes of major histocompatibility complex and peptide. Nat Immunol *7*, 1191-1199.

Huster, K. M., Busch, V., Schiemann, M., Linkemann, K., Kerksiek, K. M., Wagner, H., and Busch, D. H. (2004). Selective expression of IL-7 receptor on memory T cells identifies early CD40L-dependent generation of distinct CD8+ memory T cell subsets. Proc Natl Acad Sci U S A *101*, 5610-5615.

Jameson, S. C., Hogquist, K. A., and Bevan, M. J. (1995). Positive selection of thymocytes. Annu Rev Immunol *13*, 93-126.

Janeway, C. A., Jr., and Medzhitov, R. (2002). Innate immune recognition. Annu Rev Immunol *20*, 197-216.

Johnson, L. A., Heemskerk, B., Powell, D. J., Jr., Cohen, C. J., Morgan, R. A., Dudley, M. E., Robbins, P. F., and Rosenberg, S. A. (2006). Gene transfer of tumor-reactive TCR confers both high avidity and tumor reactivity to nonreactive peripheral blood mononuclear cells and tumor-infiltrating lymphocytes. J Immunol *177*, 6548-6559.

Kalams, S. A., and Walker, B. D. (1998). The critical need for CD4 help in maintaining effective cytotoxic T lymphocyte responses. J Exp Med *188*, 2199-2204.

Kalergis, A. M., Boucheron, N., Doucey, M. A., Palmieri, E., Goyarts, E. C., Vegh, Z., Luescher, I. F., and Nathenson, S. G. (2001). Efficient T cell activation requires an optimal dwell-time of interaction between the TCR and the pMHC complex. Nat Immunol *2*, 229-234.

Kalia, V., Sarkar, S., Gourley, T. S., Rouse, B. T., and Ahmed, R. (2006). Differentiation of memory B and T cells. Curr Opin Immunol *18*, 255-264.

Karjalainen, K. (1994). High sensitivity, low affinity--paradox of T-cell receptor recognition. Curr Opin Immunol *6*, 9-12.

Kaufmann, S. H. (1995). Immunity to intracellular microbial pathogens. Immunol Today *16*, 338-342.

Kentsch, J., Durr, M., Schnelle, T., Gradl, G., Muller, T., Jager, M., Normann, A., and Stelzle, M. (2003). Microdevices for separation, accumulation, and analysis of biological micro- and nanoparticles. IEE Proc Nanobiotechnol *150*, 82-89.

Kern, P. S., Teng, M. K., Smolyar, A., Liu, J. H., Liu, J., Hussey, R. E., Spoerl, R., Chang, H. C., Reinherz, E. L., and Wang, J. H. (1998). Structural basis of CD8 coreceptor function revealed by crystallographic analysis of a murine CD8alphaalpha ectodomain fragment in complex with H-2Kb. Immunity *9*, 519-530.

Kessels, H. W., Wolkers, M. C., van den Boom, M. D., van der Valk, M. A., and Schumacher, T. N. (2001). Immunotherapy through TCR gene transfer. Nat Immunol *2*, 957-961.

Knabel, M., Franz, T. J., Schiemann, M., Wulf, A., Villmow, B., Schmidt, B., Bernhard, H., Wagner, H., and Busch, D. H. (2002). Reversible MHC multimer staining for functional isolation of T-cell populations and effective adoptive transfer. Nat Med *8*, 631-637.

Krogsgaard, M., Li, Q. J., Sumen, C., Huppa, J. B., Huse, M., and Davis, M. M. (2005). Agonist/endogenous peptide-MHC heterodimers drive T cell activation and sensitivity. Nature *434*, 238-243.

Krogsgaard, M., Prado, N., Adams, E. J., He, X. L., Chow, D. C., Wilson, D. B., Garcia, K. C., and Davis, M. M. (2003). Evidence that structural rearrangements and/or flexibility during TCR binding can contribute to T cell activation. Mol Cell *12*, 1367-1378.

Kuball, J., Schmitz, F. W., Voss, R. H., Ferreira, E. A., Engel, R., Guillaume, P., Strand, S., Romero, P., Huber, C., Sherman, L. A., and Theobald, M. (2005). Cooperation of human tumor-reactive CD4+ and CD8+ T cells after redirection of their specificity by a high-affinity p53A2.1-specific TCR. Immunity *22*, 117-129.

Lawson, T. M., Man, S., Wang, E. C., Williams, S., Amos, N., Gillespie, G. M., Moss, P. A., and Borysiewicz, L. K. (2001). Functional differences between influenza A-specific cytotoxic T lymphocyte clones expressing dominant and subdominant TCR. Int Immunol *13*, 1383-1390.

Lee, J. K., Stewart-Jones, G., Dong, T., Harlos, K., Di Gleria, K., Dorrell, L., Douek, D. C., van der Merwe, P. A., Jones, E. Y., and McMichael, A. J. (2004). T cell cross-reactivity and conformational changes during TCR engagement. J Exp Med *200*, 1455-1466.

Leen, A. M., Rooney, C. M., and Foster, A. E. (2006). Improving T Cell Therapy for Cancer. Annu Rev Immunol.

Liedberg, B., Nylander, C., and Lundstrom, I. (1983). Surface plasmon resonance for gas detection and biosensing. Sensors and Actuators *4*, 299-304.

Lin, A. Y., Devaux, B., Green, A., Sagerstrom, C., Elliott, J. F., and Davis, M. M. (1990). Expression of T cell antigen receptor heterodimers in a lipid-linked form. Science *249*, 677-679.

Liu, Y., Xiong, Y., Naidenko, O. V., Liu, J. H., Zhang, R., Joachimiak, A., Kronenberg, M., Cheroutre, H., Reinherz, E. L., and Wang, J. H. (2003). The crystal structure of a TL/CD8alphaalpha complex at 2.1 A resolution: implications for modulation of T cell activation and memory. Immunity *18*, 205-215.

Lyman, M. A., Nugent, C. T., Marquardt, K. L., Biggs, J. A., Pamer, E. G., and Sherman, L. A. (2005). The fate of low affinity tumor-specific CD8+ T cells in tumor-bearing mice. J Immunol *174*, 2563-2572.

Lyons, D. S., Lieberman, S. A., Hampl, J., Boniface, J. J., Chien, Y., Berg, L. J., and Davis, M. M. (1996). A TCR binds to antagonist ligands with lower affinities and faster dissociation rates than to agonists. Immunity *5*, 53-61.

Manning, T. C., Schlueter, C. J., Brodnicki, T. C., Parke, E. A., Speir, J. A., Garcia, K. C., Teyton, L., Wilson, I. A., and Kranz, D. M. (1998). Alanine scanning mutagenesis of an alphabeta T cell receptor: mapping the energy of antigen recognition. Immunity *8*, 413-425.

Marshall, N. A., Christie, L. E., Munro, L. R., Culligan, D. J., Johnston, P. W., Barker, R. N., and Vickers, M. A. (2004). Immunosuppressive regulatory T cells are abundant in the reactive lymphocytes of Hodgkin lymphoma. Blood *103*, 1755-1762.

Masopust, D., Kaech, S. M., Wherry, E. J., and Ahmed, R. (2004). The role of programming in memory T-cell development. Curr Opin Immunol *16*, 217-225.

Matsui, K., Boniface, J. J., Reay, P. A., Schild, H., Fazekas de St Groth, B., and Davis, M. M. (1991). Low affinity interaction of peptide-MHC complexes with T cell receptors. Science *254*, 1788-1791.

Medzhitov, R., and Janeway, C. A., Jr. (1998). Innate immune recognition and control of adaptive immune responses. Semin Immunol *10*, 351-353.

Miyahira, Y., Murata, K., Rodriguez, D., Rodriguez, J. R., Esteban, M., Rodrigues, M. M., and Zavala, F. (1995). Quantification of antigen specific CD8+ T cells using an ELISPOT assay. J Immunol Methods *181*, 45-54.

Modlin, R. L., and Sieling, P. A. (2005). Immunology. Now presenting: gammadelta T cells. Science *309*, 252-253.

Mombaerts, P., Arnoldi, J., Russ, F., Tonegawa, S., and Kaufmann, S. H. (1993). Different roles of alpha beta and gamma delta T cells in immunity against an intracellular bacterial pathogen. Nature *365*, 53-56.

Morel, P. A., and Oriss, T. B. (1998). Crossregulation between Th1 and Th2 cells. Crit Rev Immunol *18*, 275-303.

Morgan, R. A., Dudley, M. E., Wunderlich, J. R., Hughes, M. S., Yang, J. C., Sherry, R. M., Royal, R. E., Topalian, S. L., Kammula, U. S., Restifo, N. P., *et al.* (2006). Cancer regression in patients after transfer of genetically engineered lymphocytes. Science *314*, 126-129.

Morgan, R. A., Dudley, M. E., Yu, Y. Y., Zheng, Z., Robbins, P. F., Theoret, M. R., Wunderlich, J. R., Hughes, M. S., Restifo, N. P., and Rosenberg, S. A. (2003). High efficiency TCR gene transfer into primary human lymphocytes affords avid recognition of melanoma tumor antigen glycoprotein 100 and does not alter the recognition of autologous melanoma antigens. J Immunol *171*, 3287-3295.

Mosmann, T. R., and Sad, S. (1996). The expanding universe of T-cell subsets: Th1, Th2 and more. Immunol Today *17*, 138-146.

Nakamoto, Y., Guidotti, L. G., Pasquetto, V., Schreiber, R. D., and Chisari, F. V. (1997). Differential target cell sensitivity to CTL-activated death pathways in hepatitis B virus transgenic mice. J Immunol *158*, 5692-5697.

Neuenhahn, M., Kerksiek, K. M., Nauerth, M., Suhre, M. H., Schiemann, M., Gebhardt, F. E., Stemberger, C., Panthel, K., Schroder, S., Chakraborty, T., *et al.* (2006). CD8alpha+ dendritic cells are required for efficient entry of Listeria monocytogenes into the spleen. Immunity *25*, 619-630.

Newcom, S. R., and Gu, L. (1995). Transforming growth factor beta 1 messenger RNA in Reed-Sternberg cells in nodular sclerosing Hodgkin's disease. J Clin Pathol *48*, 160-163.

Niehans, G. A., Brunner, T., Frizelle, S. P., Liston, J. C., Salerno, C. T., Knapp, D. J., Green, D. R., and Kratzke, R. A. (1997). Human lung carcinomas express Fas ligand. Cancer Res *57*, 1007-1012.

Nugent, C. T., Morgan, D. J., Biggs, J. A., Ko, A., Pilip, I. M., Pamer, E. G., and Sherman, L. A. (2000). Characterization of CD8+ T lymphocytes that persist after peripheral tolerance to a self antigen expressed in the pancreas. J Immunol *164*, 191-200.

O'Garra, A. (1998). Cytokines induce the development of functionally heterogeneous T helper cell subsets. Immunity *8*, 275-283.

Ochsenbein, A. F., Klenerman, P., Karrer, U., Ludewig, B., Pericin, M., Hengartner, H., and Zinkernagel, R. M. (1999). Immune surveillance against a solid tumor fails because of immunological ignorance. Proc Natl Acad Sci U S A *96*, 2233-2238.

Palermo, B., Campanelli, R., Mantovani, S., Lantelme, E., Manganoni, A. M., Carella, G., Da Prada, G., della Cuna, G. R., Romagne, F., Gauthier, L., *et al.* (2001). Diverse expansion potential and heterogeneous avidity in tumor-associated antigen-specific T lymphocytes from primary melanoma patients. Eur J Immunol *31*, 412-420.

Pamer, E., and Cresswell, P. (1998). Mechanisms of MHC class I--restricted antigen processing. Annu Rev Immunol *16*, 323-358.

Parker, K. C., and Strominger, J. L. (1983). Localization of the sites of iodination of human beta 2-microglobulin: quaternary structure implications for histocompatibility antigens. Biochemistry *22*, 1145-1153.

Plitz, T., Huffstadt, U., Endres, R., Schaller, E., Mak, T. W., Wagner, H., and Pfeffer, K. (1999). The resistance against Listeria monocytogenes and the formation of germinal centers depend on a functional death domain of the 55 kDa tumor necrosis factor receptor. Eur J Immunol *29*, 581-591.

Prussin, C., and Metcalfe, D. D. (1995). Detection of intracytoplasmic cytokine using flow cytometry and directly conjugated anti-cytokine antibodies. J Immunol Methods *188*, 117-128.

Rees, W., Bender, J., Teague, T. K., Kedl, R. M., Crawford, F., Marrack, P., and Kappler, J. (1999). An inverse relationship between T cell receptor affinity and antigen dose during CD4(+) T cell responses in vivo and in vitro. Proc Natl Acad Sci U S A *96*, 9781-9786.

Rogers, P. R., Huston, G., and Swain, S. L. (1998). High antigen density and IL-2 are required for generation of CD4 effectors secreting Th1 rather than Th0 cytokines. J Immunol *161*, 3844-3852.

Romagnani, S. (1992). Induction of TH1 and TH2 responses: a key role for the 'natural' immune response? Immunol Today *13*, 379-381.

Rooney, C. M., Smith, C. A., Ng, C. Y., Loftin, S., Li, C., Krance, R. A., Brenner, M. K., and Heslop, H. E. (1995). Use of gene-modified virus-specific T lymphocytes to control Epstein-Barr-virus-related lymphoproliferation. Lancet *345*, 9-13.

Rosenberg, S. A. (2001). Progress in human tumour immunology and immunotherapy. Nature *411*, 380-384.

Rosenberg, S. A., Sherry, R. M., Morton, K. E., Scharfman, W. J., Yang, J. C., Topalian, S. L., Royal, R. E., Kammula, U., Restifo, N. P., Hughes, M. S., *et al.* (2005). Tumor progression can occur despite the induction of very high levels of self/tumor antigen-specific CD8+ T cells in patients with melanoma. J Immunol *175*, 6169-6176.

Rubio-Godoy, V., Dutoit, V., Rimoldi, D., Lienard, D., Lejeune, F., Speiser, D., Guillaume, P., Cerottini, J. C., Romero, P., and Valmori, D. (2001). Discrepancy between ELISPOT IFN-gamma secretion and binding of A2/peptide multimers to TCR reveals interclonal dissociation of CTL effector function from TCR-peptide/MHC complexes half-life. Proc Natl Acad Sci U S A *98*, 10302-10307.

Rudolph, M. G., Stanfield, R. L., and Wilson, I. A. (2006). How TCRs bind MHCs, peptides, and coreceptors. Annu Rev Immunol *24*, 419-466.

Saito, H., Kranz, D. M., Takagaki, Y., Hayday, A. C., Eisen, H. N., and Tonegawa, S. (1984). A third rearranged and expressed gene in a clone of cytotoxic T lymphocytes. Nature *312*, 36-40.

Sallusto, F., Lenig, D., Forster, R., Lipp, M., and Lanzavecchia, A. (1999). Two subsets of memory T lymphocytes with distinct homing potentials and effector functions. Nature *401*, 708-712.

Savage, P. A., Boniface, J. J., and Davis, M. M. (1999). A kinetic basis for T cell receptor repertoire selection during an immune response. Immunity *10*, 485-492.

Savage, P. A., and Davis, M. M. (2001). A kinetic window constricts the T cell receptor repertoire in the thymus. Immunity *14*, 243-252.

Schaft, N., Willemsen, R. A., de Vries, J., Lankiewicz, B., Essers, B. W., Gratama, J. W., Figdor, C. G., Bolhuis, R. L., Debets, R., and Adema, G. J. (2003). Peptide fine specificity of anti-glycoprotein 100 CTL is preserved following transfer of engineered TCR alpha beta genes into primary human T lymphocytes. J Immunol *170*, 2186-2194.

Schlueter, C. J., Manning, T. C., Schodin, B. A., and Kranz, D. M. (1996). A residue in the center of peptide QL9 affects binding to both Ld and the T cell receptor. J Immunol *157*, 4478-4485.

Schuck, P. (1996). Kinetics of ligand binding to receptor immobilized in a polymer matrix, as detected with an evanescent wave biosensor. I. A computer simulation of the influence of mass transport. Biophys J *70*, 1230-1249.

Sedlik, C., Dadaglio, G., Saron, M. F., Deriaud, E., Rojas, M., Casal, S. I., and Leclerc, C. (2000). In vivo induction of a high-avidity, high-frequency cytotoxic T-lymphocyte response is associated with antiviral protective immunity. J Virol *74*, 5769-5775.

Sha, W. C., Nelson, C. A., Newberry, R. D., Kranz, D. M., Russell, J. H., and Loh, D. Y. (1988). Selective expression of an antigen receptor on CD8-bearing T lymphocytes in transgenic mice. Nature *335*, 271-274.

Slifka, M. K., and Whitton, J. L. (2001). Functional avidity maturation of CD8(+) T cells without selection of higher affinity TCR. Nat Immunol *2*, 711-717.

Sloan-Lancaster, J., and Allen, P. M. (1996). Altered peptide ligand-induced partial T cell activation: molecular mechanisms and role in T cell biology. Annu Rev Immunol *14*, 1-27.

Song, E., Chen, J., Ouyang, N., Su, F., Wang, M., and Heemann, U. (2001). Soluble Fas ligand released by colon adenocarcinoma cells induces host lymphocyte apoptosis: an active mode of immune evasion in colon cancer. Br J Cancer *85*, 1047-1054.

Speiser, D. E., Kyburz, D., Stubi, U., Hengartner, H., and Zinkernagel, R. M. (1992). Discrepancy between in vitro measurable and in vivo virus neutralizing cytotoxic T cell reactivities. Low T cell receptor specificity and avidity sufficient for in vitro proliferation or cytotoxicity to peptide-coated target cells but not for in vivo protection. J Immunol *149*, 972-980.

Speiser, D. E., Miranda, R., Zakarian, A., Bachmann, M. F., McKall-Faienza, K., Odermatt, B., Hanahan, D., Zinkernagel, R. M., and Ohashi, P. S. (1997). Self antigens expressed by solid tumors Do not efficiently stimulate naive or activated T cells: implications for immunotherapy. J Exp Med *186*, 645-653.

Sprent, J., and Kishimoto, H. (2002). The thymus and negative selection. Immunol Rev *185*, 126-135.

Stanislawski, T., Voss, R. H., Lotz, C., Sadovnikova, E., Willemsen, R. A., Kuball, J., Ruppert, T., Bolhuis, R. L., Melief, C. J., Huber, C.*, et al.* (2001). Circumventing tolerance to a human MDM2-derived tumor antigen by TCR gene transfer. Nat Immunol *2*, 962-970.

Straathof, K. C., Pule, M. A., Yotnda, P., Dotti, G., Vanin, E. F., Brenner, M. K., Heslop, H. E., Spencer, D. M., and Rooney, C. M. (2005). An inducible caspase 9 safety switch for T-cell therapy. Blood *105*, 4247-4254.

Suzuki, T., Tahara, H., Narula, S., Moore, K. W., Robbins, P. D., and Lotze, M. T. (1995). Viral interleukin 10 (IL-10), the human herpes virus 4 cellular IL-10 homologue, induces local anergy to allogeneic and syngeneic tumors. J Exp Med *182*, 477-486.

Teague, R. M., Sather, B. D., Sacks, J. A., Huang, M. Z., Dossett, M. L., Morimoto, J., Tan, X., Sutton, S. E., Cooke, M. P., Ohlen, C., and Greenberg, P. D. (2006). Interleukin-15 rescues tolerant CD8+ T cells for use in adoptive immunotherapy of established tumors. Nat Med *12*, 335-341.

Teng, M. K., Smolyar, A., Tse, A. G., Liu, J. H., Liu, J., Hussey, R. E., Nathenson, S. G., Chang, H. C., Reinherz, E. L., and Wang, J. H. (1998). Identification of a common docking topology with substantial variation among different TCR-peptide-MHC complexes. Curr Biol *8*, 409-412.

Ueno, T., Tomiyama, H., Fujiwara, M., Oka, S., and Takiguchi, M. (2004). Functionally impaired HIV-specific CD8 T cells show high affinity TCR-ligand interactions. J Immunol *173*, 5451-5457.

Valitutti, S., Muller, S., Cella, M., Padovan, E., and Lanzavecchia, A. (1995). Serial triggering of many T-cell receptors by a few peptide-MHC complexes. Nature *375*, 148-151.

Valmori, D., Dutoit, V., Schnuriger, V., Quiquerez, A. L., Pittet, M. J., Guillaume, P., Rubio-Godoy, V., Walker, P. R., Rimoldi, D., Lienard, D.*, et al.* (2002). Vaccination with a Melan-A peptide selects an oligoclonal T cell population with increased functional avidity and tumor reactivity. J Immunol *168*, 4231-4240.

Walter, E. A., Greenberg, P. D., Gilbert, M. J., Finch, R. J., Watanabe, K. S., Thomas, E. D., and Riddell, S. R. (1995). Reconstitution of cellular immunity against cytomegalovirus in recipients of allogeneic bone marrow by transfer of T-cell clones from the donor. N Engl J Med *333*, 1038-1044.

Walter, J. B., Garboczi, D. N., Fan, Q. R., Zhou, X., Walker, B. D., and Eisen, H. N. (1998). A mutant human beta2-microglobulin can be used to generate diverse multimeric class I peptide complexes as specific probes for T cell receptors. J Immunol Methods *214*, 41-50.

Wang, J. H., Meijers, R., Xiong, Y., Liu, J. H., Sakihama, T., Zhang, R., Joachimiak, A., and Reinherz, E. L. (2001). Crystal structure of the human CD4 N-terminal two-domain fragment complexed to a class II MHC molecule. Proc Natl Acad Sci U S A *98*, 10799-10804.

Wang, X. L., and Altman, J. D. (2003). Caveats in the design of MHC class I tetramer/antigen-specific T lymphocytes dissociation assays. J Immunol Methods *280*, 25-35.

Willemsen, R. A., Weijtens, M. E., Ronteltap, C., Eshhar, Z., Gratama, J. W., Chames, P., and Bolhuis, R. L. (2000). Grafting primary human T lymphocytes with cancer-specific chimeric single chain and two chain TCR. Gene Ther *7*, 1369-1377.

Wong, P., Lara-Tejero, M., Ploss, A., Leiner, I., and Pamer, E. G. (2004). Rapid development of T cell memory. J Immunol *172*, 7239-7245.

Wooldridge, L., van den Berg, H. A., Glick, M., Gostick, E., Laugel, B., Hutchinson, S. L., Milicic, A., Brenchley, J. M., Douek, D. C., Price, D. A., and Sewell, A. K. (2005). Interaction between the CD8 coreceptor and major histocompatibility complex class I stabilizes T cell receptor-antigen complexes at the cell surface. J Biol Chem *280*, 27491-27501.

Xue, S. A., Gao, L., Hart, D., Gillmore, R., Qasim, W., Thrasher, A., Apperley, J., Engels, B., Uckert, W., Morris, E., and Stauss, H. (2005). Elimination of human leukemia cells in NOD/SCID mice by WT1-TCR gene-transduced human T cells. Blood *106*, 3062-3067.

Yee, C., Savage, P. A., Lee, P. P., Davis, M. M., and Greenberg, P. D. (1999). Isolation of high avidity melanoma-reactive CTL from heterogeneous populations using peptide-MHC tetramers. J Immunol *162*, 2227-2234.

Zeh, H. J., 3rd, Perry-Lalley, D., Dudley, M. E., Rosenberg, S. A., and Yang, J. C. (1999). High avidity CTLs for two self-antigens demonstrate superior in vitro and in vivo antitumor efficacy. J Immunol *162*, 989-994.

Zhao, Y., Zheng, Z., Robbins, P. F., Khong, H. T., Rosenberg, S. A., and Morgan, R. A. (2005). Primary human lymphocytes transduced with NY-ESO-1 antigen-specific TCR genes recognize and kill diverse human tumor cell lines. J Immunol *174*, 4415-4423.

Zinkernagel, R. M., and Doherty, P. C. (1974). Restriction of in vitro T cell-mediated cytotoxicity in lymphocytic choriomeningitis within a syngeneic or semiallogeneic system. Nature *248*, 701-702.

7 ACKNOWLEDGEMENTS

With this paragraph I would like to take the opportunity to thank all the people who have helped me and supported me throughout the last years during my thesis work.

First of all I want to thank Prof. Dr. Dirk H. Busch for giving me the opportunity to work on this fascinating project. His vision and enthusiasm were of essential importance for the success of this work. He was always open for questions, willing to share his vast immunological knowledge and gave me great guidance throughout the recent years. Also, he was always there to give me a push when I needed one. Furthermore I would like to thank Prof. Hermann Wagner for giving me the opportunity to work at such a renowned institute and for providing excellent research infrastructure.

I also want to thank Prof. Dirk Haller who agreed to supervise this work and Prof. Siegfried Scherer who agreed to act as chairman of this dissertation.

Special thanks go to the whole Busch group, which provided a very comfortable, supporting and stimulating work environment. Your strong company was something I could always rely on, especially during stretches of slow progress and frustration. A special mention goes to the technicians Anna Hochholzer, Evelyn Ziegler and Martina Koffler for expert technical assistance and help in all questions of lab routine, to Dr. Mathias Schiemann for excellent assistance in all IT- and flow cytometry-related questions, to Dr. Katharina Huster for fruitful discussions and genuine human warmth and to Anja Kriegeskorte, Christian Stemberger and Florian Anderl for discussions, for being there, for sharing the experience of being a Ph D student as well as for excellent tabletop football matches.

Very special thanks also to Dr. Jörg Mages of the Lang group, whose excellent programming skills have transformed weeks of data analysis into mere days. Thanks also to Dr. Frank Schmitz of the Wagner group for help in all questions related to confocal microscopy, to Dr. Lothar Germeroth, Dr. Thomas Schmidt and Dr. Gerd Holzapfel of IBA GmbH Göttingen for providing Streptactin-PE and for help in all questions related to the Streptag technology and to Dr. Thomas Müller and Dr. Thomas Schnelle of Evotec GmbH Berlin for great help with the Evotec Cytocon400 system. Thanks also to Dr. Rafaela Holtappels-Geginat and Prof. Dr. Matthias Reddehase from the Institute for Virolgy at the University of Mainz for providing mCMV specific T cell lines.

Last but not least I would like to thank my dear friends Harry, Jörg, Marc, Nina and Rio. I know I do not have to say anything special. Thanks for being with me.

7 ACKNOWLEDGEMENTS

Obviously, my parents have supported me not only during the last years of this work, but throughout my entire life. The strength of my family has made me never give up during my studies or during this thesis work. For that I am very grateful (as well as for the occasional financial support).

My great love Melinda, who I have found exactly at the time that I started to write this thesis and who has been turning my world upside down ever since, I cannot thank enough. You have always been there for me and you were always willing to listen to my lamentations. The mere thought of you makes me smile. I love you Baby!

Thanks to all of you!!!